



Attorney's Docket No.: 17979-006002 / 02045P US DIV  
IFW

IN THE UNITED STATES PATENT AND TRADEMARK OFFICE

Applicant : Krahmer et al. Art Unit : Unknown  
Serial No. : 10/817,527 Examiner : Unknown  
Filed : April 1, 2004  
Title : OBJECTIVE WITH FLUORIDE CRYSTAL LENSES

Commissioner for Patents  
P.O. Box 1450  
Alexandria, VA 22313-1450

TRANSMITTAL OF CERTIFIED TRANSLATIONS OF PRIORITY DOCUMENTS

Applicant hereby submits Certified Translations of the following Priority Documents:

DE 101 23 725 A

DE 101 23 727 A1

DE 101 25 487 A1

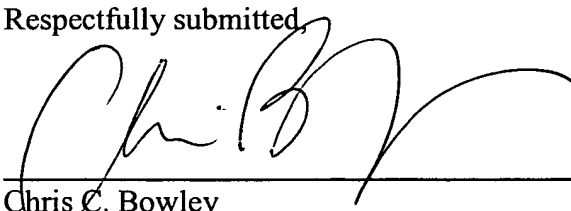
DE 101 27 320 A1

DE 102 10 782 A1

Please apply any charges or credits to Deposit Account No. 06-1050.

Respectfully submitted,

Date: 8/9/2005

  
Chris C. Bowley  
Reg. No. 55,016

Fish & Richardson P.C.  
225 Franklin Street  
Boston, MA 02110  
Telephone: (617) 542-5070  
Facsimile: (617) 542-8906

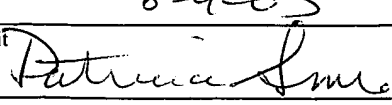
21141677.doc

CERTIFICATE OF MAILING BY FIRST CLASS MAIL

I hereby certify under 37 CFR §1.8(a) that this correspondence is being deposited with the United States Postal Service as first class mail with sufficient postage on the date indicated below and is addressed to the Commissioner for Patents, P.O. Box 1450, Alexandria, VA 22313-1450.

8-9-05

Date of Deposit



Signature

Patricia Smith

Typed or Printed Name of Person Signing Certificate

**DR. WALTER E. KUPPER**

65 Barnsdale Road  
Madison, NJ 07940

Telephone: 973 301-1989 Fax: 973 822-9096 E-mail: wekupper@att.net

June 15, 2005

TO WHOM IT MAY CONCERN:

**TRANSLATOR'S CERTIFICATE**

The undersigned hereby certifies that he is bilingually proficient in German and English, that he has personally prepared the attached translation

**"Microlithography Projection Exposure Apparatus, Optical System and Manufacturing Method"**

of the published German Patent Application

**"Offenlegungsschrift DE 101 23 725 A,  
Projektionsbelichtungsanlage der Mikrolithographie, Optisches System und Herstellverfahren"**

and that the translation is accurate.



Walter Kupper

Microlithography Projection Exposure Apparatus, Optical System  
and Manufacturing Method

[0001] The invention relates to a microlithography projection exposure apparatus in accordance with the introductory part of claim 1.

[0002] Projection exposure apparatus of this kind are known, e.g., from the not pre-published document DE 100 10 131.3 of March 3, 2000 (U.S. Serial No. 09/797,961 of March 5, 2001). In that reference (see claim 8), it is proposed to compensate for undesirable effects that optical components can have on the distribution of the polarization by making adjustments in other components, however specifically in relation to the polarization-selective reflection and to stress-induced birefringence.

[0003] The patent application PCT/EP00/13184 presents purely refractive and catadioptric projection objectives that are suitable for projection exposure apparatus of this kind, with numerical aperture values of 0.8 and 0.9, and at an operating wavelength of 157 nm.

[0004] The concept of using birefringent elements of locally varying thickness to compensate for polarization effects that vary across a bundle of light rays is known from DE 198 07 120 A (U.S. Serial No. 09/252,636).

[0005] U.S. Patent 6,201,634 B describes that technical fluoride crystals which are suitable for this application show a stress-induced birefringence effect that is direction-dependent in relation to the crystallographic axes.

[0006] From the Internet publication "Preliminary Determination of an Intrinsic Birefringence in CaF<sub>2</sub> by John H. Burnett, Eric L. Shirley, and Zachary H. Levine, NIST, Gaithersburg, MD 20899, USA (posted May 7, 2001), it is known that calcium fluoride single crystals also exhibit intrinsic birefringence in addition to the stress-induced birefringence.

[0007] All referenced documents in their entirety are intended to also be incorporated in the present patent application. This applies likewise to the simultaneously filed patent application by the same inventors, entitled "Optical Element, Projection Objective and Microlithography Projection Exposure Apparatus with Fluoride Crystal Lenses", in which measures are proposed that are advantageous also in combination with the present invention.

[0008] These birefringence effects are relevant only at short wavelengths of less than about 200 nm. This includes in particular the wavelength of 193 nm and to an even greater extent 157 nm, which are the preferred wavelengths in high-resolution microlithography.

[0009] Because of its dependence on the direction of the light ray in relation to the crystallographic axes, this form of birefringence varies as a function of the aperture angle as well as the angle of rotation about the optical axis (azimuth angle).

[0010] In an optical element that is oriented with rotational symmetry about the crystallographic (111)-axis, particularly in a lens (which can also take the shape of a planar-parallel plate, for example as an end plate or a filter), the birefringence effect has its minimum for a light ray passing perpendicularly through the element. However, with an

aperture angle of about 35° and at three angles of rotation (azimuth angles) oriented at 120° to each other, the direction of incidence equals the (110)-orientation of the crystal, where the maximum amount of birefringence occurs.

[0011] In an arrangement that is rotationally symmetric relative to one of the (100)-, (010)-, or (001)-axes, the (110)-equivalent axes which are associated with maximum birefringence are oriented at an aperture angle of 45°, now with fourfold symmetry. This is described in more detail in the aforementioned simultaneous patent application of the same inventors.

[0012] Considering that the aperture angle equals 31° for a 157 nm light ray exiting with the numerical aperture of 0.8 from an element of CaF<sub>2</sub> with a refractive index of about 1.56 at the transition, and that the angle is about 35° for a numerical aperture of 0.9, one concludes that the direction-dependent birefringence represents a problem in systems with such high numerical aperture values.

[0013] It is therefore the object of the present invention to propose a compensation of the undesirable effects of direction-dependent birefringence through a solution that allows projection objectives of even the highest aperture values to be operated optimally.

[0014] The foregoing objective is attained in a projection exposure apparatus according to claim 1, further through an optical system according to claim 9 or 12, and through manufacturing methods according to claims 15 and 17.

[0015] The invention is based on the observation that on the one hand - with birefringence amounting to about 6 nm per cm

and a light path length of about 10 cm occurring in lenses with high aperture angles - the birefringence-related undesirable effect represents primarily a phase shift of up to about one-quarter of a wavelength for two rays that are polarized orthogonally to each other, and further on the observation that large ray angles occur in elements that are close to the image plane (or a field plane) and have ray-vs-angle distribution functions that present themselves as spatial distributions in a Fourier-transformed pupil plane.

[0016] This leads to the surprising conclusion that the undesirable effect can be corrected by placing an element with a location-dependent phase shift (or location-dependent rotation of the polarization) near a pupil plane. However, as mentioned above, such elements and their manufacture through location-specific polishing, in particular ion beam polishing, are known, and they are available to be used also in this new context.

[0017] The position "near" a pupil plane, preferably the system aperture plane, represents a practical approximation where the location-dependent distribution of polarization and phase in the corrective element receives a sufficiently faithful transformation into the angular distribution of the element in which the angle-dependent birefringence occurs. This aspect has to be matched in particular to the optical design of the projection objective.

[0018] Besides this solution which is expressed in claims 1 and 9, the birefringent effects in a plurality of such elements can also be lessened according to claim 12 by installing the elements with mutually rotated orientations, a concept that can be applied either by itself or in combination (see claims 13, 14).

[0019] It is admittedly common practice that imperfections in individual production units of mounted elements are compensated in the assembly and adjustment process by rotating the elements against each other. In the case of the present invention, however, the loss of rotational symmetry caused by the angle-dependent birefringence is used in the optical design to prescribe a rotation of elements relative to each other and to thereby lessen the undesirable effect.

[0020] In the example of two calcium fluoride elements in (111)-orientation which are of equal thickness and are traversed by the light at the same angles, one would rotate the two elements by 60° relative to each other, so that the maxima of birefringence in one element are superimposed on the minima of the other element and vice versa, whereby the effect is approximately cut in half. A corrective plate for this arrangement will have sixfold rotational symmetry.

[0021] Given that the undesirable effect itself as well as the required shape change on the corrective element are relatively small, it is possible to completely assemble and adjust a projection objective in a first phase of the manufacturing process and to subsequently measure and rework the objective in accordance with claim 15. With this procedure, intrinsic birefringence and unit-specific stress birefringence can be compensated at the same time.

[0022] Advantageous embodiments are the subject of the subordinate claims.

[0023] In the embodiment according to claim 8, a conversion of radial into tangential polarization in the projection objective is performed by an optically active element, a

concept that is explained in detail in the simultaneously filed patent application "Optisches Abbildungssystem mit Polarisationsmitteln und Quarzkristallplatte hierfür" ("Optical Imaging System with Polarization Means and Quartz Crystal Plate for the Imaging System"), inventor Dr. Michael Gerhard. This application in its entirety is also incorporated in the present application.

[0024] The invention will be explained in detail with reference to the drawing.

[0025] Fig. 1 schematically illustrates a projection exposure apparatus according to the invention.

[0026] With an optical axis 0 as a reference, Fig. 1 shows a light source 1 which is preferably a laser with a narrow-band emission at 157 nm or 193 nm. The light of the light source is delivered to an illumination system 2 which as a special feature may include means 21 that serve to produce a radial polarization, as known from DE 195 35 392 A1 and the aforementioned patent application by the inventor Gerhard. A microlithography reticle 3, which is attached to a reticle-holding and -positioning system 31, is illuminated by the light from the illumination system. The projection objective 4 which follows next projects an image of the reticle onto the object 5 which is arranged in the image plane - typically a wafer.

[0027] The object 5 is equipped with an object-holding and -positioning system.

[0028] The objective 4 includes a group 41 with lenses and, if necessary, also one or more mirrors, a pupil plane or system aperture plane P and - between the plane P and the

plane of the object 5 - lenses 42, 43 whose exit angle  $\alpha$  is determined by the image-side numerical aperture NA of the projection objective.

[0029] At least one of the lenses 42, 43 consists of a material with angle-dependent birefringence, for example calcium fluoride whose (111)-orientation coincides with the optical axis O or deviates by up to about 5°.

[0030] If both of the lenses 42, 43 shown in the drawing (of course, in most cases more lenses will be required in this area) meet the description of the preceding paragraph, they are preferably installed with a mutual rotation in regard to their azimuth angle, i.e., rotated relative to each other about the optical axis O.

[0031] For each light ray, an aperture angle that occurs at one of the lenses 42, 43 close to the field is transformed in the proximity of the pupil plane P into a distance from the optical axis O. By having a variable thickness and thus a phase shift or rotation of the polarization that depends on the distance from the optical axis O, the corrective element 44 of birefringent or optically active material, which according to the invention is arranged in that place, can therefore compensate for the angle-dependent birefringence of the lenses 42, 43.

[0032] The means 21 and the corrective element 44 can be configured in the sense of the above-referenced patent application by the inventor Gerhard and can thus produce radial polarization on the object 5, in which case the corrective element 44 in the sense of the present invention simultaneously compensates for the angle-dependent birefringence.

[0033] If the projection objective 4 has additional pupil planes, which is the case for example in configurations with an intermediate image, a corrective element can also be arranged in an additional pupil plane.

[0034] If the refractive effects of the thickness profile of the corrective element 44 are found to be undesirable, they can be compensated by compensation plates of a material that has little or no birefringence, as known from DE 198 07 120. Also, it is possible to rework the shape of lens surfaces, e.g., by ion beam etching.

[0035] The effect of angle-dependent birefringence of fluoride crystals which has been described above can be taken into account in the optical design of large-aperture projection objectives. This requires that the variation over the azimuth angle be taken into account. Based on these factors, the shape of the corrective element 44 can be prescribed in the design.

[0036] As an alternative or supplementary measure, it is also possible to measure the irregularity in the image caused by the angle-dependent birefringence and to use the measurement as a basis to specify how the corrective element 44 is to be reworked. This procedure allows a unit-specific birefringence distribution to be corrected at the same time.

[0037] The measures which are herein described, cited from references, and claimed can be used in the widest diversity of combinations, even though this is not described in detail.

## Patent Claims:

1. Microlithography projection exposure apparatus with:
  - a light source (1), in particular with a wavelength in the range from 200 to 100 nm,
  - an illumination system (2),
  - a mask-positioning system (31),
  - a projection objective (4), preferably with an image-side numerical aperture (NA) in the range from 0.7 to 0.95, with a system aperture plane (P) and with an image plane (5), comprising at least one lens (42, 43) of a material that exhibits a birefringence which is dependent on the passage angle ( $\alpha$ ), in particular arranged close to the image plane (5),
  - an object-positioning system (51),characterized in that an optical element (44) is provided in the illumination system (2) or in the projection objective (4) near a pupil plane (P), which element has a location-dependent polarization-rotating or phase-shifting effect and compensates at least partially for the birefringence effects in the image plane (5) that are produced by the at least one lens (42, 43).
2. Projection exposure apparatus according to claim 1, characterized in that the material of the at least one lens is a cubic fluoride crystal, in particular  $\text{CaF}_2$ ,  $\text{BaF}_2$  or  $\text{SrF}_2$ .
3. Projection exposure apparatus according to claim 1 or claim 2, characterized in that the passage-angle-dependent birefringence and the location-dependent, polarization-rotating or phase-shifting effect have the same manifold, in particular three- or fourfold rotational symmetry.

4. Projection exposure apparatus according to at least one of the claims 1 to 3, characterized in that the at least one lens of said material which exhibits a passage-angle-dependent birefringence is arranged between the system aperture plane and the image plane, in particular as a last lens on the image side.
5. Projection exposure apparatus according to at least one of the claims 1 to 4, characterized in that the element with the location-dependent phase-shifting effect is arranged near the system aperture plane of the projection objective.
6. Projection exposure apparatus according to at least one of the claims 1 to 5, characterized in that the element with the location-dependent phase-shifting effect is an optically active element, in particular of quartz, or a birefringent element with a thickness that varies with location.
7. Projection exposure apparatus according to at least one of the claims 1 to 6, characterized in that a tangential or radial polarization is present in the image plane.
8. Projection exposure apparatus according to claim 6 and claim 7, characterized in that radial polarization is produced in the illumination system or in the object-facing part of the projection objective and that an optically active element, in particular of quartz, is arranged near the system aperture plane, which element by means of a suitable location-dependent thickness distribution effects a rotation of the polarization into tangential polarization with a superimposed compensation

- of the birefringent effects coming from the at least one lens.
9. Optical system, in particular a microlithography projection objective, with
- at least one first optical element which effects a polarization-dependent irregularity over the angular range of the light rays in the propagation of a bundle of light rays traversing the element,
  - characterized in that
  - at least one second optical element is provided which influences the polarization in a manner which depends on the location of the light rays of the light bundle at the second optical element, in such a way that the irregularity caused by the first optical element is at least partially compensated.
10. Optical system according to claim 9, characterized in that
- the system comprises at least one field plane and
  - further comprises at least one pupil plane that is a Fourier transform of the field plane, and that
  - the first optical element is arranged near said field plane and
  - the second optical element is arranged near one of said pupil planes.
11. Optical system according to claim 9 or 10, characterized in that the irregularity of the propagation and the influence on the polarization have the same manifold, in particular threefold or fourfold rotational symmetry.
12. Optical system, in particular a microlithography projection objective, with at least one first and one second optical element, both of which effect a

polarization-dependent irregularity of the propagation over the angular range of the light rays of a light bundle traversing the elements, characterized in that the first and the second optical element are rotated relative to each other about a common symmetry axis in such a manner that the respective rotation-angle ranges of maximal birefringence of the first and second element are offset relative to each other.

13. Optical system according to claim 12, characterized in that additionally the features of at least one of the claims 9-11 are met.
14. Microlithography projection exposure apparatus, comprising an optical system according to at least one of the claims 9 to 13.
15. Method of manufacturing a microlithography projection objective, wherein the objective is completely assembled and the wave front in the image plane is measured, characterized in that a manifold, in particular three- or fourfold rotationally symmetric irregularity is evaluated and, dependent on the evaluation, the thickness profile of an optical element which is arranged in particular near a pupil plane is varied with the same manifold rotational symmetry, so that the manifold rotationally symmetric irregularity of the wave front in the image plane is at least partially compensated.
16. Manufacturing method according to claim 15, characterized in that the microlithography projection objective is an optical system according to at least one of the claims 9 to 13 and/or is a part of a projection exposure apparatus according to at least one of the claims 1 to 8 and 14.

---

17. Method of producing a microlithography structure, characterized by the use of a projection exposure apparatus according to at least one of the claims 1 to 8 and 14, or comprising an optical system according to at least one of the claims 9 to 13, or manufactured according to claim 15 or 16.

---

Attached hereto: 1 page(s) of drawings

---

**Summary****Microlithography Projection Exposure Apparatus, Optical System  
and Manufacturing Method**

(Fig. 1)

In a projection exposure apparatus, in particular with a wavelength of 157 nm or 193 nm and an image-side numerical aperture NA of 0.8 to 0.95, and with fluoride crystal lenses (42, 43), the undesirable effect of angle-dependent birefringence of the fluoride crystal lenses is reduced by rotating them relative to each other about the optical axis (O) and/or by means of a corrective element (44) that is placed near a pupil plane (P).

**DR. WALTER E. KUPPER**

65 Barnsdale Road  
Madison, NJ 07940

Telephone: 973 301-1989 Fax: 973 822-9096 E-mail: wekupper@att.net

June 27, 2005

TO WHOM IT MAY CONCERN:

**TRANSLATOR'S CERTIFICATE**

The undersigned hereby certifies that he is bilingually proficient in German and English, that he has personally prepared the attached translation

**"Optical Element, Projection Objective and Microlithography Projection Exposure Apparatus with Fluoride Crystal Lenses"**

of the published German Patent Application

**"Offenlegungsschrift DE 101 23 727 A1,  
Optisches Element, Projektionsobjektiv und Mikrolithographie-  
Projektionsbelichtungsanlage mit Fluoridkristall-Linsen "**

and that the translation is accurate.



Walter Kupper

Optical Element, Projection Objective and Microlithography  
Projection Exposure Apparatus with Fluoride Crystal Lenses

Description

[0001] The invention relates to an optical element in accordance with the introductory part of claim 1.

[0002] Optical elements of this kind are known from U.S. Patent 6,201,634 which discloses that, ideally, in the manufacture of the optical elements, the element axes of the optical elements are aligned perpendicularly to the crystallographic (111)-planes of the fluoride crystals in order to minimize the stress-related birefringence. The implied assumption in U.S. Patent 6,201,634 is that fluoride crystals have no intrinsic birefringence.

[0003] However, as is known from the Internet publication "Preliminary Determination of an Intrinsic Birefringence in CaF<sub>2</sub>" by John H. Burnett, Eric L. Shirley, and Zachary H. Levine, NIST, Gaithersburg, MD 20899, USA (posted May 7, 2001), calcium fluoride single crystals also exhibit birefringence that is not stress-induced, i.e., intrinsic birefringence. The measurements presented in that reference demonstrate that with a light ray propagation in the crystallographic (110)-direction, the birefringence in calcium fluoride amounts to  $(6.5 \pm 0.4)$  nm/cm at a wavelength of  $\lambda=156.1$  nm, to  $(3.6 \pm 0.2)$  nm/cm at a wavelength of  $\lambda=193.09$  nm, and to  $(1.2 \pm 0.1)$  nm/cm at a wavelength of  $\lambda=253.65$  nm. However, with a light ray propagation in the crystallographic (100)-direction and in the crystallographic (111)-direction, no intrinsic birefringence occurs in calcium fluoride, as is also predicted by theory. Thus, the intrinsic

birefringence is strongly direction-dependent and becomes noticeably more pronounced as the wavelength decreases.

[0004] Because of the symmetries of cubic crystals, any statements made hereinafter in regard to light propagating in the crystallographic (110)-direction will always be applicable likewise to light propagating in the crystallographic (101)-direction and in the crystallographic (011)-direction. The same applies also to statements relating to light propagating in the crystallographic (100)-, (010)-, and (001)-directions. The crystallographic direction in all cases indicates the direction of the normal vector of the respective crystallographic plane. As an example, the crystallographic direction (100) indicates the direction of the normal vector of the crystallographic plane (100). Statements relating to crystallographic directions that correspond to each other based on the crystallographic symmetry or, in other words, crystallographic planes that are obtained merely by permutating the digits 0 and 1, will therefore not be explicitly mentioned, but should be considered as implied in all cases where statements are made relative to one of these crystallographic directions or crystallographic planes.

[0005] Projection objectives and microlithography projection exposure apparatus are known, e.g., from the patent application PCT/EP00/13184 of the present applicant and the references that are cited in that application. The embodiments presented in that application illustrate suitable purely refractive and catadioptric projection objectives with numerical aperture values of 0.8 and 0.9 at an operating wavelength of 193 nm as well as 157 nm.

[0006] The present invention has the object to propose optical elements for a projection objective as well as

projection objectives for a microlithography projection exposure apparatus, wherein the influence of intrinsic birefringence is minimized.

[0007] The object just described is solved by an optical element according to claim 1, a projection objective according to claim 4 and claim 19, a microlithography projection exposure apparatus according to claim 20, and a method for the manufacture of semiconductor components according to claim 21. Advantageous embodiments of the invention are presented in the characterizing portions of the dependent claims.

[0008] As a means for reducing the influence of intrinsic birefringence, claim 1 proposes to align the element axes in optical elements made of a fluoride crystal with an orientation where the element axis coincides with the crystallographic (100)-direction within a maximum deviation 5°. The element axis in this context is defined, e.g., by a symmetry axis of the optical element or, if the optical element is exposed to radiation, by the center of the incident light bundle, or by a straight line in relation to which the ray angles of all light rays within the optical elements are minimal. Optical elements can include, e.g., refractive or diffractive lenses as well as correction plates with free-form corrective surfaces. Orienting the element axis in the crystallographic (100)-direction has the advantage that the undesirable influence of the intrinsic birefringence which occurs with a light propagation in the crystallographic (110)-direction becomes noticeable only at very large aperture angles of the light rays. The term aperture angle in the present context refers to the angle between a light ray and the element axis inside the optical element. Only as the aperture angle falls into the angular range between the crystallographic (100)- and (110)-directions does the

influence of birefringence manifest itself in the respective light rays. The angle between the crystallographic (110)- and (100)-directions amounts to 45°. If the element axis were, on the other hand, oriented in the crystallographic (111)-direction, the undesirable influence of intrinsic birefringence would be noticeable already at smaller aperture angles, as the angle between the crystallographic (110)- and (111)-directions is only 35°.

[0009] If this angle-dependence of the birefringence is caused, e.g., by the manufacturing process of the fluoride crystal or by mechanical stress applied to the optical element, the conceptual solutions disclosed herein can, of course be used to lessen the undesirable influence of the birefringence.

[0010] With preference, the optical elements in the present context are rotationally symmetric lenses. In this case, the symmetry axis of the lenses coincides with the element axis of the optical elements.

[0011] The preferred material to use for the optical elements in projection objectives is calcium fluoride, because when used together with quartz at an operating wavelength of 193 nm, calcium fluoride is particularly well suited for the color correction, and with an operating wavelength of 157 nm, it still has a sufficient transmissivity. However, the foregoing statements are likewise applicable to the fluoride crystals strontium fluoride and barium fluoride, as they are crystals of the same type of cubic crystal structure.

[0012] According to claim 4, optical elements whose element axis are oriented approximately perpendicular to the crystallographic (100)-planes are used with preference in

projection objectives of a microlithography projection exposure apparatus. It is not necessary for all optical elements of the projection objective to share this orientation of the crystallographic planes. Those optical elements in which the element axes are perpendicular to the crystallographic (100)-planes will hereinafter also be referred to as special optical elements.

[0013] Projection objectives have an optical axis that runs from the object plane to the image plane. With preference, the optical elements are arranged in centered alignment relative to this optical axis, so that the element axes also coincide with the optical axis.

[0014] The undesirable influence of intrinsic birefringence becomes particularly noticeable if the light rays inside the optical elements have large aperture angles. This is the case in projection objectives with an image-side numerical aperture larger than 0.75, in particular larger than 0.85.

[0015] In projection objectives with such large numerical aperture values, there will be aperture angles larger than  $25^\circ$ , and in particular larger than  $30^\circ$ , occurring inside the special optical elements. It is precisely with these large aperture angles that the inventive concept of orienting the element axes in the crystallographic (100)-direction proves to be successful. If the element axes were oriented in the crystallographic (111)-direction, the influence of birefringence, which has its maximum at  $34^\circ$ , would be clearly noticed in the light rays with aperture angles larger than  $25^\circ$ , in particular larger than  $30^\circ$ .

[0016] Since on the other hand, the undesirable influence of intrinsic birefringence can have a maximum at an aperture

angle of  $45^\circ$ , it is advantageous to design the projection objective in such a way that all aperture angles of the light rays are smaller than  $45^\circ$ , in particular smaller than

$\arcsin\left(\frac{NA}{n_{FK}}\right)$ , wherein NA stands for the image-side numerical

aperture and  $n_{FK}$  stands for the refractive index of the fluoride crystal. This is achieved by a design in which the lenses that are arranged near the image plane, have light-collecting lens surfaces or at most slightly dispersing lens surfaces.

[0017] Large aperture angles occur primarily in optical elements near field planes, in particular the image plane. The special optical elements should therefore preferably be used in the vicinity of the field planes. The range where the special optical elements should be used can be determined by way of the ratio between the element diameter and the diameter of the aperture stop. Thus, the element diameter of the special optical element is preferably at most 85%, in particular at most 80% of the aperture stop diameter.

[0018] In projection objectives with an image-side numerical aperture larger than 0.75, the largest aperture angles occur as a rule in the optical element closest to the image plane. It is therefore preferred to align the element axis of this optical element in the crystallographic (100)-direction.

[0019] The intrinsic birefringence under discussion here is dependent not only on the aperture angle of a light ray, but also on the azimuth angle of the light ray relative to rotation about the element axis. The azimuth angle as it pertains to the present discussion is determined as follows: If the element axis is oriented, e.g., in the crystallographic (100)-direction, the light ray is projected into the

crystallographic (100)-plane. The directional vectors of the crystallographic (101)-, (110)-, (10 $\bar{1}$ )- and (1 $\bar{1}$ 0)-directions of maximum intrinsic birefringence are likewise projected into the crystallographic (100)-plane. The azimuth angle is now determined as the angle between the projected light ray and the projected directional vector of the crystallographic (101)-direction. Of course, analogous definitions apply also for the cases in which the element axis is oriented in the crystallographic (010)- or (001)-direction. The intrinsic birefringence thus has a fourfold symmetry if the element axis is oriented in the crystallographic (100)-direction. A maximum for the intrinsic birefringence occurs here at azimuth angles of 0°, 90°, 180° and 270°, while it nearly vanishes for angles of 45°, 135°, 225° and 315°. If a plurality of special optical elements are used in a projection objective, it is advantageous if the special optical elements are arranged with a rotation relative to each other about the optical axis. With this measure, it can be avoided that the undesirable effects of intrinsic birefringence are additively superimposed on each other.

[0020] For example, if two special optical elements are used, it is advantageous if the angle of rotation between the optical elements is approximately 45°.

[0021] The rotation of the individual special optical elements is particularly effective, if the special optical elements are arranged next to each other.

[0022] Intrinsic birefringence becomes noticeably stronger with decreasing working wavelength. Thus, the intrinsic birefringence at a wavelength of 193 nm is more than twice as strong, and at a wavelength of 157 nm it is more than five times as strong as at a wavelength of 248 nm. The invention

can therefore be used to particular advantage if the light rays have wavelengths smaller than 200 nm, in particular smaller than 160 nm.

[0023] The projection objective in the present context can be a purely refractive objective that consists of a multitude of lenses arranged with rotational symmetry about the optical axis.

[0024] But the imaging performance is also improved in projection objectives of the catadioptric type of objectives, if the lenses with large aperture angles of the light rays are oriented so that the symmetry axes of the lenses point in the crystallographic (100)-direction.

[0025] Since the influence of intrinsic birefringence is dependent on the azimuth angle of a light ray, the imaging performance of a projection objective can be enhanced by arranging the optical elements with a rotation relative to each other about the optical axis. The rotation of each of the individual optical elements refers to the orientation of its crystallographic structure. Thus, a light ray on its path from the object plane to the image plane should only to a limited extent pass through areas with azimuth-angle ranges of increased intrinsic birefringence. The azimuth-angle ranges of increased intrinsic birefringence are in this case given by the crystallographic (110)-direction or the crystallographic directions obtained by permutation of the indices 1, 1, 0.

[0026] Projection objectives of this kind can be used advantageously in microlithography projection exposure apparatus which include a light source to begin with, an illumination system, a mask-positioning system, a structure-

carrying mask, a projection objective, an object-positioning system, and a light-sensitive substrate.

[0027] This microlithography projection exposure apparatus can be used to produce micro-structured semiconductor elements.

[0028] The invention will be explained in more detail with reference to the drawings.

[0029] Figure 1 illustrates a cross-section of a fluoride crystal perpendicular to the crystallographic (100)-planes with an optical element according to the invention shown in a schematic representation;

[0030] Figure 2 shows an optical element according to the invention in a schematic three-dimensional representation;

[0031] Figure 3 shows a coordinate system for the definition of the aperture angle and the azimuth angle;

[0032] Figure 4 represents the profile of the intrinsic birefringence as a function of the aperture angle  $\theta$ ;

[0033] Figure 5 represents the profile of the intrinsic birefringence as a function of the azimuth angle  $\alpha$ ;

[0034] Figure 6 represents the lens section of a refractive projection objective;

[0035] Figure 7 represents the lens section of a catadioptric projection objective; and

[0036] Figure 8 illustrates a microlithography projection exposure apparatus in a schematic representation.

[0037] Figure 1 schematically illustrates a section through a fluoride crystal block 3. The section is selected so that the crystallographic (100)-planes 5 can be seen as individual lines, i.e., the crystallographic (100)-planes 5 are oriented perpendicular to the plane of the paper. The fluoride crystal block 3 serves as raw material for the optical element 1. In the illustrated example, the optical element 1 is a bi-convex lens with the element axis EA which is at the same time the symmetry axis of the lens. The optical element 1 is now formed out of the crystal block in such a manner that the element axis EA stands perpendicular to the crystallographic (100)-planes.

[0038] Figure 2 visualizes again in a three-dimensional representation why it is particularly advantageous to orient the element axis EA of the optical elements in the crystallographic (100)-direction. The optical element shown in Figure 2 is a circular planar-parallel plate 201 of calcium fluoride. The element axis EA points in the crystallographic (100)-direction. Besides the crystallographic (100)-direction, the (101)-, (110)-, (10 $\bar{1}$ )-, and (1 $\bar{1}$ 0)-directions are likewise represented as arrows. The intrinsic birefringence is represented schematically by four lobes 207, whose surfaces represent the amount of the intrinsic birefringence for the respective ray direction of a light ray.

[0039] The maxima for the intrinsic birefringence occur, respectively, in the crystallographic (101)-, (110)-, (10 $\bar{1}$ )-, and (1 $\bar{1}$ 0)-directions, i.e., for light rays with an aperture angle of 45° and an azimuth angle of 0°, 90°, 180° and 270°. The intrinsic birefringence vanishes for azimuth angles of

45°, 135°, 225° and 315° as well as for an aperture angle of 0°.

[0040] The definition of aperture angle  $\theta$  and azimuth angle  $\alpha$  is illustrated in Figure 3. In relation to the example of Figure 2, the z-axis indicates the crystallographic (100)-direction, and the x-axis represents the crystallographic (101)-direction.

[0041] It is known from measurements, that with a light ray propagation in the crystallographic (110)-direction, a birefringence of  $(6.5 \pm 0.4)$  nm/cm occurs at a wavelength of  $\lambda = 156.1$  nm in calcium fluoride.

[0042] Represented in Figure 4 is the intrinsic birefringence as a function of the aperture angle  $\theta$  for the azimuth angle  $\alpha = 0^\circ$ . The value of 6.5 nm/cm for the intrinsic birefringence at an aperture angle of  $\theta = 45^\circ$  represents the measured value. The curve profile is based on the model assumption that the intrinsic birefringence shows a strong increase only after exceeding an aperture angle  $\theta = 25^\circ$ .

[0043] Figure 5 represents the intrinsic birefringence as a function of the azimuth angle  $\alpha$  for an aperture angle  $\theta = 45^\circ$ . The fourfold symmetry is evident. The curve profile takes into account that the intrinsic birefringence vanishes at an azimuth angle of 45°, 135°, 225° and 315°.

[0044] Figure 6 represents the lens section of a refractive projection objective 611 for the wavelength of 157 nm. The optical data for this objective are listed in Table 1. This example is taken from the applicant's patent application PCT/EP00/13184 where it corresponds to Figure 7 and Table 6. For a detailed description of the function of the objective,

see PCT/EP00/13184. All lenses of this objective consist of calcium fluoride crystal. The image-side numerical aperture of the objective is 0.9. The imaging performance of the objective is corrected so well that the deviation from a wave front of an ideal spherical wave is smaller than 1.8 thousandths of a wavelength at  $\lambda = 157$  nm. Especially with these high-performance objectives, it is necessary for the undesirable effects of intrinsic birefringence to be reduced to the farthest extent possible.

[0045] For the embodiment of Figure 6, a calculation was made of the aperture angles  $\alpha$  of the marginal ray 609 for the individual optical elements L601 to L630. The marginal ray 609 originates from the object point with the coordinates  $x = 0$  mm and  $y = 0$  mm, and in the image plane has an angle relative to the optical axis that corresponds to the image-side numerical aperture. The reason why the marginal ray 609 is singled out is that it is associated with close to the maximum aperture angles inside the optical elements. The aperture angles  $\alpha$  for the marginal ray 609 are listed in Table 2.

Table 2

Lens No.	Aperture Angle $\alpha$ [°]	Lens No.	Aperture Angle $\alpha$ [°]
L601	8.1	L616	-1.3
L602	8.7	L617	26.4
L603	7.8	L618	33.5
L604	10.7	L619	26.5
L605	9.4	L620	19.3
L606	10.3	L621	6.7
L607	21.8	L622	-10.3
L608	25.4	L623	-11.9
L609	16.3	L624	0.3
L610	12.2	L625	6.0
L611	2.3	L626	-24.0
L612	2.3	L627	-35.6
L613	-18.3	L628	-39.4
L614	-18.7	L629	-35.3
L615	-14.0	L630	-35.3

[0046] As can be seen in Table 2, the aperture angles  $\theta$  for the lenses L608, L617, L618, L619, L627, L628, L629 and L630 are larger than  $25^\circ$ , and for the lenses L618, L627, L628, L629 and L630 even larger than  $30^\circ$ . At least for these lenses, the element axis should therefore be aligned in the crystallographic (100)-direction. Particularly affected by the large aperture angles are the lenses L627 to L630, which are closest to the image plane. To prevent a cumulative addition of the undesirable effect of the intrinsic birefringence in these four lenses, they should be rotated relative to each other about the optical axis. The angle of rotation between two adjacent lenses can for example be  $45^\circ$ , so that a light ray passes e.g. through an azimuth-angle range of maximum intrinsic birefringence in one lens and through an azimuth-angle range of minimum intrinsic birefringence in the next lens. It is also possible to set the four last lenses in the light path at such angles of rotation that the respective azimuth-angle ranges of maximum intrinsic birefringence are rotated by 22.5 degrees. It is further possible to use arbitrary angles of rotation. The only important consideration is that the undesirable influence of the intrinsic birefringence on the overall wave front is minimized.

[0047] The projection objective was designed so that the maximum aperture angle of all light rays is smaller than  $45^\circ$ . The maximum aperture angle for the marginal ray is  $39.4^\circ$  in the lens L628. Also helpful was the use of two thick planar lenses L629 and L630 immediately ahead of the image plane.

[0048] The diameter of the aperture stop located between the lenses L621 and L622 is 270 mm. The diameter of the lens L618 is 207 mm and the diameters of the lenses L627 to L630 are all

smaller than 190 mm. Thus, the diameters of these lenses, which are associated with large aperture angles, are smaller than 80% of the aperture stop diameter.

[0049] Figure 7 represents the lens section of a catadioptric projection objective 711 for the wavelength of 157 nm. The optical data for this objective are listed in Table 3. This example is taken from the applicant's patent application PCT/EP00/13184 where it corresponds to Figure 9 and Table 8. For a detailed description of the function of the objective, see PCT/EP00/13184. All lenses of this objective consist of calcium fluoride crystal. The image-side numerical aperture of the objective is 0.8.

[0050] For the embodiment of Figure 7, a calculation was made of the aperture angles  $\alpha$  of the marginal ray for the individual optical elements L801 to L817. The marginal ray in this example originates from the object point with the coordinates  $x = 0$  mm and  $y = 0$  mm, and in the image plane has an angle relative to the optical axis that corresponds to the image-side numerical aperture. It is normal practice to perform the calculation for this theoretical ray, even though it does not represent a physical light ray, because objectives of this type have an off-axis field. The aperture angles  $\alpha$  for the axial ray are listed in Table 4.

Table 4

Lens No.	Aperture Angle $\alpha$ [°]	Lens No.	Aperture Angle $\alpha$ [°]
L801	5.5	L807	5.5
L802	15.5	L808	4.1
L803	20.5	L809	3.3
L803	21.5	L810	5.0
L802	16.4	L811	12.8
L804	6.3	L812	6.4
L805	8.3	L813	4.8
L806	4.3	L814	5.3
		L815	25.2
		L816	26.6
		L817	30.2

[0051] As can be seen in Table 4, the aperture angles  $\theta$  for the lenses L815 to L817 are larger than  $25^\circ$ . At least for these lenses, the element axis should therefore be aligned in the crystallographic (100)-direction. In this embodiment, too, the lenses L815 to L817, which are closest to the image plane, have large aperture angles. To prevent a cumulative addition of the undesirable influence of the intrinsic birefringence in these lenses, they should be arranged with a mutual rotation about the optical axis relative to each other. The angle of rotation between two adjacent lenses can for example be  $45^\circ$ , so that a light ray passes e.g. through an azimuth-angle range of maximum intrinsic birefringence in one lens and through an azimuth-angle range of minimum intrinsic birefringence in the next lens. It is also possible to set these three last lenses in the light path at such angles of rotation that the respective azimuth-angle ranges of maximum intrinsic birefringence are rotated by 30 degrees. It is also possible to use arbitrary angles of rotation. The only important consideration is that the undesirable influence of the intrinsic birefringence on the overall wave front is minimized.

[0052] The design of the lenses L815 to L817 achieved the result that the maximum aperture angle is smaller than

$$\arcsin\left(\frac{NA}{n_{FK}}\right) = \arcsin\left(\frac{0.8}{1.5597}\right) = 30.9^\circ. \quad \text{The maximum aperture}$$

angle for the marginal ray is  $30.2^\circ$  in the lens L817.

[0053] Simulations with the model data given in Figure 4 and Figure 5 in regard to the intrinsic birefringence have led to the result that in the embodiment of Figure 7, the intrinsic birefringence amounts to 16 nm, if the element axes in all lenses point in the crystallographic (100)-direction and all lenses are oriented equally, i.e., not rotated in relation to each other. With a suitable rotation of the lenses, the birefringence can be reduced to 8 nm. On the other hand, if one arranges all lenses so that the element axes point in the crystallographic (111)-direction, the intrinsic birefringence amounts to 49 nm, if all lenses are oriented equally. With a suitable rotation of the lenses, the birefringence can be reduced to 25 nm. The example demonstrates that in objectives with an image-side numerical aperture larger than 0.8, the intrinsic birefringence can be reduced by more than a factor of three, if the element axes of the lenses are not oriented in the crystallographic (111)-direction, but in the crystallographic (100)-direction.

[0054] The diameter of the aperture stop located between the lenses L811 and L812 is 193 mm. The diameters of the lenses L815 to L817 are all smaller than 162 mm. Thus, the diameters of these lenses, which are associated with large aperture angles, are smaller than 85% of the aperture stop diameter.

[0055] The following description of the principal configuration of a microlithography projection exposure apparatus is based on Figure 8. The projection exposure

apparatus 81 has an illumination device 83 and a projection objective 85. The projection objective 85 includes a lens arrangement 819 with an aperture stop AP, wherein an optical axis 87 is defined by the lens arrangement 89. Embodiments of the lens arrangement 89 are presented in Figure 6 and Figure 7. Arranged between the illumination device 83 and the projection objective 85 is a mask 89 which is held in the light path by means of a mask holder 811. Masks 89 of this type, which are used in microlithography, have a micrometer-nanometer structure that is projected into the image plane 813 by means of the projection objective 85, reduced for example by a factor of 4 or 5. In the image plane 813, a light-sensitive substrate 815 positioned by a substrate holder 817, more specifically a wafer, is held in place.

[0056] The smallest structure dimensions that can still be resolved depend on the wavelength  $\lambda$  of the light that is used for the illumination and they also depend on the image-side numerical aperture of the projection objective 85, with the maximally achievable resolution of the projection exposure apparatus 81 increasing as the wavelength  $\lambda$  of the illumination device 83 decreases and the numerical aperture of the projection objective 85 increases. With the embodiments shown in Figures 6 and 7, it is possible to realize resolutions smaller than 150 nm. This is also the reason why effects such as the intrinsic birefringence need to be minimized, even if such effects cause a deterioration of the wave front of an order of magnitude of only 10 nm. The invention has been successful in strongly reducing the undesirable influence of the intrinsic birefringence in particular in projection objectives with large image-side numerical aperture values.

M1587a

TABLE 1

LENSES	RADI	THICKNESS VALUES	GLASSES	REFR. INDEX AT 157.629nm	1/2 FREE DIAMETER
0	0.000000000	27.171475840 0.602670797	N2 N2	1.00031429 1.00031429	46.200 52.673
L601	900.198243311AS -235.121108435	15.151284556 9.531971079	CaF2 CaF2	1.55929035 1.00031429	53.454 54.049
L602	-167.185917779 -132.673519510	8.294716452 14.020355779	CaF2 CaF2	1.55929035 1.00031429	54.178 54.901
L603	-333.194588652 -155.450516203	9.893809820 15.930502944	CaF2 N2	1.55929035 1.00031429	53.988 54.132
L604	-73.572316296 -68.248613899AS	7.641977580 2.881720302	CaF2 N2	1.55929035 1.00031429	53.748 55.167
L605	-86.993585564AS -238.150965327	5.094651720 5.379130780	CaF2 N2	1.55929035 1.00031429	52.580 53.729
L606	-165.613920870 153.417884485	5.094651720 34.150169591	CaF2 N2	1.55929035 1.00031429	53.730 56.762
L607	-92.061009990 8491.086261873AS	5.094651720 19.673523795	CaF2 N2	1.55929035 1.00031429	58.081 74.689
L608	-407.131300451 -140.620317156	30.380807138 0.761662684	CaF2 N2	1.55929035 1.00031429	87.291 91.858
L609	-4831.804853654AS -192.197373609	50.269660218 1.688916911	CaF2 N2	1.55929035 1.00031429	117.436 121.408
L610	-367.718684892 -233.628547894	21.227715500 2.224071019	CaF2 N2	1.55929035 1.00031429	127.704 129.305
L611	709.585855080 1238.859445357	28.736922725 9.120684720	CaF2 N2	1.55929035 1.00031429	137.016 137.428
L612	1205.457051945 -285.321880705	49.281218258 1.625271224	CaF2 N2	1.55929035 1.00031429	138.288 138.379
L613	137.549591710 -4380.301012978AS	56.718543740 0.623523902	CaF2 N2	1.55929035 1.00031429	108.652 106.138
L614	2663.880214408 149.184979730	6.792868960 15.779049257	CaF2 N2	1.55929035 1.00031429	103.602 84.589
L615	281.093108064 184.030288413	6.792868960 32.341552355	CaF2 N2	1.55929035 1.00031429	83.373 77.968
L616	-222.157416308 101.254238115AS	5.094651720 56.792834221	CaF2 N2	1.55929035 1.00031429	77.463 71.826
L617	-106.980638018 1612.305471130	5.094651720 20.581065398	CaF2 N2	1.55929035 1.00031429	72.237 89.760
L618	-415.596135628 -204.680044631	26.398111993 0.713343960	CaF2 N2	1.55929035 1.00031429	96.803 103.409
L619	-646.696622394 -231.917626896	25.867340760 0.766268682	CaF2 N2	1.55929035 1.00031429	116.636 118.569
L620	-790.657607677 -294.872053725	23.400482872 0.721402031	CaF2 N2	1.55929035 1.00031429	128.806 130.074
L621	786.625567756 -431.247283013	40.932308205 12.736629300	CaF2 N2	1.55929035 1.00031429	141.705 142.089
L622	0.000000000 295.022653593AS	-8.491086200 20.185109438	N2 CaF2	1.00031429 1.55929035	134.586 139.341
L623	449.912291916 358.934076212	0.619840486 48.662890509	N2 CaF2	1.00031429 1.55929035	137.916 136.936
L624	-622.662988878 -224.404889753	30.955714157 12.736629300	N2 CaF2	1.00031429 1.55929035	135.288 134.760
L625	-251.154571510AS -193.582989843AS	16.079850229 16.510083506	N2 CaF2	1.00031429 1.55929035	134.853 134.101
L626	-198.077570749 206.241795157	0.880353872 19.927993542	N2 CaF2	1.00031429 1.55929035	136.109 101.240
L627	338.140581666 111.017549581	0.925956949 24.580089962	N2 CaF2	1.00031429 1.55929035	97.594 85.023
L628	169.576109839 117.982165264	0.777849447 31.161065630	N2 CaF2	1.00031429 1.55929035	81.164 75.464
L629	921.219058213AS 0.000000000	6.934980174 22.260797322	N2 CaF2	1.00031429 1.55929035	69.501 63.637
L630	0.000000000 0.000000000	8.491086200 4.245543100	N2 CaF2	1.00031429 1.00031429	48.606 41.032
	0.000000000 0.000000000	0.000000000 21.227715500	N2 CaF2	1.000000000 1.55929035	26.698 11.550

---

Wavelength and refractive index are stated relative to vacuum.

ASPHERIC CONSTANTS

Asphere of lens L601

K	0.0000
C1	1.28594437e-007
C2	8.50731836e-013
C3	1.16375620e-016
C4	2.28674275e-019
C5	-1.23202729e-022
C6	3.32056239e-026
C7	-4.28323389e-030
C8	0.00000000e+000
C9	0.00000000e+000

Asphere of lens L604

K	-1.3312
C1	-4.03355456e-007
C2	2.25776586e-011
C3	-2.19259878e-014
C4	4.32573397e-018
C5	-7.92477159e-022
C6	7.57618874e-026
C7	-7.14962797e-030
C8	0.00000000e+000
C9	0.00000000e+000

Asphere of lens L605

K	-1.1417
C1	1.33637337e-007
C2	1.56787758e-011
C3	-1.64362484e-014
C4	3.59793786e-018
C5	-5.11312568e-022
C6	1.70636633e-026
C7	1.82384731e-030
C8	0.00000000e+000
C9	0.00000000e+000

Asphere of lens L607

K	0.0000
C1	1.34745120e-007
C2	-2.19807543e-011
C3	1.20275881e-015
C4	4.39597377e-020
C5	-2.37132819e-023
C6	2.87510939e-027
C7	-1.42065162e-031
C8	0.00000000e+000
C9	0.00000000e+000

## Asphere of lens L609

K	0.0000
C1	6.85760526e-009
C2	-4.84524868e-013
C3	-6.28751350e-018
C4	-3.72607209e-022
C5	3.25276841e-026
C6	-4.05509974e-033
C7	-3.98843079e-035
C8	0.00000000e+000
C9	0.00000000e+000

## Asphere of lens L613

K	0.0000
C1	2.24737416e-008
C2	-4.45043770e-013
C3	-4.10272049e-017
C4	4.31632628e-021
C5	-3.27538237e-025
C6	1.44053025e-029
C7	-2.76858490e-034
C8	0.00000000e+000
C9	0.00000000e+000

## Asphere of lens L616

K	0.0000
C1	-2.83553693e-008
C2	-1.12122261e-011
C3	-2.05192812e-016
C4	-1.55525080e-020
C5	-4.77093112e-024
C6	8.39331135e-028
C7	-8.97313681e-032
C8	0.00000000e+000
C9	0.00000000e+000

## Asphere of lens L622

K	0.0421
C1	7.07310826e-010
C2	-2.00157185e-014
C3	-9.33825109e-020
C4	1.27125854e-024
C5	1.94008709e-027
C6	-6.11989858e-032
C7	2.92367322e-036
C8	0.00000000e+000
C9	0.00000000e+000

## Asphere of lens L624

K	0.0000
C1	3.02835805e-010
C2	-2.40484062e-014
C3	-3.22339189e-019
C4	1.64516979e-022
C5	-8.51268614e-027
C6	2.09276792e-031
C7	-4.74605669e-036
C8	0.00000000e+000
C9	0.00000000e+000

## Asphere of lens L625

K	0.0000
C1	-3.99248993e-010
C2	5.79276562e-014
C3	3.53241478e-018
C4	-4.57872308e-023
C5	-6.29695208e-027
C6	1.57844931e-031
C7	-2.19266130e-036
C8	0.00000000e+000
C9	0.00000000e+000

## Asphere of lens L628

K	0.0000
C1	4.40737732e-008
C2	1.52385268e-012
C3	-5.44510329e-016
C4	6.32549789e-020
C5	-4.58358203e-024
C6	1.92230388e-028
C7	-3.11311258e-033
C8	0.00000000e+000
C9	0.00000000e+000

TABLE 3

L61

LENSES	RADI	THICKNESS VALUES	GLASSES	REFR. INDEX AT 157.629nm	1/2 FREE DIAMETER
0	0.000000000	34.000000000		1.00000000	82.150
	0.000000000	0.100000000		1.00000000	87.654
L801	276.724757380	40.000000000	CaF2	1.55970990	90.112
	1413.944109416AS	95.000000000		1.00000000	89.442
SP1	0.000000000	11.000000000		1.00000000	90.034
	0.000000000	433.237005445		1.00000000	90.104
L802	-195.924336384	17.295305525	CaF2	1.55970990	92.746
	-467.658808527	40.841112468		1.00000000	98.732
L803	-241.385736441	15.977235467	CaF2	1.55970990	105.512
	-857.211727400AS	21.649331094		1.00000000	118.786
SP2	0.000000000	0.000010000		1.00000000	139.325
	253.074839896	21.649331094		1.00000000	119.350
L803'	857.211727400AS	15.977235467	CaF2	1.55970990	118.986
	241.385736441	40.841112468		1.00000000	108.546
L802'	467.658808527	17.295305525	CaF2	1.55970990	102.615
	195.924336384	419.981357165		1.00000000	95.689
SP3	0.000000000	6.255658280		1.00000000	76.370
	0.000000000	42.609155219		1.00000000	76.064
Z1	0.000000000	67.449547115		1.00000000	73.981
L804	432.544479547	37.784311058	CaF2	1.55970990	90.274
	-522.188532471	113.756133662		1.00000000	92.507
L805	-263.167605725	33.768525968	CaF2	1.55970990	100.053
	-291.940616829AS	14.536591424		1.00000000	106.516
L806	589.642961222AS	20.449887046	CaF2	1.55970990	110.482
	-5539.698828792	443.944079795		1.00000000	110.523
L807	221.780582003	9.000000000	CaF2	1.55970990	108.311
	153.071443064	22.790060084		1.00000000	104.062
L808	309.446967518	38.542735318	CaF2	1.55970990	104.062
	-2660.227900099	0.100022286		1.00000000	104.098
L809	23655.354584194	12.899131182	CaF2	1.55970990	104.054
	-1473.189213176	9.318886362		1.00000000	103.931
L810	-652.136459374	16.359499814	CaF2	1.55970990	103.644
	-446.489459129	0.100000000		1.00000000	103.877
L811	174.593507050	25.900313780	CaF2	1.55970990	99.267
	392.239615259AS	14.064505431		1.00000000	96.610
	0.000000000	2.045119392		1.00000000	96.552
L812	7497.306838492	16.759051656	CaF2	1.55970990	96.383
	318.210831711	8.891640764		1.00000000	94.998
L813	428.724465129	41.295806263	CaF2	1.55970990	95.548
	3290.097860119AS	7.377912006		1.00000000	95.040
L814	721.012739719	33.927118706	CaF2	1.55970990	95.443
	-272.650872353	6.871397517		1.00000000	95.207
L815	131.257556743	38.826450065	CaF2	1.55970990	81.345
	632.112566477AS	4.409527396		1.00000000	74.847
L816	342.127616157AS	37.346293509	CaF2	1.55970990	70.394
	449.261078744	4.859754445		1.00000000	54.895
L817	144.034814702	34.792179308	CaF2	1.55970990	48.040
	-751.263321098AS	11.999872684		1.00000000	33.475
0'	0.000000000	0.000127776		1.00000000	16.430

## ASPHERIC CONSTANTS

Asphere of lens L801

K	0.0000
C1	4.90231706e-009
C2	3.08634889e-014
C3	-9.53005325e-019
C4	-6.06316417e-024
C5	6.11462814e-028
C6	-8.64346302e-032
C7	0.00000000e+000
C8	0.00000000e+000
C9	0.00000000e+000

Asphere of lens L803

K	0.0000
C1	-5.33460884e-009
C2	9.73867225e-014
C3	-3.28422058e-018
C4	1.50550421e-022
C5	0.00000000e+000
C6	0.00000000e+000
C7	0.00000000e+000
C8	0.00000000e+000
C9	0.00000000e+000

Asphere of lens L803'

K	0.0000
C1	5.33460884e-009
C2	-9.73867225e-014
C3	3.28422058e-018
C4	-1.50550421e-022
C5	0.00000000e+000
C6	0.00000000e+000
C7	0.00000000e+000
C8	0.00000000e+000
C9	0.00000000e+000

Asphere of lens L805

K	0.0000
C1	2.42569449e-009
C2	3.96137865e-014
C3	-2.47855149e-018
C4	7.95092779e-023
C5	0.00000000e+000
C6	0.00000000e+000
C7	0.00000000e+000
C8	0.00000000e+000
C9	0.00000000e+000

## Asphere of lens L806

K	0.0000
C1	-6.74111232e-009
C2	-2.57289693e-014
C3	-2.81309020e-018
C4	6.70057831e-023
C5	5.06272344e-028
C6	-4.81282974e-032
C7	0.00000000e+000
C8	0.00000000e+000
C9	0.00000000e+000

## Asphere of lens L811

K	0.0000
C1	2.28889624e-008
C2	-1.88390559e-014
C3	2.86010656e-017
C4	-3.18575336e-021
C5	1.45886017e-025
C6	-1.08492931e-029
C7	0.00000000e+000
C8	0.00000000e+000
C9	0.00000000e+000

## Asphere of lens L813

K	0.0000
C1	3.40212872e-008
C2	-1.08008877e-012
C3	4.33814531e-017
C4	-7.40125614e-021
C5	5.66856812e-025
C6	0.00000000e+000
C7	0.00000000e+000
C8	0.00000000e+000
C9	0.00000000e+000

## Asphere of lens L815

K	0.0000
C1	-3.15395039e-008
C2	4.30010133e-012
C3	3.11663337e-016
C4	-3.64089769e-020
C5	1.06073268e-024
C6	0.00000000e+000
C7	0.00000000e+000
C8	0.00000000e+000
C9	0.00000000e+000

## Asphere of lens L816

K	0.0000
C1	-2.16574623e-008
C2	-6.67182801e-013
C3	4.46519932e-016
C4	-3.71571535e-020
C5	0.00000000e+000
C6	0.00000000e+000
C7	0.00000000e+000
C8	0.00000000e+000
C9	0.00000000e+000

## Asphere of lens L817

K	0.0000
C1	2.15121397e-008
C2	-1.65301726e-011
C3	-5.03883747e-015
C4	1.03441815e-017
C5	-6.29122773e-021
C6	1.44097714e-024
C7	0.00000000e+000
C8	0.00000000e+000
C9	0.00000000e+000

## Patent Claims:

1. Optical element (1, 201, L627-L630, L815-L817) of a fluoride crystal, in particular for a projection objective of a microlithography projection exposure apparatus, wherein the optical element has an element axis (EA), characterized in that the element axis is oriented approximately perpendicular to the crystallographic (100)-planes or to the crystallographic (010)-planes or to the crystallographic (001)-planes of the fluoride crystal.
2. Optical element (1, 201, L627-L630, L815-L817) according to claim 1, wherein the optical element is a rotationally symmetric lens with a symmetry axis and the symmetry axis coincides with the element axis of the optical element.
3. Optical element (1, 201, L627-L630, L815-L817) according to one of the claims 1 or 2, wherein the fluoride crystal is a calcium fluoride crystal, a strontium fluoride crystal or a barium fluoride crystal.
4. Projection objective (611, 711, 85) for a microlithography projection exposure apparatus with a plurality of optical elements (L601-L630, L801-L817), wherein at least one special optical element (201, L627-L630, L815-L817) is an optical element according to one of the claims 1 to 3.
5. Projection objective (611, 711, 85) according to claim 4, with an optical axis (OA), wherein the element axis of the special optical element coincides with the optical axis of the projection objective.
6. Projection objective according to claim 4 or 5, wherein the projection objective has an image-side numerical

aperture NA and the image-side numerical aperture NA is larger than 0.75, in particular larger than 0.85.

7. Projection objective according to one of the claims 4 to 6, wherein light rays run inside the projection objective from an object plane (O) to an image plane (O') and at least one light ray (609) has inside the special optical element a ray angle relative to the element axis that is larger than 25°, in particular larger than 30°.
8. Projection objective according to one of the claims 4 to 7, wherein light rays run inside the projection objective from an object plane (O) to an image plane (O') and all light rays inside the special optical element have ray angles of maximally 45° relative to the element axis, in particular maximally  $\arcsin\left(\frac{NA}{n_{FK}}\right)$ , wherein NA stands for the image-side numerical aperture and  $n_{FK}$  stands for the refractive index of the fluoride crystal.
9. Projection objective according to one of the claims 4 to 8, with an aperture stop plane, wherein the aperture stop plane has an aperture stop diameter and the special optical element has an element diameter, with said element diameter being smaller than 85%, in particular smaller than 80%, of the aperture stop diameter.
10. Projection objective according to one of the claims 4 to 9, wherein the special optical element (L630, L817) is the optical element nearest to the image plane.
11. Projection objective according to one of the claims 4 to 10, wherein the projection objective includes at least a

first special optical element (L629, L816) and a second special optical element (L630, L817), and the first special optical element is arranged relative to the second special optical element with a rotational angle about the optical axis in order to minimize the influence of birefringence.

12. Projection objective according to claim 11, wherein the rotational angle between the first special optical element and the second special optical element is approximately 45°.
13. Projection objective according to one of the claims 11 and 12, wherein the first special optical element and the second special optical element are arranged adjacent to each other.
13. Projection objective according to one of the claims 4 to 13, wherein the light rays have wavelengths shorter than 200 nm.
15. Projection objective according to one of the claims 4 to 14, wherein the light rays have wavelengths shorter than 160 nm.
16. Projection objective according to one of the claims 4 to 15, wherein the projection objective (611) is a refractive objective with lenses.
17. Projection objective according to one of the claims 4 to 15, wherein the projection objective is a catadioptric objective with lenses and at least one concave mirror (Sp2).

18. Projection objective according to one of the claims 4 to 17, wherein all refractive optical elements are of calcium fluoride.
19. Projection objective for a microlithography projection exposure apparatus with an optical axis, which comprises a plurality of optical elements of a fluoride crystal, wherein the optical elements have element axes arranged so that they are centered on the optical axis, and wherein the optical elements, dependent on their crystallographic structure, have azimuth-angle ranges of increased birefringence, characterized in that at least two optical elements are arranged with a rotation relative to each other about the optical axis in order to minimize the influence of birefringence.
20. Microlithography projection exposure apparatus (81), comprising
  - an illumination system (83),
  - a projection objective (85) according to one of the claims 1 to 19, which projects a structure-carrying mask (89) onto a light-sensitive substrate (815).
21. Method for the manufacture of semiconductor components by means of a microlithography projection exposure apparatus (81) according to claim 20.

---

Attached hereto: 8 page(s) of drawings

---

**Summary:****Optical Element, Projection Objective and Microlithography****Projection exposure apparatus with Fluoride Crystal Lenses**

(Fig. 1)

Optical element (1) of a fluoride crystal, in particular for a projection objective of a microlithography projection exposure apparatus, wherein the optical element has an element axis (EA) that is oriented approximately perpendicular to the crystallographic (100)-planes or to the crystallographic (010)-planes or to the crystallographic (001)-planes of the fluoride crystal. Optical elements of this kind find application in projection objectives for a microlithography projection exposure apparatus. In order to further reduce the undesirable influence of the birefringence, the optical elements of fluoride crystal are arranged with a rotation relative to each other about the optical axis.

**DR. WALTER E. KUPPER**

65 Barnsdale Road  
Madison, NJ 07940

Telephone: 973 301-1989 Fax: 973 822-9096 E-mail: wekupper@att.net

June 29, 2005

TO WHOM IT MAY CONCERN:

**TRANSLATOR'S CERTIFICATE**

The undersigned hereby certifies that he is bilingually proficient in German and English, that he has personally prepared the attached translation

**"Optical Element, Projection Objective and Microlithography Projection Exposure System with Fluoride Crystal Lenses"**

of the published German Patent Application

**"Offenlegungsschrift DE 101 25 487 A1,  
Optisches Element, Projektionsobjektiv und Mikrolithographie-  
Projektionsbelichtungsanlage mit Fluoridkristall-Linsen"**

and that the translation is accurate.



Walter Kupper

Optical Element, Projection Objective and Microlithography  
Projection Exposure System with Fluoride Crystal Lenses

Description

[0001] The invention relates to a projection objective in accordance with the introductory part of claim 1.

[0002] Projection objectives of this kind are known from U.S. Patent 6,201,634 which discloses that, ideally, in the manufacture of fluoride crystal lenses, the lens axes are aligned perpendicularly to the crystallographic {111}-planes of the fluoride crystals in order to minimize the stress-related birefringence. The implied assumption in U.S. Patent 6,201,634 is that fluoride crystals have no intrinsic birefringence.

[0003] However, as is known from the Internet publication "Preliminary Determination of an Intrinsic Birefringence in CaF<sub>2</sub> by John H. Burnett, Eric L. Shirley, and Zachary H. Levine, NIST, Gaithersburg, MD 20899, USA (posted May 7, 2001), calcium fluoride single crystals also exhibit birefringence that is not stress-induced, i.e., intrinsic birefringence. The measurements presented in that reference demonstrate that with a light ray propagation in the crystallographic <110>-direction, the birefringence in calcium fluoride amounts to  $(6.5 \pm 0.4)$  nm/cm at a wavelength of  $\lambda=156.1$  nm,  $(3.6 \pm 0.2)$  nm/cm at a wavelength of  $\lambda=193.09$  nm, and  $(1.2 \pm 0.1)$  nm/cm at a wavelength of  $\lambda=253.65$  nm. However, with a light ray propagation in the crystallographic <100>-direction and in the crystallographic <111>-direction, no intrinsic birefringence occurs in calcium fluoride, as is also predicted by theory. Thus, the intrinsic birefringence

is strongly direction-dependent and becomes noticeably more pronounced as the wavelength decreases.

[0004] Because of the symmetries of cubic crystals, any statements made hereinafter in regard to light propagating in the crystallographic  $\langle 110 \rangle$  direction will always be applicable likewise to light propagating in the crystallographic  $\langle 101 \rangle$ -,  $\langle 10\bar{1} \rangle$ -,  $\langle \bar{1}01 \rangle$ -,  $\langle \bar{1}0\bar{1} \rangle$ -,  $\langle 011 \rangle$ -,  $\langle 0\bar{1}1 \rangle$ -,  $\langle 01\bar{1} \rangle$ -,  $\langle 0\bar{1}\bar{1} \rangle$ -,  $\langle \bar{1}10 \rangle$ -,  $\langle \bar{1}1\bar{0} \rangle$ -, and  $\langle \bar{1}\bar{1}0 \rangle$ -directions. The same applies also to statements relating to light propagating in the crystallographic  $\langle 100 \rangle$ -,  $\langle 010 \rangle$ -, and  $\langle 001 \rangle$ -directions, and in the directions where the index "1" has a negative sign, i.e.,  $\bar{1}$ . The crystallographic direction in all cases indicates the direction of the normal vector of the respective crystallographic plane. As an example, the crystallographic direction  $\langle 100 \rangle$  indicates the direction of the normal vector of the crystallographic plane  $\{100\}$ . Statements relating to crystallographic directions that are equivalent based on the crystallographic symmetry and which are obtained as a rule by merely permutating the digits 0,  $\bar{1}$  and 1 will therefore not be explicitly mentioned, but should be considered as implied in all cases where statements are made relative to one of these crystallographic directions or the respective crystallographic planes.

[0005] Projection objectives and microlithography projection exposure systems are known, e.g., from the patent application PCT/EP00/13184 of the present applicant and the references that are cited in that application. The embodiments presented in that application illustrate suitable purely refractive and catadioptric projection objectives with numerical aperture values of 0.8 and 0.9 at an operating wavelength of 193 nm as well as 157 nm.

[0006] The concept of rotating lens elements in order to compensate birefringence effects is also described in the present applicant's patent application "Microlithography Projection Exposure System, Optical System and Manufacturing Method" identified by applicant's file reference 01055P, with a filing date of May 15, 2001. The content of that application is hereby incorporated by reference in the present application.

[0007] The present invention has the object to propose a microlithography projection exposure system, wherein the influence of intrinsic birefringence is minimized.

[0008] The object just described is solved by a projection objective according to claim 1, 17, 26 and 49, a microlithography projection exposure system according to claim 35, a method for the manufacture of semiconductor components according to claim 36, and a method of reducing birefringence according to claim 37, 38 and 39.

[0009] Advantageous embodiments of the invention are presented in the features of the dependent claims.

[0010] As a means for reducing the influence of intrinsic birefringence, claim 1 proposes to orient the lens axes of lenses made of a fluoride crystal so that the lens axes coincide with the crystallographic <100>-direction within a maximum deviation 5°. In this arrangement, it is not necessary for all of the fluoride crystal lenses of the projection objective to have the aforementioned orientation. Those lenses in which the lens axes are oriented perpendicular to the crystallographic {100}-plane will hereinafter also be referred to as (100)-lenses. Orienting the lens axis in the crystallographic <100>-direction has the advantage that the

undesirable influence of the intrinsic birefringence which occurs with a light propagation in the crystallographic  $<110>$ -direction becomes noticeable at aperture angles of the light rays that are larger than with an orientation of the lens axis in the crystallographic  $<111>$ -direction. The term aperture angle in the present context refers to the angle between a light ray and the optical axis outside of a lens and between a light ray and the lens axis inside a lens. Only as the aperture angle falls into the angular range between the crystallographic  $<100>$ - and  $<110>$ - directions does the influence of birefringence manifest itself in the respective light rays. The angle between the crystallographic  $<110>$ - and  $<100>$ -directions amounts to about  $45^\circ$ . If the element axis were, on the other hand, oriented in the crystallographic  $<111>$ -direction, the undesirable influence of intrinsic birefringence would be noticeable already at smaller aperture angles, as the angle between the crystallographic  $<110>$ - and  $<111>$ -directions is only  $35^\circ$ .

[0011] If the angle-dependence of the birefringence is caused, e.g., by the manufacturing process of the fluoride crystal or by mechanical stress applied to the lens, the conceptual solutions disclosed herein can, of course, likewise be used to lessen the undesirable influence of the birefringence.

[0012] The lens axis is constituted, e.g., by a symmetry axis of a rotationally symmetrical lens. If the lens has no symmetry axis, the lens axis can be defined by the center of an incident bundle of light rays or by a straight line in relation to which the ray angles of all light rays inside the lens are minimal. The lenses can be, e.g., refractive or diffractive lenses as well as corrective plates with free-form corrective surfaces. Planar-parallel plates, too, are

considered as lenses, if they are arranged in the light path of the projection objective. The lens axis of a planar-parallel plate is perpendicular to the planes of the lens surfaces.

[0013] With preference, however, the lenses are rotationally symmetric lenses.

[0014] Projection objectives have an optical axis that runs from the object plane to the image plane. With preference, the (100)-lenses are arranged in centered alignment relative to this optical axis, so that the lens axes also coincide with the optical axis.

[0015] In projection objectives with large numerical aperture values on the image side, in particular larger than 0.7, aperture angles larger than 25° and in particular larger than 30° will occur inside the (100)-lenses. It is especially at these large aperture angles that the inventive concept of orienting the lens axes in the crystallographic <100>-direction proves to be useful. If the lens axes were oriented in the crystallographic <111>-direction, the undesirable influence of the birefringence, which in this case has its maximum at aperture angles of 35°, would manifest itself more noticeably at aperture angles larger than 25° and in particular larger than 30°.

[0016] Since on the other hand, the undesirable influence of intrinsic birefringence can have a maximum at an aperture angle of 45°, it is advantageous to design the projection objective in such a way that all aperture angles of the light rays are smaller than 45°, in particular smaller than or equal to  $\arcsin\left(\frac{NA}{n_{FK}}\right)$ , wherein NA stands for the image-side numerical

aperture and  $n_{FK}$  stands for the refractive index of the fluoride crystal. The expression  $\arcsin\left(\frac{NA}{n_{FK}}\right)$  represents the aperture angle that corresponds to the image-side numerical aperture inside a fluoride crystal lens if no refraction takes place at the interface. This is achieved by a design in which the lenses that are arranged near the image plane, have light-collecting lens surfaces, planar lens surfaces or at most slightly dispersing lens surfaces, if in the direction of the light path the light-dispersing lens surface is followed by a lens surface of a stronger light-collecting power.

[0017] Large aperture angles occur primarily in lenses near field planes, in particular near the image plane. The (100)-lenses should therefore be used with preference in the vicinity of the field planes. The range where the (100)-lenses should be used can be determined by way of the ratio between the lens diameter and the diameter of the aperture stop. Thus, the lens diameter of the (100)-lenses is preferably at most 85%, in particular at most 80% of the aperture stop diameter.

[0018] In projection objectives, the largest aperture angles occur as a rule in the lens closest to the image plane. It is therefore preferred to align the lens axis of this lens in the crystallographic <100>-direction.

[0019] The intrinsic birefringence under discussion here is dependent not only on the aperture angle of a light ray, but also on the azimuth angle of the light ray. The azimuth angle as it pertains to the present discussion is determined as follows: If the lens axis is oriented, e.g., in the crystallographic <100>-direction, the light ray is projected into the crystallographic {100}-plane. The directional

vectors of the crystallographic  $\langle 101 \rangle$ -,  $\langle 110 \rangle$ -,  $\langle 10\bar{1} \rangle$ - and  $\langle 1\bar{1}0 \rangle$ -directions of maximum intrinsic birefringence are likewise projected into the crystallographic  $\{100\}$ -plane. The azimuth angle is now determined between the projected light ray and the projected directional vector of the crystallographic  $\langle 110 \rangle$ -direction. Of course, analogous definitions apply also for the cases in which the lens axis is oriented in the crystallographic  $\langle 010 \rangle$ - or  $\langle 001 \rangle$ -direction. The intrinsic birefringence of an individual lens has a fourfold symmetry if the lens axis is oriented in the crystallographic  $\langle 100 \rangle$ -direction. A maximum for the intrinsic birefringence occurs here at azimuth angles of  $0^\circ$ ,  $90^\circ$ ,  $180^\circ$  and  $270^\circ$ , while it nearly vanishes for angles of  $45^\circ$ ,  $135^\circ$ ,  $225^\circ$  and  $315^\circ$ . The angle-dependence of the intrinsic birefringence can be represented by the birefringence distribution  $\Delta n(\theta, \alpha)$  which occurs in a bundle of light rays originating from an object point in the object plane. Each ray in the bundle is characterized by its aperture angle  $\theta$  relative to the optical axis and by its azimuth angle  $\alpha$  relative to a reference direction in the object plane. The birefringence distribution  $\Delta n(\theta, \alpha)$  is determined in the image plane, after the bundle of light rays has been propagated through the entire projection objective. For every ray in the bundle, the respective optical path differences in each lens between two mutually orthogonal states of linear polarization are determined and added up. The sum of the optical path differences is subsequently divided by the sum of the path lengths of the light rays inside the lenses for each of the rays. As a result of this calculation, one obtains the birefringence distribution. The birefringence distribution can also be stated for the contribution of individual lenses by evaluating the optical path differences for the individual lenses. If several  $(100)$ -lenses are used in a projection objective, it is advantageous if the  $(100)$ -lenses are arranged

with a rotation relative to each other about the optical axis. Through this measure, one can prevent the undesirable influence of the birefringence from adding up cumulatively, which it would if the (100)-lenses were installed with uniform orientation. With the rotated arrangement of the (100)-lenses, the magnitude of the birefringence distribution  $\Delta n(\theta, \alpha)$  can be significantly reduced. Thus, the maximum amount of the birefringence can be lowered by as much as 20% and in particular cases by as much as 25% in comparison to (100)-lenses that are installed with uniform orientation.

[0020] By installing the (100)-lenses in rotated positions, the dependence on the azimuth angle  $\alpha$  in particular can be noticeably reduced, so that a birefringence distribution is obtained that is close to rotational symmetry.

[0021] The orientation of the (100)-lenses relative to each other is defined by way of the angles of rotation  $\beta$  which represent the angle between two reference directions. The reference direction of a (100)-lens in this context is perpendicular to the lens axis and points in a principal crystallographic direction. The principal crystallographic directions for the (100)-lenses are the  $<010>$ -,  $<001>$ -,  $<0\bar{1}0>$ -, or  $<00\bar{1}>$ -direction. For the purpose of reducing the birefringence, it is advantageous to consider a group of (100)-lenses, wherein the (100)-lenses are rotated relative to each other in such a manner that for each two of the (100)-lenses of a group, the angle of rotation is represented by the following expression:

$$\beta = \frac{90^\circ}{n} + m \cdot 90^\circ \pm 5^\circ, \text{ wherein } n \text{ represents the number of the}$$

(100)-lenses of a group and  $m$  represents a positive integer. If the group has two (100)-lenses, the angle of rotation between these two lenses is ideally  $45^\circ$ ,  $135^\circ$ ,  $225^\circ$  ... Since

the (100)-lenses have a fourfold azimuthal symmetry, the correction of the birefringence is indifferent in regard to rotations of the (100)-lenses by  $90^\circ$ . This degree of freedom as well as the tolerance of  $\pm 5^\circ$  can be used for the conventional adjustment of the projection objective, e.g., for the purpose of correcting irregularities that are not rotationally symmetric.

[0022] The lenses of a group are determined, e.g., according to the criterion that an outermost aperture ray of a bundle of rays has similar aperture angles inside these lenses. It is of advantage if the aperture angles of the outermost aperture ray are larger than  $15^\circ$  in these lenses, in particular if they are larger than  $20^\circ$ . The term "outermost aperture ray" refers to a ray that originates from an object point and whose ray height in the aperture stop plane equals the radius of the aperture stop, so that in the image plane this ray has an angle corresponding to the image-side numerical aperture. The reason why the outermost aperture rays are used to define the groups is that they normally have the largest aperture angles inside the lenses and are thus affected the most by the undesirable effects of the birefringence. By determining the optical path difference for two mutually orthogonal states of linear polarization for the outermost aperture rays, one can therefore arrive at conclusions about the maximum irregularity of a wave front due to birefringence.

[0023] It is further advantageous if the outermost aperture ray in each of these lenses has a ray path of the same length. This measure has the result of a good compensation of the contributions to the birefringence that are caused by the individual lenses of the group.

[0024] It is advantageous for an optimal compensation of the lenses of a group, if the outermost aperture ray is subjected in each of these lenses to an optical path difference of similar magnitude between two mutually orthogonal states of linear polarization. The state of polarization of the ray is defined by the electromagnetic field components.

[0025] In the case of two adjacent planar-parallel lenses, the rotation of the lenses has the result of a birefringence distribution that is close to rotationally symmetric. In lenses with curved surfaces, it is likewise possible through a judicious selection of the lenses or through an appropriate choice of the thicknesses and radii of the lenses to achieve an approximately rotation-symmetric birefringence distribution through a rotated arrangement of two (100)-lenses.

[0026] The concept of rotating the individual (100)-lenses relative to each other is particularly effective if the (100)-lenses are arranged adjacent to each other. It is particularly advantageous to split a lens into two halves and to wring the lens halves together in rotated positions relative to each other. As a further advantageous embodiment, it is proposed to manufacture a lens from a material block that was produced by wringing together two (111)-plates with a rotation of 60° relative to each other and two (100)-plates with a rotation of 45° relative to each other.

[0027] In a projection objective with a multitude of lenses it is advantageous to form a plurality of groups of (100)-lenses. In this arrangement, the (100)-lenses of a group are rotated in such a manner that the birefringence distribution of the group has a profile that is nearly independent of the azimuth angle.

[0028] The concept of reducing the birefringence effect by rotating the (100)-lenses against each other can also be used to advantage in fluoride crystal lenses whose lens axes are perpendicular to the crystallographic {111}- or equivalent planes within a tolerance of 5°, e.g., the crystallographic { $\bar{1}11$ }- or { $\bar{1}\bar{1}\bar{1}$ }-planes. These lenses will hereinafter be referred to as (111)-lenses.

[0029] The intrinsic birefringence of an individual lens has a threefold azimuthal symmetry if the lens axis is oriented in the crystallographic <111>-direction. A maximum of the intrinsic birefringence is found at azimuth angles of 0°, 120°, and 240°, while the effect vanishes at angles of 60°, 180°, and 300°. What has been said above about the rotation of the (100)-lenses against each other applies analogously to the rotation of the (111)-lenses, except for the way in which the ideal rotation angles  $\gamma$  are defined if the birefringence is to be lowered with a group of (111)-lenses. The angle of rotation between each two of the (111)-lenses of this group is defined by the following expression:

$$\beta = \frac{120^\circ}{k} + l \cdot 120^\circ \pm 8^\circ, \text{ wherein } k \text{ represents the number of}$$

(111)-lenses of a group and  $l$  represents a positive integer.  
If the group has two (111)-lenses, the angle of rotation  
between the two lenses will ideally be 60°, 180°, 300°, ...

[0030] While rotating the (100)-lenses against each other or the (111)-lenses against each other has now made the distribution function of the birefringence nearly independent of the azimuth angle, the absolute value of the birefringence distribution can be noticeably reduced by an arrangement where the projection objective has a group of (100)-lenses as well as a group of (111)-lenses. This is possible, because the birefringence has not only an absolute value, but also a

direction. If one considers the (100)-birefringence that is caused by a group of (100)-lenses in which the rotation angle is optimized and the (111)-birefringence that is caused by a group of (111)-lenses in which the rotation angle is optimized, one will find that the direction of the (100)-birefringence is rotated relative to the direction of the (111)-birefringence by an angle close to 90°. If the absolute values of the (100)-birefringence are of similar magnitude as the absolute values of the (111)-birefringence, the two birefringence distributions will compensate each other almost completely. By using a group of (100)-lenses in combination with a group of (111)-lenses, it is therefore possible to reduce the maximum value of the birefringence to such an extent that it will amount to only 20% of the maximum birefringence value that would be obtained by using either only (111)-lenses or only (100)-lenses in particular for lenses that have a large aperture angle.

[0031] The preferred material to use for the lenses in projection objectives is calcium fluoride, because when used together with quartz at an operating wavelength of 193 nm, calcium fluoride is particularly well suited for the color correction, and with an operating wavelength of 157 nm, it still has a sufficient transmissivity. However, the foregoing statements are likewise applicable to the fluoride crystals strontium fluoride and barium fluoride, as they are crystals of the same type of cubic crystal structure.

[0032] The undesirable influence of intrinsic birefringence becomes particularly noticeable if the light rays inside the (100)-lenses or (111)-lenses have large aperture angles. This is the case in projection objectives with an image-side numerical aperture larger than 0.7, in particular larger than 0.8.

[0033] The intrinsic birefringence becomes noticeably stronger with decreasing working wavelength. Thus, the intrinsic birefringence at a wavelength of 193 nm is more than twice as strong, and at a wavelength of 157 nm it is more than five times as strong as it is at a wavelength of 248 nm. The invention can therefore be used to particular advantage if the light rays have wavelengths smaller than 200 nm, in particular smaller than 160 nm.

[0034] The projection objective in the present context can be a purely refractive objective that consists of a multitude of lenses arranged with rotational symmetry about the optical axis.

[0035] But the imaging performance is also improved in projection objectives of the catadioptric type of objectives, if the lenses with large aperture angles of the light rays are oriented so that the symmetry axes of the lenses point in the crystallographic <100>-direction and/or so that, in the case of groups of (100)- or (111)-lenses of fluoride crystal, the lenses are arranged with a rotation relative to each other.

[0036] Projection objectives of this kind can be used advantageously in microlithography projection exposure systems which include a light source followed by an illumination system, a mask-positioning system, a structure-carrying mask, a projection objective, an object-positioning system, and a light-sensitive substrate.

[0037] This microlithography projection exposure system can be used to produce micro-structured semiconductor elements.

[0038] The invention also provides methods that are suitable to reduce the birefringence to a noticeable extent. The method is used in a projection objective which includes at least two fluoride crystal lenses in <100>-orientation or <111>-orientation. Also known is the orientation of the reference directions in these lenses, which are defined by the principal crystallographic directions perpendicular to the crystallographic <100>- or <111>-directions. The method makes use of the inventive observation that the maximum values of the birefringence distribution can be reduced significantly by rotating the fluoride crystal lenses about the optical axis. Using suitable simulation methods, a bundle of light rays originating from an object point is propagated through a projection objective, and the resulting birefringence distribution in the image plane is calculated on the basis of the known optical properties of the fluoride crystal lenses. In an optimizing step, the fluoride crystal lenses are rotated until the birefringence values are within tolerance. It is possible to take further boundary constraints into account in the optimizing step, such as for example the compensation of rotationally non-symmetric lens errors that are compensated by rotating the lenses, whereby the overall imaging performance of the objective is improved. This optimizing step can reduce the maximum birefringence value by up to 30%, in particular cases up to 50%, in comparison to a projection objective in which the fluoride crystal lenses are arranged with uniform orientation. The optimizing routine can also contain an intermediate step in which groups are formed among the fluoride crystal lenses, where the lenses in each group produce similar optical path differences between two mutually orthogonal states of linear polarization in an outermost aperture ray. In the subsequent optimizing step, the lenses are rotated only within the groups in order to reduce the birefringence.

[0039] The method of the foregoing description can be applied to particular advantage, if one or more groups of (111)-lenses are used in addition to the one or more groups of (100)-lenses in the projection objective. In this case, the optimizing step provides that the (100)-lenses are first rotated so that the (100)-birefringence caused by them is reduced, and that subsequently the (111)-lenses are rotated so that the (111)-birefringence caused by them is reduced. The allocation of the fluoride crystal lenses to lenses with (100)-orientation and (111)-orientation, respectively, has to be made in such a manner in the optimization that the resultant (100)-birefringence and the resultant (111)-birefringence compensate each other to a large extent.

[0040] The invention will be explained in more detail with reference to the drawings.

[0041] Figure 1 illustrates a cross-section of a fluoride crystal block perpendicular to the crystallographic {100}-planes together with a lens of a projection objective in a schematic representation;

[0042] Figures 2A-B show, respectively, a planar-parallel lens with (100)-orientation and a planar-parallel lens with (111)-orientation in a schematic three-dimensional representation;

[0043] Figure 3 shows a coordinate system for the definition of the aperture angle and the azimuth angle;

[0044] Figures 4A-D represent the birefringence distributions of (100)-lenses in different representations;

[0045] Figures 5A-D represent the birefringence distributions of (111)-lenses in different representations;

[0046] Figure 6 represents the lens section of a refractive projection objective;

[0047] Figure 7 represents the lens section of a catadioptric projection objective; and

[0048] Figure 8 illustrates a microlithography projection exposure system in a schematic representation.

[0049] Figure 1 schematically illustrates a section through a fluoride crystal block 3. The section is selected so that the crystallographic (100)-planes 5 can be seen as individual lines, i.e., the crystallographic {100}-planes 5 are oriented perpendicular to the plane of the paper. The fluoride crystal block 3 serves as raw material for the (100)-lens 1. In the illustrated example, the (100)-lens 1 is a bi-convex lens with the lens axis EA which is at the same time the symmetry axis of the lens. The lens 1 is now formed out of the fluoride crystal block in such a manner that the element axis EA stands perpendicular to the crystallographic {100}-planes.

[0050] Figure 2A visualizes in a three-dimensional representation how the intrinsic birefringence is related to the crystallographic directions in the case where the lens axis EA points in the crystallographic <100>-direction. The lens shown in Figure 2A is a circular planar-parallel plate 201 of calcium fluoride. The lens axis EA points in the crystallographic <100>-direction. Besides the crystallographic <100>-direction, the <101>-, <1 $\bar{1}$ 0>-, <10 $\bar{1}$ >-, and <110>-directions are likewise represented as arrows. The intrinsic birefringence is represented schematically by four

lobes 203, whose surface areas represent the amount of the intrinsic birefringence for the respective ray direction of a light ray. The maxima for the intrinsic birefringence occur, respectively, in the crystallographic  $<101>-$ ,  $<1\bar{1}0>-$ ,  $<10\bar{1}>-$ , and  $<110>-$ -directions, i.e., for light rays with an aperture angle of  $45^\circ$  and an azimuth angle of  $0^\circ$ ,  $90^\circ$ ,  $180^\circ$  and  $270^\circ$ . The minima of the intrinsic birefringence are associated with azimuth angles of  $45^\circ$ ,  $135^\circ$ ,  $225^\circ$  and  $315^\circ$ . The intrinsic birefringence vanishes at an aperture angle of  $0^\circ$ .

[0051] Figure 2B visualizes in a three-dimensional representation how the intrinsic birefringence is related to the crystallographic directions in the case where the lens axis EA points in the crystallographic  $<111>$ -direction. The lens shown in Figure 2B is a circular planar-parallel plate 205 of calcium fluoride. The lens axis EA points in the crystallographic  $<111>$ -direction. Besides the crystallographic  $<111>$ -direction, the  $<011>-$ ,  $<101>-$ , and  $<110>-$ -directions are likewise represented as arrows. The intrinsic birefringence is represented schematically by three lobes 207, whose surface areas represent the amount of the intrinsic birefringence for the respective ray direction of a light ray. The maxima for the intrinsic birefringence occur, respectively, in the crystallographic  $<011>-$ ,  $<101>-$ , and  $<110>-$ -directions, i.e., for light rays with an aperture angle of  $35^\circ$  and an azimuth angle of  $0^\circ$ ,  $120^\circ$ , and  $240^\circ$ . The minima of the intrinsic birefringence are associated with azimuth angles of  $60^\circ$ ,  $180^\circ$ , and  $300^\circ$ . The intrinsic birefringence vanishes at an aperture angle of  $0^\circ$ .

[0052] The definition of aperture angle  $\theta$  and azimuth angle  $\alpha$  is illustrated in Figure 3. In relation to the example of Figure 2, the z-axis indicates the crystallographic  $<100>-$

direction, and the x-axis represents the crystallographic (010)-direction.

[0053] As disclosed in the internet publication cited hereinabove, in measurements with a light ray propagation in the crystallographic <110>-direction, a birefringence of  $(6.5 \pm 0.4)$  nm/cm was found at a wavelength of  $\lambda = 156.1$  nm in calcium fluoride. Taking this measured value as a normative factor, it is possible to theoretically calculate the birefringence distribution  $\Delta n(\theta, \alpha)$  dependent on the crystal structure. The computations are based on the formalisms known from the field of crystal optics for the calculation of the index ellipsoids dependent on the direction of the light ray. The theoretical basis can be found, e.g., in "Lexikon der Optik", Spektrum Akademischer Verlag Heidelberg Berlin 1999 under the term "Kristalloptik".

[0054] Represented in Figure 4A is the intrinsic birefringence as a function of the aperture angle  $\theta$  for the azimuth angle  $\alpha = 0^\circ$  for a (100)-lens. The value of 6.5 nm/cm for the intrinsic birefringence at an aperture angle of  $\theta = 45^\circ$  represents the measured value. The curve profile was determined according to the formulae that are known from the theory of crystal optics.

[0055] Figure 4B illustrates the intrinsic birefringence as a function of the azimuth angle  $\alpha$  for the aperture angle  $\theta = 45^\circ$  for a (100)-lens. The fourfold symmetry is evident.

[0056] Figure 4C illustrates the birefringence distribution  $\Delta n(\theta, \alpha)$  for individual ray directions in the  $(\theta, \alpha)$ -continuum for a (100)-lens. Each line represents the amount and the direction for a ray direction that is defined by the aperture angle  $\theta$  and the azimuth angle  $\alpha$ . The length of the lines is

proportional to the amount of the birefringence or, more specifically, the length difference between the principal axes of the elliptical section, while the direction of the line indicates the orientation of the longer principal axis of the elliptical section.

[0057] The elliptical section is obtained by intersecting the index ellipsoid for the ray of the direction  $(\theta, \alpha)$  with a plane that is perpendicular to the ray direction and passes through the center point of the index ellipsoid. The directions as well as the lengths of the lines indicate the fourfold structure of the distribution. The length of the lines, and thus the amount of the birefringence, has its maxima at the azimuth angles of  $0^\circ$ ,  $90^\circ$ ,  $180^\circ$ , and  $270^\circ$ .

[0058] Figure 4D illustrates the birefringence distribution  $\Delta n(\theta, \alpha)$  that is obtained by arranging two adjacent planar-parallel (100)-lenses of equal thickness with a rotation of  $45^\circ$  relative to each other. As is evident, the resulting birefringence distribution  $\Delta n(\theta, \alpha)$  is independent of the azimuth angle  $\alpha$ . The longer principal axes of the elliptical sections run in the tangential direction. The resultant optical path differences between two mutually orthogonal states of polarization are obtained by combining the birefringence values with the path length inside the material. Rotationally symmetric birefringence distributions are likewise obtained by arranging  $n$  planar-parallel (100)-lenses of equal thickness in such a manner that the angle of rotation between two lenses conforms to the equation:

$$\beta = \frac{90^\circ}{n} + m \cdot 90^\circ \pm 5^\circ$$

wherein  $n$  stands for the number of planar-parallel (100)-lenses and  $m$  represents an integer number. In comparison to an arrangement of uniformly oriented lenses, the maximum value

of the birefringence for the aperture angle  $\theta = 30^\circ$  can be reduced by 30%. A rotationally symmetric birefringence distribution is also obtained for arbitrary types of lenses if all rays of a bundle have equal aperture angles and cover equal path lengths inside the lenses. Therefore, the lenses should be combined into groups where the rays conform as much as possible to the foregoing condition.

[0059] Figure 5A represents the intrinsic birefringence as a function of the aperture angle  $\theta$  for the azimuth angle  $\alpha = 0^\circ$  in a (111)-lens. The value of 6.5 nm/cm for the intrinsic birefringence at an aperture angle of  $\theta = 35^\circ$  represents the measured value. The curve profile was determined according to the formulae that are known from crystal optics.

[0060] Figure 5B illustrates the intrinsic birefringence as a function of the azimuth angle  $\alpha$  for the aperture angle  $\theta = 35^\circ$  for a (111)-lens. The threefold symmetry is evident.

[0061] Figure 5C illustrates the birefringence distribution  $\Delta n(\theta, \alpha)$  for individual ray directions in the  $(\theta, \alpha)$ -continuum for a (111)-lens in an analogous representation as was used already in Figure 4C. The directions as well as the lengths of the lines indicate the threefold structure of the distribution. The length of the lines, and thus the amount of the birefringence, has its maxima at the azimuth angles of  $0^\circ$ ,  $120^\circ$ , and  $240^\circ$ . In contrast to a (100)-lens, the orientation of the birefringence rotates by  $90^\circ$  if a ray passes through the lens with an azimuth angle of  $180^\circ$  instead of with an azimuth angle of  $0^\circ$ . Thus, the birefringence can be compensated, e.g., by two (111)-lenses of equal orientation, if the ray angles of a ray bundle change signs between the two lenses.

[0062] Figure 5D illustrates the birefringence distribution  $\Delta n(\theta, \alpha)$  that is obtained by arranging two adjacent planar-parallel (111)-lenses of equal thickness with a rotation of  $60^\circ$  relative to each other. As is evident, the resulting birefringence distribution  $\Delta n(\theta, \alpha)$  is independent of the azimuth angle  $\alpha$ . However, in contrast to Figure 4C, the longer principal axes of the elliptical sections run in the radial direction. The resultant optical path differences between two mutually orthogonal states of polarization are obtained by combining the birefringence values with the path length inside the material. Rotationally symmetric birefringence distributions are likewise obtained by arranging  $n$  planar-parallel (111)-lenses of equal thickness in such a manner that the angle of rotation between two lenses conforms to the equation:

$$\gamma = \frac{120^\circ}{k} + l \cdot 120^\circ \pm 5^\circ$$

wherein  $k$  stands for the number of planar-parallel (111)-lenses and  $l$  represents an integer number. In comparison to an arrangement of uniformly oriented lenses, the value of the birefringence for the aperture angle  $\theta = 30^\circ$  can be reduced by 68%. A rotationally symmetric birefringence distribution is also obtained for arbitrary types of lenses if all rays of a bundle in the lenses have equal aperture angles and cover equal path lengths inside the lenses. Therefore, the lenses should be combined into groups where the rays conform as much as possible to the foregoing condition.

[0063] Based on the foregoing discussion, if one combines groups of (100)-lenses and groups of (111)-lenses within a projection objective, it is possible to compensate the birefringence contributions of these lenses to a large extent. To accomplish this, it is first necessary that within the groups a birefringence distribution close to rotational

symmetry is obtained by rotating the lenses, and then that by combining a group of (100)-lenses with a group of (111)-lenses their respective birefringence distributions will compensate each other. To achieve this result, one makes use of the fact that the orientations of the longer principal axes of the elliptical sections for the birefringence distribution of a group of rotated (100)-lenses are perpendicular to the orientations of the longer principal axes of the elliptical sections for the birefringence distribution of a group of rotated (111)-lenses, as can be concluded from Figures 4D and 5D. In this respect, it is of critical importance that on the one hand the individual groups produce a birefringence distribution close to rotational symmetry and on the other hand the sum of the contributions of the groups of (100)-lenses closely matches the sum of the contributions of the groups of (111)-lenses.

[0064] Figure 6 represents the lens section of a refractive projection objective 611 for the wavelength of 157 nm. The optical data for this objective are listed in Table 1. This example is taken from the applicant's patent application PCT/EP00/13184 where it corresponds to Figure 7 and Table 6. For a detailed description of the function of the objective, see PCT/EP00/13184. All lenses of this objective consist of calcium fluoride crystal. The image-side numerical aperture of the objective is 0.9. The imaging performance of the objective is corrected so well that the deviation from a wave front of an ideal spherical wave is smaller than 1.8 thousandths of a wavelength at  $\lambda = 157$  nm. Especially with these high-performance objectives, it is necessary for the undesirable effects of intrinsic birefringence to be reduced to the farthest extent possible.

[0065] For the embodiment of Figure 6, a calculation was made of the aperture angles  $\theta$  and path lengths  $OP_L$  of the outermost aperture ray 609 for the individual lenses L601 to L630. The outermost aperture ray 609 originates from the object point with the coordinates  $x = 0$  mm and  $y = 0$  mm, and in the image plane has an angle relative to the optical axis that corresponds to the image-side numerical aperture. The reason why the outermost aperture ray 609 is selected is that it is associated with close to the maximum aperture angles inside the lenses.

Table 2

Lens	Aperture angle $\theta$ [°]	Ray path $OP_L$ [mm]	Optical path difference (111)-lens $\alpha_{AR}-\alpha_L=0^\circ$ [nm]	Optical path difference (111)-lens $\alpha_{AR}-\alpha_L=60^\circ$ [nm]	Optical path difference (100)-lens $\alpha_{AR}-\alpha_L=0^\circ$ [nm]	Optical path difference (100)-lens $\alpha_{AR}-\alpha_L=45^\circ$ [nm]
L601	8.1	15.1	2.9	-2.2	-0.8	-0.4
L602	8.7	8.2	1.7	-1.2	-0.5	-0.2
L603	7.8	9.5	1.7	-1.3	-0.4	-0.2
L604	10.7	7.2	1.9	-1.3	-0.6	-0.3
L605	9.4	6.5	1.5	-1.0	-0.4	-0.2
L606	10.3	8.5	2.1	-1.4	-0.7	-0.3
L607	21.8	12.7	6.6	-2.7	-3.9	-1.8
L608	25.4	22.2	12.8	-4.4	-8.7	-3.9
L609	16.3	36.1	14.3	-7.6	-6.8	-3.3
L610	12.2	15.2	4.5	-2.9	-1.7	-0.8
L611	2.3	26.6	1.4	-1.3	-0.1	-0.1
L612	2.3	32.2	1.6	-1.5	-0.1	-0.1
L613	-18.3	30.4	-6.6	13.5	-7.0	-3.3
L614	-18.7	22.0	-4.8	10.0	-5.3	-2.5
L615	-14.0	10.2	-2.0	3.5	-1.5	-0.7
L616	-1.3	29.8	-0.8	0.9	0.0	0.0
L617	26.4	31.6	18.6	-6.1	-13.0	-5.7
L618	33.5	14.3	9.3	-2.0	-7.9	-3.1
L619	26.5	7.5	4.4	-1.4	-3.1	-1.4
L620	19.3	6.4	3.0	-1.4	-1.6	-0.8
L621	6.7	8.0	1.3	-1.0	-0.3	-0.1
L622	-10.3	7.7	-1.3	1.9	-0.6	-0.3
L623	-11.9	9.6	-1.8	2.8	-1.0	-0.5
L624	0.3	17.8	0.1	-0.1	0.0	0.0
L625	6.0	16.3	2.3	-1.8	-0.5	-0.2
L626	-24.0	9.0	-1.9	5.0	-3.2	-1.5
L627	-35.6	8.0	-0.9	5.2	-4.7	-1.7
L628	-39.4	12.0	-1.0	7.6	-7.5	-2.5
L629	-35.3	27.3	-3.3	17.7	-15.7	-5.9
L630	-35.3	26.0	-3.1	16.9	-15.0	-5.6
Sum			64.5	42.3	112.9	47.4

[0066] In addition to the aperture angles  $\theta$  and the path lengths  $OP_L$  for the outermost aperture ray, Table 2 also lists the optical path differences between two mutually orthogonal states of linear polarization for different lens orientations. The optical path differences are shown for (111)-lenses as well as for (100)-lenses, where the differences between the azimuth angle  $\alpha_{AR}$  of the outermost aperture ray and the azimuth angle  $\alpha_L$  of the lens are  $0^\circ$  and  $60^\circ$  for a (111)-lens, and  $0^\circ$  and  $45^\circ$  for a (100)-lens.

[0067] As can be seen in Table 2, the aperture angles  $\theta$  for the lenses L608, L617, L618, L619, L627, L628, L629 and L630 are larger than  $25^\circ$ , and for the lenses L618, L627, L628, L629 and L630 even larger than  $30^\circ$ . Particularly affected by the large aperture angles are the lenses L627 to L630, which are closest to the image plane.

[0068] The projection objective was designed so that the maximum aperture angle of all light rays is smaller than  $45^\circ$ . The maximum aperture angle for the outermost aperture ray is  $39.4^\circ$  in the lens L628. It was helpful to use two thick planar lenses L629 and L630 immediately ahead of the image plane.

[0069] The diameter of the aperture stop located between the lenses L621 and L622 is 270 mm. The diameter of the lens L618 is 207 mm and the diameters of the lenses L627 to L630 are all smaller than 190 mm. Thus, the diameters of these lenses, which are associated with large aperture angles, are smaller than 80% of the aperture stop diameter.

[0070] As can be concluded from Table 2, it is advantageous to orient individual lenses with large aperture angles in the (100)-direction, as the birefringence values will overall be lower. The reason for this lies in the fact that in (100)-lenses the influence of the crystallographic <110>-direction begins to manifest itself only at larger angles than it does in (111)-lenses. As an example the optical path differences in the lenses L608, L609 and L617 are more than 30% smaller.

[0071] The example of the two planar-parallel lenses L629 and L630 provides a good way of demonstrating how the birefringence can be noticeably reduced by rotating lenses in relation to each other.

[0072] Both lenses have equal aperture angles of 35.3° for the outermost aperture ray and similar path lengths of 27.3 and 26.0 mm, respectively. If the two lenses were installed as (100)-lenses with equal orientation, there would be a resultant optical path difference of 30.7 nm. However, if the two (100)-lenses are rotated relative to each other by 45°, the optical path difference is reduced to 20.9 nm, i.e., by 32%. If the two lenses were installed as (111)-lenses with equal orientation, there would be a resultant optical path difference of 34.6 nm; but if the two (111)-lenses are rotated relative to each other by 60°, the optical path difference is reduced to 13.6 nm, i.e., by 61%.

[0073] A near-perfect compensation of the optical path differences for two mutually orthogonal states of linear polarization due to intrinsic birefringence in the lenses L629 and L630 can be achieved if the lens L629 is split up into the lenses L6291 and L6292, and the lens L630 is split up into the lenses L6301 and L6302, wherein the lens L6291 is a (100)-lens with a thickness of 9.15 mm, the lens 6292 is a (111)-lens

with a thickness of 13.11 mm, the lens L6301 is a (100)-lens with a thickness of 8.33 mm and the lens L6302 is a (111)-lens with a thickness of 12.9 mm. The lenses L6291 and L6301 are rotated against each other by 45°, while the lenses L6292 and L6302 are rotated by 60°. The resultant maximum optical path difference in this case amounts to 0.2 nm. The lenses L6291 and L6292, as well as the lenses L6301 and L6302, can be joined together with an optically seamless connection, e.g., by wringing. This concept is also applicable if the projection objective has only one crystal lens. In this case, the crystal lens is split into at least two lenses that are arranged with a rotation relative to each other. The joining can be accomplished by wringing. As another possibility, individual plates of the desired crystallographic orientation are joined through an optically seamless connection in a first step, and the lens is fabricated from the combined plates in a further process step.

[0074] Figure 7 represents the lens section of a catadioptric projection objective 711 for the wavelength of 157 nm. The optical data for this objective are listed in Table 3. This example is taken from the applicant's patent application PCT/EP00/13184 where it corresponds to Figure 9 and Table 8. For a detailed description of the function of the objective, see PCT/EP00/13184. All lenses of this objective consist of calcium fluoride crystal. The image-side numerical aperture of the objective is 0.8.

[0075] For the embodiment of Figure 7, a calculation was made of the aperture angles  $\theta$  and the ray paths  $OP_L$  of the upper outermost aperture ray 713 and the lower outermost aperture ray 715 for the individual lenses L801 to L817. The outermost aperture rays 713 and 715 in this example originate from the object point with the coordinates  $x = 0$  mm and  $y = -82.15$  mm

mm, and in the image plane have angles relative to the optical axis that correspond to the image-side numerical aperture. The calculation was made for the upper and lower outermost aperture rays because this example has an off-axis object field, so that the aperture rays are not symmetric in relation to the optical axis as was the case for the outermost aperture ray of the embodiment of Figure 6.

[0076] The data for the upper outermost aperture ray are listed in Table 4 and for the lower outermost aperture ray in Table 5.

Table 4

Lens	Aperture angle $\theta$ [°]	Ray path $OP_L$ [mm]	Optical path difference (111)-lens $\alpha_{AR}-\alpha_L=0^\circ$ [nm]	Optical path difference (111)-lens $\alpha_{AR}-\alpha_L=60^\circ$ [nm]	Optical path difference (100)-lens $\alpha_{AR}-\alpha_L=0^\circ$ [nm]	Optical path difference (100)-lens $\alpha_{AR}-\alpha_L=45^\circ$ [nm]
801	1.4	28.1	0.8	-0.8	0.0	0.0
802	-10.8	30.7	-5.3	8.0	-2.7	-1.3
803	-15.6	32.4	-6.8	12.4	-5.7	-2.7
803	-24.4	31.8	-6.5	17.8	-11.7	-5.2
802	-19.5	26.6	-5.8	12.4	-6.8	-3.2
804	6.4	20.1	3.0	-2.4	-0.6	-0.3
805	10.8	34.4	9.0	-6.0	-3.0	-1.5
806	0.2	10.0	0.1	-0.1	0.0	0.0
807	-11.1	22.0	-3.9	5.9	-2.1	-1.0
808	0.1	18.5	0.0	0.0	0.0	0.0
809	-0.8	9.0	-0.1	0.2	0.0	0.0
810	1.1	12.4	0.3	-0.3	0.0	0.0
811	-16.8	9.4	-2.0	3.8	-1.9	-0.9
812	-10.4	29.8	-5.0	7.5	-2.4	-1.2
813	-8.8	34.7	-5.2	7.3	-2.1	-1.0
814	-9.4	17.5	-2.8	4.0	-1.2	-0.6
815	-27.4	28.1	-5.3	16.9	-12.2	-5.3
816	-28.7	40.2	-7.1	24.8	-18.6	-7.9
817	-30.8	39.0	-6.3	24.7	-19.6	-8.1
Sum			-48.9	136.1	-90.9	-40.3

Table 5

Lens	Aperture angle $\theta$ [°]	Ray path OP <sub>L</sub> [mm]	Optical path difference (111)-lens $\alpha_{AR}-\alpha_L=0^\circ$ [nm]	Optical path difference (111)-lens $\alpha_{AR}-\alpha_L=60^\circ$ [nm]	Optical path difference (100)-lens $\alpha_{AR}-\alpha_L=0^\circ$ [nm]	Optical path difference (100)-lens $\alpha_{AR}-\alpha_L=45^\circ$ [nm]
801	-11.6	32.1	-5.8	9.0	-3.2	-1.6
802	19.5	28.3	13.3	-6.1	-7.3	-3.4
803	24.7	33.8	19.1	-6.9	-12.7	-5.7
803	17.7	34.3	14.7	-7.4	-7.5	-3.6
802	12.7	31.6	9.7	-6.0	-3.8	-1.8
804	-5.2	27.7	-2.7	3.3	-0.6	-0.3
805	-4.5	34.6	-3.0	3.5	-0.5	-0.3
806	-8.6	19.5	-2.9	4.0	-1.1	-0.6
807	-0.5	16.5	-0.2	0.2	0.0	0.0
808	-8.2	25.6	-3.7	5.0	-1.3	-0.7
809	-7.5	10.1	-1.3	1.8	-0.4	-0.2
810	-9.1	13.1	-2.0	2.9	-0.8	-0.4
811	9.0	9.9	2.1	-1.5	-0.6	-0.3
812	2.6	30.7	1.8	-1.6	-0.2	-0.1
813	0.9	34.0	0.6	-0.6	0.0	0.0
814	1.3	10.4	0.3	-0.3	0.0	0.0
815	23.5	16.3	8.9	-3.4	-5.7	-2.6
816	24.6	37.2	21.0	-7.6	-13.9	-6.2
817	29.4	29.6	18.5	-5.1	-14.1	-5.9
Sum			88.3	-16.8	-73.7	-33.5

[0077] As can be seen in Tables 4 and 5, the aperture angles  $\theta$  for the lenses L815 to L817 are larger than  $25^\circ$ . In this embodiment, too, the lenses L815 to L817 which are closest to the image plane have large aperture angles. The lenses L815 to L817 were designed so that the maximum aperture angle is

$$\text{smaller than or equal to } \arcsin\left(\frac{NA}{n_{FK}}\right) = \arcsin\left(\frac{0.8}{1.5597}\right) = 30.9^\circ.$$

The maximum aperture angle for the outermost aperture ray is  $30.8^\circ$  in the lens L817.

[0078] The aperture stop that is located between the lenses L811 and L812 has a diameter of 193 mm. All of the lenses L815 to L817 have diameters of less than 162 mm. Thus, the diameters of these lenses, which are associated with large

aperture angles, are smaller than 85% of the aperture stop diameter.

[0079] Tables 4 and 5 lead to the conclusion that it is advantageous if lenses with large aperture angles are oriented in the (100)-direction, as the birefringence values are lower overall. For example in the lenses L815 to L817, the optical path differences are smaller by more than 20%.

[0080] The embodiment of Figure 7 will now be used to demonstrate how the intrinsic birefringence can be compensated to a large extent by using groups of (100)-lenses that are rotated relative to each other in parallel with groups of (111)-lenses that are rotated relative to each other.

[0081] As a first step, all calcium fluoride in (111)-orientation are installed without rotating the (111)-lenses relative to each other. As a result, there will be a maximum optical path difference between two mutually orthogonal states of linear polarization of 136 nm. By rotating the (111)-lenses, the maximum optical path difference can be reduced to about 38 nm. This is achieved by combining the lenses L801 and L804 in a group and the lenses L802 and L803 in a further group, wherein the angle of rotation between the lenses is 60°. The lenses L808, L809 and L810 are combined into a group of three, and so are the lenses L815, L816 and L817, wherein the angle of rotation between each two of these lenses is 40°. The lenses L811, L812, L813 and L814 are combined into a group of four with an angle of rotation of 30°.

[0082] If all calcium fluoride in (100)-orientation are installed without rotating the (100)-lenses, the resultant maximum optical path difference between two mutually orthogonal states of linear polarization will be 90.6 nm. By

rotating the (100)-lenses, the maximum optical path difference can be reduced to about 40 nm. This is achieved by combining the lenses L801 and L804 in a group and the lenses L802 and L803 in a further group, wherein the angle of rotation between the lenses is in each case 45°. The lenses L808, L809 and L810 are combined into a group of three, and so are the lenses L815, L816 and L817, wherein the angle of rotation between two lenses in a group is 30°. The lenses L811, L812, L813 and L814 are combined into a group of four with an angle of rotation of 22.5°.

[0083] A maximum of 7 nm is obtained in the optical path difference for two mutually orthogonal states of linear polarization, if groups of (100)-lenses are combined with groups of (111)-lenses. The lenses L801 and L804 are combined into a group of (111)-lenses in which the angle of rotation between the lenses is 60°. The lenses L802 and L803 are combined into a group of (100)-lenses in which the angle of rotation between the lenses is 45°. A group of three (100)-lenses is formed of the lenses L808, L809 and L810, wherein the angle of rotation between each two of these lenses is 30°. A group of three (111)-lenses is formed of the lenses L815, L816 and L817, wherein the angle of rotation between each two of these lenses is 40°. The lenses L811, L812, L813 and L814 are combined into a group of four (100)-lenses with an angle of rotation of 22.5°. The lens axes of the lenses L805 and L807 which are not combined in a group are oriented in the crystallographic <111>-direction, while the lens axis of the lens L806 is oriented in the crystallographic <100>-direction.

[0084] As described above, the birefringence in crystals for light in the ultraviolet range can be compensated by arranging crystal elements with different orientations of the crystallographic axis following each other. If one arranges

lenses with different crystallographic directions following each other in an optical system, one encounters the problem that lenses are in many cases traversed by a light ray at different angles, in which case it is possible that a compensation may be achievable only to a limited extent. In optical systems that contain only one crystal lens, this kind of compensation is not possible at all.

[0085] As a possible solution, a lens can in the design be split into two lenses that are wrung together with a rotation relative to each other. In practice, this procedure suffers from the drawback that stresses deform the joint surface and also that the two halves have to be positioned with an accuracy of micrometers in the lateral direction.

[0086] It is proposed to make blanks from individual plates that are wrung together and are rotated relative to each other in regard to the orientation of their crystallographic axes and which are then made into lenses by milling and polishing. Everything that was said hereinabove in regard to the orientation is likewise applicable to this concept. In addition to the traditional technique of wringing in the optical manufacturing process, any other joining techniques that produce an intimate contact and minimize the occurrence of stress represent possible solutions and are encompassed within the scope of the invention. The wringing can be supported in particular by layers consisting, e.g., of quartz glass. It is important that no refraction or reflection occurs at the joining interface, which would be detrimental to the desired result.

[0087] The selection of the orientations is made according to the rules described above.

[0088] The following description of the principal configuration of a microlithography projection exposure system is based on Figure 8. The projection exposure system 81 has an illumination device 83 and a projection objective 85. The projection objective 85 includes a lens arrangement 819 with an aperture stop AP, wherein an optical axis 87 is defined by the lens arrangement 89. Examples for the lens arrangement 89 are presented in Figure 6 and Figure 7. Arranged between the illumination device 83 and the projection objective 85 is a mask 89 which is held in the light path by means of a mask holder 811. Masks 89 of this type, which are used in microlithography, have a micrometer-nanometer structure, which is projected into the image plane 813 by means of the projection objective 85, reduced for example by a factor of 4 or 5. In the image plane 813, a light-sensitive substrate 815, more specifically a wafer positioned on a substrate holder 817, is held in place.

[0089] The smallest structure dimensions that can still be resolved depend on the wavelength  $\lambda$  of the light that is used for the illumination and they also depend on the image-side numerical aperture of the projection objective 85, i.e., the maximally achievable resolution of the projection exposure system 81 increases with decreasing wavelength  $\lambda$  of the illumination device 83 and with increasing image-side numerical aperture of the projection objective 85. With the embodiments shown in Figures 6 and 7, it is possible to realize resolutions smaller than 150 nm. This is also the reason why effects such as the intrinsic birefringence need to be minimized. The invention has been successful in strongly reducing the undesirable influence of the intrinsic birefringence in particular in projection objectives with large image-side numerical aperture values.

M1587a

TABLE 1

LENSES	RADI	THICKNESS VALUES	GLASSES	REFR. INDEX AT 157.629nm	1/2 FREE DIAMETER
0	0.000000000	27.171475840	N2	1.00031429	46.200
	0.000000000	0.602670797	N2	1.00031429	52.673
L601	900.198243311AS	15.151284556	CaF2	1.55929035	53.454
	-235.121108435	9.531971079	N2	1.00031429	54.049
L602	-167.185917779	8.294716452	CaF2	1.55929035	54.178
	-132.673519510	14.020355779	N2	1.00031429	54.901
L603	-333.194588652	9.893809820	CaF2	1.55929035	53.988
	-155.450516203	15.930502944	N2	1.00031429	54.132
L604	-73.572316296	7.641977580	CaF2	1.55929035	53.748
	-68.248613899AS	2.881720302	N2	1.00031429	55.167
L605	-86.993585564AS	5.094651720	CaF2	1.55929035	52.580
	-238.150965327	5.379130780	N2	1.00031429	53.729
L606	-165.613920870	5.094651720	CaF2	1.55929035	53.730
	153.417884485	34.150169591	N2	1.00031429	56.762
L607	-92.061009990	5.094651720	CaF2	1.55929035	58.081
	8491.086261873AS	19.673523795	N2	1.00031429	74.689
L608	-407.131300451	30.380807138	CaF2	1.55929035	87.291
	-140.620317156	0.761662684	N2	1.00031429	91.858
L609	-4831.804853654AS	50.269660218	CaF2	1.55929035	117.436
	-192.197373609	1.688916911	N2	1.00031429	121.408
L610	-367.718684892	21.227715500	CaF2	1.55929035	127.704
	-233.628547894	2.224071019	N2	1.00031429	129.305
L611	709.5858555080	28.736922725	CaF2	1.55929035	137.016
	1238.859445357	9.120684720	N2	1.00031429	137.428
L612	1205.457051945	49.281218258	CaF2	1.55929035	138.288
	-285.321880705	1.625271224	N2	1.00031429	138.379
L613	137.549591710	56.718543740	CaF2	1.55929035	108.652
	-4380.301012978AS	0.623523902	N2	1.00031429	106.138
L614	2663.880214408	6.792868960	CaF2	1.55929035	103.602
	149.184979730	15.779049257	N2	1.00031429	84.589
L615	281.093108064	6.792868960	CaF2	1.55929035	83.373
	184.030288413	32.341552355	N2	1.00031429	77.968
L616	-222.157416308	5.094651720	CaF2	1.55929035	77.463
	101.254238115AS	56.792834221	N2	1.00031429	71.826
L617	-106.980638018	5.094651720	CaF2	1.55929035	72.237
	1612.305471130	20.581065398	N2	1.00031429	89.760
L618	-415.596135628	26.398111993	CaF2	1.55929035	96.803
	-204.680044631	0.713343960	N2	1.00031429	103.409
L619	-646.696622394	25.867340760	CaF2	1.55929035	116.636
	-231.917626896	0.766268682	N2	1.00031429	118.569
L620	-790.657607677	23.400482872	CaF2	1.55929035	128.806
	-294.872053725	0.721402031	N2	1.00031429	130.074
L621	786.625567756	40.932308205	CaF2	1.55929035	141.705
	-431.247283013	12.736629300	N2	1.00031429	142.089
	0.000000000	-8.491086200	N2	1.00031429	134.586
L622	295.022653593AS	20.185109438	CaF2	1.55929035	139.341
	449.912291916	0.619840486	N2	1.00031429	137.916
L623	358.934076212	48.662890509	CaF2	1.55929035	136.936
	-622.662988878	30.955714157	N2	1.00031429	135.288
L624	-224.404889753	12.736629300	CaF2	1.55929035	134.760
	-251.154571510AS	16.079850229	N2	1.00031429	134.853
L625	-193.582989843AS	16.510083506	CaF2	1.55929035	134.101
	-198.077570749	0.880353872	N2	1.00031429	136.109
L626	206.241795157	19.927993542	CaF2	1.55929035	101.240
	338.140581666	0.925956949	N2	1.00031429	97.594
L627	111.017549581	24.580089962	CaF2	1.55929035	85.023
	169.576109839	0.777849447	N2	1.00031429	81.164
L628	117.982165264	31.161065630	CaF2	1.55929035	75.464
	921.219058213AS	6.934980174	N2	1.00031429	69.501
L629	0.000000000	22.260797322	CaF2	1.55929035	63.637
	0.000000000	4.245543100	N2	1.00031429	48.606
L630	0.000000000	21.227715500	CaF2	1.55929035	41.032
	0.000000000	8.491086200	N2	1.00031429	26.698
	0.000000000	0.000000000		1.000000000	11.550

---

Wavelength and refractive index are stated relative to vacuum.

ASPHERIC CONSTANTS

Asphere of lens L601

K	0.0000
C1	1.28594437e-007
C2	8.50731836e-013
C3	1.16375620e-016
C4	2.28674275e-019
C5	-1.23202729e-022
C6	3.32056239e-026
C7	-4.28323389e-030
C8	0.00000000e+000
C9	0.00000000e+000

Asphere of lens L604

K	-1.3312
C1	-4.03355456e-007
C2	2.25776586e-011
C3	-2.19259878e-014
C4	4.32573397e-018
C5	-7.92477159e-022
C6	7.57618874e-026
C7	-7.14962797e-030
C8	0.00000000e+000
C9	0.00000000e+000

Asphere of lens L605

K	-1.1417
C1	1.33637337e-007
C2	1.56787758e-011
C3	-1.64362484e-014
C4	3.59793786e-018
C5	-5.11312568e-022
C6	1.70636633e-026
C7	1.82384731e-030
C8	0.00000000e+000
C9	0.00000000e+000

Asphere of lens L607

K	0.0000
C1	1.34745120e-007
C2	-2.19807543e-011
C3	1.20275881e-015
C4	4.39597377e-020
C5	-2.37132819e-023
C6	2.87510939e-027
C7	-1.42065162e-031
C8	0.00000000e+000
C9	0.00000000e+000

## Asphere of lens L609

K	0.0000
C1	6.85760526e-009
C2	-4.84524868e-013
C3	-6.28751350e-018
C4	-3.72607209e-022
C5	3.25276841e-026
C6	-4.05509974e-033
C7	-3.98843079e-035
C8	0.00000000e+000
C9	0.00000000e+000

## Asphere of lens L613

K	0.0000
C1	2.24737416e-008
C2	-4.45043770e-013
C3	-4.10272049e-017
C4	4.31632628e-021
C5	-3.27538237e-025
C6	1.44053025e-029
C7	-2.76858490e-034
C8	0.00000000e+000
C9	0.00000000e+000

## Asphere of lens L616

K	0.0000
C1	-2.83553693e-008
C2	-1.12122261e-011
C3	-2.05192812e-016
C4	-1.55525080e-020
C5	-4.77093112e-024
C6	8.39331135e-028
C7	-8.97313681e-032
C8	0.00000000e+000
C9	0.00000000e+000

## Asphere of lens L622

K	0.0421
C1	7.07310826e-010
C2	-2.00157185e-014
C3	-9.33825109e-020
C4	1.27125854e-024
C5	1.94008709e-027
C6	-6.11989858e-032
C7	2.92367322e-036
C8	0.00000000e+000
C9	0.00000000e+000

## Asphere of lens L624

K	0.0000
C1	3.02835805e-010
C2	-2.40484062e-014
C3	-3.22339189e-019
C4	1.64516979e-022
C5	-8.51268614e-027
C6	2.09276792e-031
C7	-4.74605669e-036
C8	0.00000000e+000
C9	0.00000000e+000

## Asphere of lens L625

K	0.0000
C1	-3.99248993e-010
C2	5.79276562e-014
C3	3.53241478e-018
C4	-4.57872308e-023
C5	-6.29695208e-027
C6	1.57844931e-031
C7	-2.19266130e-036
C8	0.00000000e+000
C9	0.00000000e+000

## Asphere of lens L628

K	0.0000
C1	4.40737732e-008
C2	1.52385268e-012
C3	-5.44510329e-016
C4	6.32549789e-020
C5	-4.58358203e-024
C6	1.92230388e-028
C7	-3.11311258e-033
C8	0.00000000e+000
C9	0.00000000e+000

TABLE 3

L61

LENSES	RADI	THICKNESS VALUES	GLASSES	REFR. INDEX AT 157.629nm	1/2 FREE DIAMETER
0	0.000000000	34.000000000		1.00000000	82.150
	0.000000000	0.100000000		1.00000000	87.654
L801	276.724757380	40.000000000	CaF2	1.55970990	90.112
	1413.944109416AS	95.000000000		1.00000000	89.442
SP1	0.000000000	11.000000000		1.00000000	90.034
	0.000000000	433.237005445		1.00000000	90.104
L802	-195.924336384	17.295305525	CaF2	1.55970990	92.746
	-467.658808527	40.841112468		1.00000000	98.732
L803	-241.385736441	15.977235467	CaF2	1.55970990	105.512
	-857.211727400AS	21.649331094		1.00000000	118.786
SP2	0.000000000	0.000010000		1.00000000	139.325
	253.074839896	21.649331094		1.00000000	119.350
L803'	857.211727400AS	15.977235467	CaF2	1.55970990	118.986
	241.385736441	40.841112468		1.00000000	108.546
L802'	467.658808527	17.295305525	CaF2	1.55970990	102.615
	195.924336384	419.981357165		1.00000000	95.689
SP3	0.000000000	6.255658280		1.00000000	76.370
	0.000000000	42.609155219		1.00000000	76.064
Z1	0.000000000	67.449547115		1.00000000	73.981
L804	432.544479547	37.784311058	CaF2	1.55970990	90.274
	-522.188532471	113.756133662		1.00000000	92.507
L805	-263.167605725	33.768525968	CaF2	1.55970990	100.053
	-291.940616829AS	14.536591424		1.00000000	106.516
L806	589.642961222AS	20.449887046	CaF2	1.55970990	110.482
	-5539.698828792	443.944079795		1.00000000	110.523
L807	221.780582003	9.000000000	CaF2	1.55970990	108.311
	153.071443064	22.790060084		1.00000000	104.062
L808	309.446967518	38.542735318	CaF2	1.55970990	104.062
	-2660.227900099	0.100022286		1.00000000	104.098
L809	23655.354584194	12.899131182	CaF2	1.55970990	104.054
	-1473.189213176	9.318886362		1.00000000	103.931
L810	-652.136459374	16.359499814	CaF2	1.55970990	103.644
	-446.489459129	0.100000000		1.00000000	103.877
L811	174.593507050	25.900313780	CaF2	1.55970990	99.267
	392.239615259AS	14.064505431		1.00000000	96.610
	0.000000000	2.045119392		1.00000000	96.552
L812	7497.306838492	16.759051656	CaF2	1.55970990	96.383
	318.210831711	8.891640764		1.00000000	94.998
L813	428.724465129	41.295806263	CaF2	1.55970990	95.548
	3290.097860119AS	7.377912006		1.00000000	95.040
L814	721.012739719	33.927118706	CaF2	1.55970990	95.443
	-272.650872353	6.871397517		1.00000000	95.207
L815	131.257556743	38.826450065	CaF2	1.55970990	81.345
	632.112566477AS	4.409527396		1.00000000	74.847
L816	342.127616157AS	37.346293509	CaF2	1.55970990	70.394
	449.261078744	4.859754445		1.00000000	54.895
L817	144.034814702	34.792179308	CaF2	1.55970990	48.040
	-751.263321098AS	11.999872684		1.00000000	33.475
0'	0.000000000	0.000127776		1.00000000	16.430

## ASPHERIC CONSTANTS

## Asphere of lens L801

K	0.0000
C1	4.90231706e-009
C2	3.08634889e-014
C3	-9.53005325e-019
C4	-6.06316417e-024
C5	6.11462814e-028
C6	-8.64346302e-032
C7	0.00000000e+000
C8	0.00000000e+000
C9	0.00000000e+000

## Asphere of lens L803

K	0.0000
C1	-5.33460884e-009
C2	9.73867225e-014
C3	-3.28422058e-018
C4	1.50550421e-022
C5	0.00000000e+000
C6	0.00000000e+000
C7	0.00000000e+000
C8	0.00000000e+000
C9	0.00000000e+000

## Asphere of lens L803'

K	0.0000
C1	5.33460884e-009
C2	-9.73867225e-014
C3	3.28422058e-018
C4	-1.50550421e-022
C5	0.00000000e+000
C6	0.00000000e+000
C7	0.00000000e+000
C8	0.00000000e+000
C9	0.00000000e+000

## Asphere of lens L805

K	0.0000
C1	2.42569449e-009
C2	3.96137865e-014
C3	-2.47855149e-018
C4	7.95092779e-023
C5	0.00000000e+000
C6	0.00000000e+000
C7	0.00000000e+000
C8	0.00000000e+000
C9	0.00000000e+000

## Asphere of lens L806

K	0.0000
C1	-6.74111232e-009
C2	-2.57289693e-014
C3	-2.81309020e-018
C4	6.70057831e-023
C5	5.06272344e-028
C6	-4.81282974e-032
C7	0.00000000e+000
C8	0.00000000e+000
C9	0.00000000e+000

## Asphere of lens L811

K	0.0000
C1	2.28889624e-008
C2	-1.88390559e-014
C3	2.86010656e-017
C4	-3.18575336e-021
C5	1.45886017e-025
C6	-1.08492931e-029
C7	0.00000000e+000
C8	0.00000000e+000
C9	0.00000000e+000

## Asphere of lens L813

K	0.0000
C1	3.40212872e-008
C2	-1.08008877e-012
C3	4.33814531e-017
C4	-7.40125614e-021
C5	5.66856812e-025
C6	0.00000000e+000
C7	0.00000000e+000
C8	0.00000000e+000
C9	0.00000000e+000

## Asphere of lens L815

K	0.0000
C1	-3.15395039e-008
C2	4.30010133e-012
C3	3.11663337e-016
C4	-3.64089769e-020
C5	1.06073268e-024
C6	0.00000000e+000
C7	0.00000000e+000
C8	0.00000000e+000
C9	0.00000000e+000

## Asphere of lens L816

K	0.0000
C1	-2.16574623e-008
C2	-6.67182801e-013
C3	4.46519932e-016
C4	-3.71571535e-020
C5	0.00000000e+000
C6	0.00000000e+000
C7	0.00000000e+000
C8	0.00000000e+000
C9	0.00000000e+000

## Asphere of lens L817

K	0.0000
C1	2.15121397e-008
C2	-1.65301726e-011
C3	-5.03883747e-015
C4	1.03441815e-017
C5	-6.29122773e-021
C6	1.44097714e-024
C7	0.00000000e+000
C8	0.00000000e+000
C9	0.00000000e+000

## Patent Claims:

1. Projection objective (611, 711) for a microlithography projection exposure system (81) with a plurality of lenses (L601-L630, L801-L817), wherein at least one lens (1) consists of a fluoride crystal, characterized in that the at least one lens (1) is a (100)-lens with a lens axis (EA) that is oriented approximately perpendicular to the crystallographic {100}-planes or to the crystallographic planes of the fluoride crystal that are equivalent to the {100}-planes.
2. Projection objective according to claim 1, wherein the (100)-lens is a rotationally symmetric lens with a symmetry axis and wherein the symmetry axis coincides with the lens axis of the (100)-lens.
3. Projection objective according to one of the claims 1 or 2, with an optical axis (OA), wherein the lens axis of the (100)-lens coincides with the optical axis of the projection objective.
4. Projection objective according to one of the claims 1 to 3, wherein light rays run inside the projection objective from an object plane (O) to an image plane (O') and at least one light ray (609, 713, 715) inside the (100)-lens has a ray angle larger than 25°, in particular larger than 30°, relative to the lens axis.
5. Projection objective according to one of the claims 1 to 4, wherein light rays run inside the projection objective from an object plane to an image plane and all light rays inside the (100)-lens have ray angles of maximally 45°, in

particular maximally  $\arcsin\left(\frac{NA}{n_{FK}}\right)$  in relation to the lens

axis, wherein NA stands for the image-side numerical aperture and  $n_{FK}$  stands for the refractive index of the fluoride crystal.

6. Projection objective according to one of the claims 1 to 5, with an aperture stop plane, wherein the aperture stop plane has an aperture stop diameter, wherein the (100)-lens has a lens diameter, and wherein the lens diameter is smaller than 85%, in particular smaller than 80%, of the aperture stop diameter.
7. Projection objective according to one of the claims 1 to 6 with an image plane, wherein the (100)-lens (L630, L817) is the lens nearest to the image plane.
8. Projection objective according to one of the claims 1 to 7, wherein a bundle of light rays originates from an object point in an object plane, each of said rays having an azimuth angle  $\alpha$  and an aperture angle  $\theta$ , wherein the bundle of rays has a birefringence distribution  $\Delta n(\theta, \alpha)$  in an image plane and the (100)-lenses are arranged in relation to each other with a rotation about the optical axis such that the birefringence distribution  $\Delta n(\theta, \alpha)$  has significantly reduced values in comparison to a non-rotated arrangement of the (100)-lenses.
9. Projection objective according to claim 8, wherein the birefringence distribution  $\Delta n(\theta, \alpha)$  for a given aperture angle  $\theta_0$  has birefringence values  $\Delta n(\theta_0, \alpha)$  which, as a function of the azimuth angle  $\alpha$ , vary by less than 20%.

10. Projection objective according to one of the claims 8 to 9, wherein the (100)-lenses have reference directions which are perpendicular to the lens axes and which point in a principal crystallographic direction, wherein rotation angles  $\beta$  are defined between the reference directions of the individual (100)-lenses, and wherein the rotation angle  $\beta$  between each two of the (100)-lenses of a group of n (100)-lenses conforms to the equation:

$$\beta = \frac{90^\circ}{n} + m \cdot 90^\circ \pm 5^\circ$$

wherein n represents the number of (100)-lenses in the group and m is an integer number.

11. Projection objective according to claim 10, wherein an outermost aperture ray (609, 713, 715) of the bundle of rays has inside each of the (100)-lenses a respective azimuth angle  $\alpha_L$  and a respective aperture angle  $\theta_L$  and wherein the aperture angles  $\theta_L$  within the (100)-lenses of the group vary by no more than 30%, in particular no more than 20%.

12. Projection objective according to one of the claims 10 to 11, wherein an outermost aperture ray (609, 713, 715) of the bundle of rays covers inside each of the (100)-lenses a respective ray path  $OP_L$  and wherein the ray paths  $OP_L$  within the (100)-lenses of the group vary by no more than 30%, in particular no more than 20%.

13. Projection objective according to one of the claims 10 to 12, wherein an outermost aperture ray (609, 713, 715) of the bundle of rays inside the (100)-lenses is subject to an optical path difference between two mutually orthogonal states of linear polarization, and wherein the optical path differences determined at a rotation angle  $\beta=0^\circ$

within the (100)-lenses of the group vary by no more than 30%, in particular no more than 20%.

14. Projection objective according to one of the claims 9 to 13, wherein the group comprises two (100)-lenses.
15. Projection objective according to claim 14, wherein the two (100)-lenses (L629, L630) are arranged adjacent to each other and are, in particular, joined to each other by wringing.
16. Projection objective according to one of the claims 9 to 15, wherein the projection objective has at least two groups of (100)-lenses and wherein the (100)-lenses in each of the two groups are rotated relative to each other.
17. Projection objective for a microlithography projection exposure system with a plurality of lenses, wherein at least two lenses consist of a fluoride crystal, wherein the at least two lenses are (111)-lenses in which the lens axes are approximately perpendicular to the crystallographic {111}-planes or on crystallographic planes of the fluoride crystal that are equivalent to the {111}-planes, and wherein the (111)-lenses are arranged in centered alignment on the optical axis, wherein a ray bundle originates from an object point in an object plane, each of the rays of the bundle having a respective azimuth angle  $\alpha$  and a respective aperture angle  $\theta$  in the object plane, wherein in an image plane the ray bundle has a birefringence distribution  $\Delta n(\theta, \alpha)$  and the (111)-lenses are arranged with a rotation relative to each other about the optical axis, such that the birefringence distribution  $\Delta n(\theta, \alpha)$  has significantly reduced values in comparison to a non-rotated arrangement of the (111)-lenses.

18. Projection objective according to claim 17, wherein the birefringence distribution  $\Delta n(\theta, \alpha)$  for a given aperture angle  $\theta_0$  has birefringence values  $\Delta n(\theta_0, \alpha)$  which, as a function of the azimuth angle  $\alpha$ , vary by less than 20%.
19. Projection objective according to one of the claims 17 to 18, wherein the (111)-lenses have reference directions which are perpendicular to the lens axes and which point in a principal crystallographic direction, wherein rotation angles  $\gamma$  are defined between the reference directions of the individual (111)-lenses, and wherein the rotation angle  $\gamma$  between each two of the (111)-lenses of a group of  $k$  (111)-lenses conforms to the equation:
$$\gamma = \frac{120^\circ}{k} + l \cdot 120^\circ \pm 8^\circ$$
wherein  $k$  represents the number of (111)-lenses in the group and  $l$  is an integer number.
20. Projection objective according to claim 19, wherein an outermost aperture ray (609, 713, 715) of the bundle of rays has inside each of the (111)-lenses a respective azimuth angle  $\alpha_L$  and a respective aperture angle  $\theta_L$  and wherein the azimuth angles  $\alpha_L$  and the aperture angles  $\theta_L$  within the (111)-lenses of the group vary by no more than 30%, in particular no more than 20%.
21. Projection objective according to one of the claims 19 to 20, wherein an outermost aperture ray (609, 713, 715) of the bundle of rays covers inside each of the (100)-lenses a respective ray path  $OP_L$  and wherein the ray paths  $OP_L$  within the (111)-lenses of the group vary by no more than 30%, in particular no more than 20%.

22. Projection objective according to one of the claims 19 to 21, wherein an outermost aperture ray (609, 713, 715) of the bundle of rays inside the (111)-lenses is subject to an optical path difference between two mutually orthogonal states of linear polarization, and wherein the optical path differences determined at a rotation angle  $\beta=0^\circ$  vary within the (111)-lenses of the group by no more than 30%, in particular no more than 20%.
23. Projection objective according to one of the claims 19 to 22, wherein the second group comprises two (111)-lenses.
24. Projection objective according to claim 23, wherein the two (111)-lenses (L629, L630) are arranged adjacent to each other and are, in particular, joined to each other by wringing.
25. Projection objective according to one of the claims 19 to 24, wherein the projection objective has at least two groups of (111)-lenses and wherein the (111)-lenses in each of the two groups are rotated relative to each other.
26. Projection objective according to one of the claims 1 to 16 and according to one of the claims 17 to 25, wherein a ray bundle originates from an object point in an object plane, each of the rays of the bundle having a respective azimuth angle  $\alpha$  and a respective aperture angle  $\theta$  in the object plane, wherein in an image plane the ray bundle has a birefringence distribution  $\Delta n(\theta, \alpha)$  and wherein the (100)-lenses and the (111)-lenses are arranged with a rotation relative to each other about the optical axis, such that the birefringence distribution  $\Delta n(\theta, \alpha)$  has significantly reduced values in comparison to a non-rotated arrangement of the (100)-lenses and (111)-lenses.

27. Projection objective according to claim 26, wherein the birefringence distribution  $\Delta n(\theta, \alpha)$  is composed of a (100)-birefringence distribution  $\Delta n_{(100)}(\theta, \alpha)$  that is due to the (100)-lenses and a (111)-birefringence distribution  $\Delta n_{(111)}(\theta, \alpha)$  that is due to the (111)-lenses, and wherein the maximum value of the birefringence distribution  $\Delta n(\theta, \alpha)$  does not exceed 20% of the maximum value of the (100)-birefringence distribution  $\Delta n_{(100)}(\theta, \alpha)$  or of the maximum value of the (111)-birefringence distribution  $\Delta n_{(111)}(\theta, \alpha)$ .
28. Projection objective according to one of the claims 1 to 27, wherein the fluoride crystal is a calcium fluoride crystal, a strontium fluoride crystal or a barium fluoride crystal.
29. Projection objective according to one of the claims 1 to 28, wherein the projection objective has an image-side numerical aperture NA, and wherein the image-side numerical aperture NA is larger than 0.7, in particular larger than 0.8.
30. Projection objective according to one of the claims 1 to 29, wherein the light rays have wavelengths shorter than 200 nm.
31. Projection objective according to one of the claims 1 to 30, wherein the light rays have wavelengths shorter than 160 nm.
32. Projection objective according to one of the claims 1 to 31, wherein the projection objective (611) is a refractive objective.

33. Projection objective according to one of the claims 1 to 32, wherein the projection objective is a catadioptric objective (711) with lenses and with at least one concave mirror (Sp2).
34. Projection objective according to one of the claims 1 to 33, wherein all lenses are of calcium fluoride.
35. Microlithography projection exposure system (81), comprising
  - an illumination system (83),
  - a projection objective (85) according to one of the claims 1 to 19, which projects a structure-carrying mask (89) onto a light-sensitive substrate (815).
36. Method for the manufacture of semiconductor components by means of a microlithography projection exposure system (81) according to claim 36.
37. Method of reducing the birefringence in a projection objective for a microlithography projection exposure system, wherein the projection objective comprises a plurality of lenses and at least two lenses consist of a fluoride crystal, wherein the at least two lenses are (100)-lenses in which the lens axes are approximately perpendicular to the crystallographic {100}-planes or to crystallographic planes of the fluoride crystal that are equivalent to the {100}-planes, and wherein the (100)-lenses are arranged in centered alignment on the optical axis,  
characterized in that  
for a ray bundle which originates from an object point in an object plane and wherein each of the rays of the bundle

has a respective azimuth angle  $\alpha$  and a respective aperture angle  $\theta$  in the object plane, the birefringence distribution  $\Delta n(\theta, \alpha)$  in the image plane of the projection objective is determined, and the (100)-lenses are arranged with a rotation about the optical axis, such that the birefringence distribution  $\Delta n(\theta, \alpha)$  has significantly reduced values in comparison to a non-rotated arrangement of the (100)-lenses.

38. Method of reducing the birefringence in a projection objective for a microlithography projection exposure system, wherein the projection objective comprises a plurality of lenses and at least two lenses consist of a fluoride crystal, wherein the at least two lenses are (111)-lenses in which the lens axes are approximately perpendicular to the crystallographic {111}-planes or to crystallographic planes of the fluoride crystal that are equivalent to the {111}-planes, and wherein the (111)-lenses are arranged in centered alignment on the optical axis,
- characterized in that for a ray bundle which originates from an object point in an object plane and wherein each of the rays of the bundle has a respective azimuth angle  $\alpha$  and a respective aperture angle  $\theta$  in the object plane, the birefringence distribution  $\Delta n(\theta, \alpha)$  in the image plane of the objective is determined, and the (111)-lenses are arranged with a rotation relative to each other about the optical axis, such that the birefringence distribution  $\Delta n(\theta, \alpha)$  has significantly reduced values in comparison to a non-rotated arrangement of the (111)-lenses.

39. Method of reducing the birefringence in a projection objective for a microlithography projection exposure system, wherein the projection objective comprises a plurality of lenses and at least two lenses consist of a fluoride crystal, wherein the at least two lenses are (100)-lenses in which the lens axes are approximately perpendicular to the crystallographic {100}-planes or to the crystallographic planes of the fluoride crystal that are equivalent to the {100}-planes, and wherein the (100)-lenses are arranged in centered alignment on the optical axis, and wherein at least two further lenses consist of a fluoride crystal, wherein the at least two further lenses are (111)-lenses in which the lens axes are approximately perpendicular to the crystallographic {111}-planes or to the crystallographic planes of the fluoride crystal that are equivalent to the {111}-planes, and wherein the (111)-lenses are arranged in centered alignment on the optical axis,

characterized in that

for a ray bundle which originates from an object point in an object plane and wherein each of the rays of the bundle has a respective azimuth angle  $\alpha$  and a respective aperture angle  $\theta$  in the object plane, the birefringence distribution  $\Delta n(\theta, \alpha)$  in the image plane of the objective is determined, and

the (100)-lenses as well as the (111)-lenses are arranged with a rotation about the optical axis, such that the birefringence distribution  $\Delta n(\theta, \alpha)$  has significantly reduced values in comparison to a non-rotated arrangement of the (100)-lenses and (111)-lenses.

40. Method according to claim 39, wherein the birefringence distribution  $\Delta n(\theta, \alpha)$  is composed of a (100)-birefringence distribution  $\Delta n_{(100)}(\theta, \alpha)$  that is due to the (100)-lenses

and a (111)-birefringence distribution  $\Delta n_{(111)}(\theta, \alpha)$  that is due to the (111)-lenses,

wherein the (100)-lenses are arranged with a rotation about the optical axis, such that the (100)-birefringence distribution  $\Delta n_{(100)}(\theta, \alpha)$  has significantly reduced values in comparison to a non-rotated arrangement of the (100)-lenses, and

wherein the (111)-lenses are arranged with a rotation about the optical axis, such that the (111)-birefringence distribution  $\Delta n_{(111)}(\theta, \alpha)$  has significantly reduced values in comparison to a non-rotated arrangement of the (111)-lenses.

41. Method for the manufacture of lenses, characterized in that a plurality of plates which consist of a crystal material, preferably fluoride crystal and in particular calcium fluoride, and which are rotated relative to each other in regard to their respective crystallographic orientations are joined together in an optically seamless manner, in particular by wringing, and are subsequently shaped and polished as a unitary blank.
42. Method for the manufacture of lenses according to claim 41, wherein two (111)-plates are joined in an optically seamless manner, wherein the respective normal vectors of (111)-plate surfaces point in the crystallographic <111>-direction or crystallographic directions equivalent to the <111>-directions, wherein the (111)-plates have reference directions that are perpendicular to the normal vectors of the surfaces and point in a principal crystallographic direction, wherein an angle of rotation  $\beta$  is defined between the reference directions of the two (111)-plates, and wherein the angle of rotation  $\beta$  conforms to the

following equation:

$$\beta = 60^\circ + m \cdot 120^\circ \pm 10^\circ, \text{ wherein } m \text{ is an integer number.}$$

43. Method for the manufacture of lenses according to claim 42, wherein the (111)-plates are of approximately equal thickness.
44. Method for the manufacture of lenses according to claim 41, wherein two (100)-plates are joined in an optically seamless manner, wherein the respective normal vectors of (100)-plate surfaces point in the crystallographic  $\langle 100 \rangle$ -direction or crystallographic directions equivalent to the  $\langle 100 \rangle$ -direction, wherein the (100)-plates have reference directions that are perpendicular to the normal vectors of the surfaces and point in a principal crystallographic direction, wherein an angle of rotation  $\gamma$  is defined between the reference directions of the two (100)-plates, and wherein the angle of rotation  $\gamma$  conforms to the following equation:  
$$\gamma = 45^\circ + l \cdot 90^\circ \pm 10^\circ, \text{ wherein } l \text{ is an integer number.}$$
45. Method for the manufacture of lenses according to claim 44, wherein the (100)-plates are of approximately equal thickness.
46. Method for the manufacture of lenses according to claim 40, wherein two (100)-plates and two (111)-plates are joined in an optically seamless manner, wherein the respective normal vectors of (100)-plate surfaces point in the crystallographic  $\langle 100 \rangle$ -direction or crystallographic directions equivalent to the  $\langle 100 \rangle$ -direction and wherein the respective normal vectors of (111)-plate surfaces point in the crystallographic  $\langle 111 \rangle$ -direction or crystallographic directions equivalent to the  $\langle 111 \rangle$ -

direction, wherein the (100)-plates and the (111)-plates, respectively, have reference directions that are perpendicular to the normal vectors of the surfaces and point in a principal crystallographic direction, wherein an angle of rotation  $\beta$  is defined between the reference directions of the two (111)-plates, and wherein the angle of rotation  $\beta$  conforms to the following equation:

$\beta = 60^\circ + m \cdot 120^\circ \pm 10^\circ$ , wherein  $m$  is an integer number, and wherein an angle of rotation  $\gamma$  is defined between the reference directions of the two (100)-plates, and wherein the angle of rotation  $\gamma$  conforms to the following equation:

$\gamma = 45^\circ + l \cdot 90^\circ \pm 10^\circ$ , wherein  $l$  is an integer number.

47. Method for the manufacture of lenses according to claim 46, wherein the (111)-plates are of an approximately equal first thickness and the (100)-plates are of an approximately equal second thickness, and wherein the ratio of the first thickness to the second thickness is  $1.5 \pm 0.2$ .
48. Lens, characterized by its manufacture according to one of the claims 41 to 47.
49. Projection objective or projection exposure system for use in the field of microlithography, characterized in that the projection objective or projection exposure system comprises a lens according to claim 48.
50. Projection objective or projection exposure system for use in the field of microlithography according to at least one of the claims 1 to 40, characterized in that the projection objective or projection exposure system comprises a lens according to claim 48.

DE 101 25 487 A1

(File Ref. 01062P)

Attached hereto: 14 page(s) of drawings

Summary:

Optical Element, Projection Objective and Microlithography

Projection Exposure System with Fluoride Crystal Lenses

(Fig. 1)

Projection objective for a microlithography projection exposure system with a plurality of lenses, wherein at least one lens consists of a fluoride crystal. This lens is a (100)-lens with a lens axis that is approximately perpendicular to the crystallographic {100}-planes of the fluoride crystal or to planes that are equivalent to the {100}-planes. In order to reduce the values of the birefringence distribution, the (100)-lenses of a group are rotated in relation to each other. The same procedure is also applicable to (111)-lenses whose crystallographic axes are approximately perpendicular to the crystallographic {111}-planes of the fluoride crystal or to planes that are equivalent to the {111}-planes. A further reduction of the undesirable influence of the birefringence is achieved by using groups of mutually rotated (100)-lenses in simultaneous combination with groups of mutually rotated (111)-lenses.

**DR. WALTER E. KUPPER**

65 Barnsdale Road  
Madison, NJ 07940

Telephone: 973 301-1989    Fax: 973 822-9096    E-mail: wekupper@att.net

July 26, 2005

TO WHOM IT MAY CONCERN:

**TRANSLATOR'S CERTIFICATE**

The undersigned hereby certifies that he is bilingually proficient in German and English,  
that he has personally prepared the attached translation

**"Objective with Fluoride Crystal Lenses"**

of the published German Patent Application

**"Offenlegungsschrift DE 101 27 320 A1,  
Objektiv mit Fluorid-Kristall-Linsen "**

and that the translation is accurate.



Walter Kupper

**Description****Objective with Fluoride Crystal Lenses**

[0001] The invention relates to an objective in accordance with the introductory part of claim 1.

[0002] Projection objectives of this kind are known from U.S. Patent 6,201,634 which discloses that, ideally, in the manufacture of fluoride crystal lenses the lens axes are aligned perpendicularly to the crystallographic {111}-planes of the fluoride crystals in order to minimize the stress-related birefringence. The implied assumption in U.S. Patent 6,201,634 is that fluoride crystals have no intrinsic birefringence.

[0003] However, as is known from the Internet publication "Preliminary Determination of an Intrinsic Birefringence in CaF<sub>2</sub> by John H. Burnett, Eric L. Shirley, and Zachary H. Levine, NIST, Gaithersburg, MD 20899, USA (posted May 7, 2001), calcium fluoride single crystals also exhibit birefringence that is not stress-induced, i.e., intrinsic birefringence. The measurements presented in that reference demonstrate that with a light ray propagation in the crystallographic <110>-direction, the birefringence in calcium fluoride amounts to  $(6.5 \pm 0.4)$  nm/cm at a wavelength of  $\lambda=156.1$  nm,  $(3.6 \pm 0.2)$  nm/cm at a wavelength of  $\lambda=193.09$  nm, and  $(1.2 \pm 0.1)$  nm/cm at a wavelength of  $\lambda=253.65$  nm. However, with a light ray propagation in the crystallographic <100>-direction and in the crystallographic <111>-direction, no intrinsic birefringence occurs in calcium fluoride, as is also predicted by theory. Thus, the intrinsic birefringence is strongly direction-dependent and becomes noticeably more pronounced as the wavelength decreases.

[0004] The indices for the crystallographic directions will hereinafter be bracketed between the symbols "<" and ">", while the indices for the crystallographic planes will be bracketed between the symbols "{" and "}". The crystallographic direction always indicates the direction of the normal vector of the corresponding crystallographic plane. For example, the crystallographic direction  $\langle 100 \rangle$  points in the direction of the normal vector of the crystallographic plane {100}. The cubic crystals, to which the fluoride crystals belong, have the principal crystallographic directions  $\langle 110 \rangle$ ,  $\langle \bar{1}10 \rangle$ ,  $\langle \bar{1}\bar{1}0 \rangle$ ,  $\langle \bar{1}\bar{1}\bar{0} \rangle$ ,  $\langle 101 \rangle$ ,  $\langle 10\bar{1} \rangle$ ,  $\langle \bar{1}01 \rangle$ ,  $\langle \bar{1}0\bar{1} \rangle$ ,  $\langle 011 \rangle$ ,  $\langle 0\bar{1}1 \rangle$ ,  $\langle 01\bar{1} \rangle$ ,  $\langle 111 \rangle$ ,  $\langle \bar{1}\bar{1}\bar{1} \rangle$ ,  $\langle \bar{1}\bar{1}1 \rangle$ ,  $\langle 1\bar{1}\bar{1} \rangle$ ,  $\langle \bar{1}\bar{1}\bar{1} \rangle$ ,  $\langle 100 \rangle$ ,  $\langle 010 \rangle$ ,  $\langle 001 \rangle$ ,  $\langle \bar{1}00 \rangle$ ,  $\langle 0\bar{1}0 \rangle$ , and  $\langle 00\bar{1} \rangle$ . Because of the symmetries of cubic crystals, the principal crystallographic directions  $\langle 100 \rangle$ ,  $\langle 010 \rangle$ ,  $\langle 001 \rangle$ ,  $\langle \bar{1}00 \rangle$ ,  $\langle 0\bar{1}0 \rangle$ , and  $\langle 00\bar{1} \rangle$  are equivalent to each other, so that crystallographic directions that point in one of these principal crystallographic directions will hereinafter be identified with the prefix "(100)-". Crystallographic planes that are perpendicular to one of the principal crystallographic directions are accordingly identified by the prefix "(100)-". The principal crystallographic directions  $\langle 110 \rangle$ ,  $\langle \bar{1}10 \rangle$ ,  $\langle \bar{1}\bar{1}0 \rangle$ ,  $\langle \bar{1}\bar{1}\bar{0} \rangle$ ,  $\langle 101 \rangle$ ,  $\langle 10\bar{1} \rangle$ ,  $\langle \bar{1}01 \rangle$ ,  $\langle \bar{1}0\bar{1} \rangle$ ,  $\langle 011 \rangle$ ,  $\langle 0\bar{1}1 \rangle$ ,  $\langle 01\bar{1} \rangle$  and  $\langle 0\bar{1}\bar{1} \rangle$  are likewise equivalent to each other, so that crystallographic directions that point in one of these principal crystallographic directions will hereinafter be identified with the prefix "(110)-". Crystallographic planes that are perpendicular to one of the principal crystallographic directions are accordingly identified by the prefix "(110)-". The principal crystallographic directions  $\langle 111 \rangle$ ,  $\langle \bar{1}\bar{1}\bar{1} \rangle$ ,  $\langle \bar{1}\bar{1}1 \rangle$ ,  $\langle \bar{1}1\bar{1} \rangle$ ,  $\langle 1\bar{1}\bar{1} \rangle$ ,  $\langle \bar{1}\bar{1}\bar{1} \rangle$ ,  $\langle 1\bar{1}1 \rangle$ ,  $\langle 11\bar{1} \rangle$  and

<111> are likewise equivalent to each other, so that crystallographic directions that point in one of these principal crystallographic directions will hereinafter be identified with the prefix "(111)-". Crystallographic planes that are perpendicular to one of the principal crystallographic directions are accordingly identified by the prefix "(111)-". Hereinafter, statements made in reference to one of the aforementioned principal crystallographic directions will always be applicable likewise to the equivalent principal crystallographic directions.

[0005] Projection objectives and microlithography exposure projection apparatus are known, e.g., from the patent application PCT/EP00/13184 of the present applicant and the references that are cited in that application. The embodiments given in that application illustrate suitable purely refractive and catadioptric projection objectives with numerical aperture values of 0.8 and 0.9 at an operating wavelength of 193 nm as well as 157 nm.

[0006] The concept of rotating lens elements in order to compensate birefringence effects is also described in the present applicant's patent application "Microlithography Projection Apparatus, Optical System and Manufacturing Method" identified by applicant's file reference 01055P, with a filing date of May 15, 2001. The content of that application is hereby incorporated by reference in the present application.

[0007] The present invention has the object to propose projection objectives for a microlithography projection exposure apparatus, wherein the influence of intrinsic birefringence is significantly reduced.

[0008] The object just described is solved by an objective according to claim 1 and 8, a microlithography projection exposure apparatus according to claim 30, a method for the manufacture of semiconductor components according to claim 31, a method for the manufacture of objectives according to claim 32, and a method for the manufacture of lenses according to claim 35.

[0009] Advantageous embodiments of the invention are presented in the features of the dependent claims.

[0010] As a means for reducing the influence of intrinsic birefringence, claim 1 proposes to align the lens axes of lenses made of a fluoride crystal so that the lens axes coincide with the crystallographic <100>-direction. The lens axes are considered to be coinciding with a principal crystallographic direction, if the maximum deviation between lens axis and principal crystallographic direction is smaller than 5°. In this arrangement, it is not necessary for all of the fluoride crystal lenses of the objective to have the aforementioned orientation of the crystallographic planes. Those lenses in which the lens axes are oriented perpendicular to the crystallographic {100}-planes will hereinafter also be referred to as (100)-lenses. Orienting the lens axis in the crystallographic <100>-direction has the advantage that the aperture angles of the light rays where the undesirable influence of the intrinsic birefringence associated with a light propagation in the crystallographic <110>-direction becomes noticeable are larger than with an orientation of the lens axis in the crystallographic <111>-direction. The term aperture angle in the present context refers to the angle between a light ray and the optical axis outside of a lens and between a light ray and the lens axis inside a lens. Only as the aperture angles enter into the angular range between the

crystallographic  $<100>$ - and  $<110>$ - directions does the influence of birefringence manifest itself in the respective light rays. The angle between the crystallographic  $<110>$ - and  $<100>$ - directions amounts to  $45^\circ$ . If the lens axis were, on the other hand, oriented in the crystallographic  $<111>$ - direction, the undesirable influence of intrinsic birefringence would be noticeable already at smaller aperture angles, as the angle between the crystallographic  $<110>$ - and  $<111>$ -directions is only  $35^\circ$ .

[0011] If the angle-dependence of the birefringence is caused, e.g., by the manufacturing process of the fluoride crystal or by mechanical stress applied to the lens, the conceptual solutions disclosed herein can, of course, be used to lessen the undesirable influence of the birefringence.

[0012] The lens axis is constituted, e.g., by a symmetry axis of a rotationally symmetrical lens. If the lens has no symmetry axis, the lens axis can be defined by the center of an incident bundle of light rays or by a straight line in relation to which the ray angles of all light rays inside the lens are minimal. The lenses can be, e.g., refractive or diffractive lenses as well as corrective plates with free-form corrective surfaces. Planar-parallel plates, too, are considered as lenses, if they are arranged in the light path of the objective. The lens axis of a planar-parallel plate is perpendicular to the planar lens surfaces.

[0013] With preference, however, the lenses in the present context are rotationally symmetric lenses.

[0014] Objectives have an optical axis that runs from the object plane to the image plane. With preference, the  $(100)$ -lenses are arranged in centered alignment relative to this

optical axis, so that the lens axes also coincide with the optical axis.

[0015] The invention can be used to good advantage in projection objectives for a microlithography projection exposure apparatus, because the requirements in regard to resolution are extremely high for these objectives. But in test objectives, too, which are used for example to test lenses for projection objectives through measurements of wave fronts with large aperture, the influence of birefringence has a detrimental effect.

[0016] In objectives with large numerical aperture values on the image side, in particular larger than 0.7, aperture angles larger than 25° and in particular larger than 30° will occur inside the (100)-lenses. It is especially at these large aperture angles that the inventive concept of orienting the lens axes in the crystallographic <100>-direction proves to be useful. If the lens axes were oriented in the crystallographic <111>-direction, the undesirable influence of the birefringence would manifest itself more noticeably at aperture angles larger than 25° and in particular larger than 30°, unless one of the corrective measures is used which are described hereinafter.

[0017] Since on the other hand, the undesirable influence of intrinsic birefringence can have a maximum at an aperture angle of 45°, it is advantageous to design the projection objective in such a way that all aperture angles of the light rays are smaller than 45°, in particular smaller than or equal to  $\arcsin\left(\frac{NA}{n_{FK}}\right)$ , wherein NA stands for the image-side numerical aperture and  $n_{FK}$  stands for the refractive index of the

fluoride crystal. The expression  $\arcsin\left(\frac{NA}{n_{FK}}\right)$  represents the aperture angle that corresponds to the image-side numerical aperture inside a fluoride crystal lens if the light ray is refracted at a planar surface. This is achieved by a design in which the lenses that are arranged near the image plane have light-collecting lens surfaces, planar lens surfaces or at most slightly dispersing lens surfaces, if in the direction of the light path the light-dispersing lens surface is followed by a lens surface of a stronger light-collecting power.

[0018] Large aperture angles occur primarily in lenses near field planes, in particular near the image plane. The (100)-lenses should therefore be used with preference in the vicinity of the field planes. The range where the (100)-lenses should be used can be determined by way of the ratio between the lens diameter and the diameter of the aperture stop. Thus, the lens diameter of the (100)-lenses is preferably at most 85%, in particular at most 80% of the aperture stop diameter.

[0019] In projection objectives, the largest aperture angles occur as a rule in the lens closest to the image plane. It is therefore preferred to align the lens axis of this lens in the crystallographic <100>-direction.

[0020] Also, the intrinsic birefringence of a fluoride crystal lens is dependent not only on the aperture angle of a light ray, but also on the azimuth angle of the light ray. Thus, every fluoride crystal lens can be characterized by a birefringence distribution  $\Delta n(\alpha_L, \theta_L)$  that is on the one hand a function of the aperture angle  $\theta_L$  and on the other hand a function of the azimuth angle  $\alpha_L$ . For a ray direction that is

defined by the aperture angle  $\theta_L$  and the azimuth angle  $\alpha_L$ , the value of the birefringence  $\Delta n$  indicates in the unit [nm/cm] the ratio between the optical path difference for two mutually orthogonal states of linear polarization and the physical ray path in the fluoride crystal. Thus, the intrinsic birefringence is independent of the ray paths and the lens shape. The optical path difference for a ray is obtained accordingly by multiplying the birefringence value with the ray path covered. The aperture angle  $\theta_L$  is determined between the ray direction and the lens axis, the azimuth angle  $\alpha_L$  between the projection of the ray direction into the crystallographic plane perpendicular to the lens axis and a reference direction that is physically fixed in the lens.

[0021] Because of the angle-dependence of the birefringence distributions of the individual fluoride crystal lenses, the rays of a bundle which merge in an image point in the image plane of the objective are subject to angle-dependent optical path differences  $\Delta OPL(\alpha_R, \theta_R)$  for two mutually orthogonal states of linear polarization. The optical path differences  $\Delta OPL$  in this expression are stated as a function of the aperture angle  $\theta_R$  and the azimuth angle  $\alpha_R$ . The aperture angle  $\theta_R$  of a ray is determined as the angle between the ray direction and the optical axis in the image plane, and the azimuth angle  $\alpha_R$  is determined as the angle between the projection of the ray direction into the image plane and a fixed reference direction in the image plane. If the objective has at least two lenses or lens parts of fluoride crystal, it is advantageous, if the lens axes of these lenses or lens parts point in a principal crystallographic direction and the lenses or lens parts are arranged with a rotation relative to each other about the lens axis such that the distribution  $\Delta OPL(\alpha_R, \theta_R)$  of the optical path differences has significantly reduced values in comparison to

an arrangement in which the lens axes point in the same crystallographic direction, but the lenses or lens parts are installed with uniform orientation. As the birefringence distributions of the lenses are azimuth-dependent, the rotated arrangement of the lenses can result in lowering the maximum value of the distribution  $\Delta OPL(\alpha_R, \theta_R)$  by as much as 20%, in particular by as much as 25%, in comparison to an installation with uniform orientation of the lenses.

[0022] Lens parts can for example refer to individual lenses that are combined into a single lens by wringing, so that they have an optically seamless joint surface. In the most general sense, lens parts are defined as the components of a single lens, wherein the lens axis of each of the lens parts points in the direction of the lens axis of the single lens.

[0023] The rotated installation of the fluoride crystal lenses can in particular lead to a noticeable reduction of the dependence of the distribution  $\Delta OPL(\alpha_R, \theta_R)$  on the azimuth angle  $\alpha_R$ , resulting in a distribution  $\Delta OPL(\alpha_R, \theta_R)$  that is close to rotational symmetry.

[0024] If the lens axis is oriented in a principal crystallographic direction, the birefringence distribution  $\Delta n(\alpha_L, \theta_L)$  of the lens will have a k-fold azimuthal symmetry. For example, the birefringence distribution of a (100)-lens whose lens axis points in the crystallographic <100>-direction, has a fourfold azimuthal symmetry, while the birefringence distribution of a (111)-lens whose lens axis points in the crystallographic <111>-direction, has a threefold azimuthal symmetry, and the birefringence distribution of a (110)-lens whose lens axis points in the crystallographic <110>-direction, has a twofold azimuthal symmetry. Depending on the rank of the azimuthal symmetry,

the individual lenses or lens parts of a group are arranged with a rotation about the lens axis by a given angle  $\gamma$  relative to each other. The rotation angles  $\gamma$  are measured between the respective reference directions of two lenses or lens parts. The lens axes of the lenses in a group are oriented in one and the same or an equivalent principal crystallographic direction. The reference directions of the lenses in a group are fixed in the lenses in such a way that the birefringence distributions  $\Delta n(\alpha_L, \theta_0)$  have the same azimuthal profile for a given aperture angle  $\theta_0$ . Thus, the azimuthal locations where the birefringence has its maxima occur at the same azimuth angles in all lenses of a group. In a group of  $n$  lenses, the angles of rotation between each two lenses are determined as follows:

$$\gamma = \frac{360^\circ}{k \cdot n} + m \cdot \frac{360^\circ}{k} \pm 10^\circ$$

where  $k$  indicates the rank of the azimuthal symmetry,  $n$  stands for the number of lenses in a group, and  $m$  stands for an arbitrary integer number. The tolerance of  $\pm 10^\circ$  allows for the fact that the angles of rotation may deviate from the theoretically ideal angles, so that other boundary constraints can be taken into account in the adjustment of the objective. A deviation from the ideal angle of rotation leads to a non-optimized azimuthal equalization of the optical path differences for the lenses in a group. However, this can be tolerated within certain limits.

[0025] Accordingly, the angles of rotation for (100)-lenses are determined as follows:

$$\gamma = \frac{90^\circ}{n} + m \cdot 90^\circ \pm 10^\circ.$$

If the group has two (100)-lenses, the ideal angle of rotation between the two lenses is  $45^\circ$ , or  $135^\circ$ ,  $225^\circ$  ...

[0026] The angles of rotation for (111)-lenses are determined as follows:

$$\gamma = \frac{120^\circ}{n} + m \cdot 120^\circ \pm 10^\circ.$$

[0027] The angles of rotation for (110)-lenses are determined as follows:

$$\gamma = \frac{180^\circ}{n} + m \cdot 180^\circ \pm 10^\circ.$$

[0028] The distribution of the optical path differences  $\Delta OPL_G(\alpha_R, \theta_R)$  can also be stated for the influence of an individual group of lenses, if they are the only lenses considered in the evaluation of the birefringence and the other lenses are assumed not to be birefringent.

[0029] The lenses of a group are determined, e.g., according to the criterion that an outermost aperture ray of a bundle of rays has similar aperture angles inside these lenses. It is of advantage if the aperture angles of the outermost aperture ray is larger than  $15^\circ$  in these lenses, in particular if it is larger than  $20^\circ$ . The term "outermost aperture ray" refers to a ray that originates from an object point and whose ray height in the aperture stop plane equals the radius of the aperture stop, so that in the image plane, this ray has an angle corresponding to the image-side numerical aperture. The reason why the outermost aperture rays are used to define the groups is that they normally have the largest aperture angles inside the lenses and are thus affected the most by the undesirable effects of the birefringence. By determining the optical path difference for two mutually orthogonal states of linear polarization for the outermost aperture rays, one can therefore arrive at conclusions about the maximum irregularity of a wave front due to birefringence.

[0030] It is further advantageous if the outermost aperture ray in each of these lenses has an equal ray path. This measure has the result of a good compensation of the azimuthal contributions to the distribution of the optical path differences that are caused by the individual lenses of a group, so that the resultant distribution of the optical path differences is close to rotationally symmetric.

[0031] It is also advantageous if with a uniform orientation of the lenses, the outermost aperture ray in each lens of a group is subjected to an optical path difference of similar magnitude between two mutually orthogonal states of linear polarization. If this condition is met, the rotated arrangement of these lenses will lead to an optimized balancing of the azimuthal contributions.

[0032] In the case of adjacent planar-parallel (100)- or (111)-lenses of equal thickness, or four adjacent planar-parallel (110)-lenses of equal thickness, the rotation of the lenses in accordance with the foregoing formulae produces a rotationally symmetric distribution of the optical path differences  $\Delta OPL$ . In lenses with curved surfaces, it is likewise possible through a judicious selection of the lenses of a group or through an appropriate choice of the thicknesses and radii of the lenses to achieve an approximately rotation-symmetric birefringence distribution already by rotating only two (100)-lenses. In the case of (100)-lenses or (111)-lenses, it is advantageous if a group has two lenses. In (110)-lenses, a distribution of the optical path differences with approximate rotational symmetry is obtained with four lenses in a group.

[0033] Rotating the lenses is particularly effective if the lenses are arranged adjacent to each other. It is particularly advantageous to split a lens into two parts and to combine the lens parts in rotated positions relative to each other with an optically seamless joint, for example by wringing.

[0034] In a projection objective with a multitude of lenses it is advantageous to form a plurality of groups of lenses. The lenses of a group are arranged with a rotation about the lens axis such that the resultant distribution  $\Delta OPL(\alpha_R, \theta_R)$  is nearly independent of the azimuth angle.

[0035] While the rotation of the lenses in a group relative to each other has the effect that the distributions  $\Delta OPL_G(\alpha_R, \theta_R)$  that are caused by the individual groups are nearly independent of the azimuth angle, the maximum value of the overall distribution  $\Delta OPL(\alpha_R, \theta_R)$  can be noticeably reduced by using at least one group of (100)-lenses as well as at least one group of (111)-lenses in the projection objective. A good compensation is also possible, if a group of (110)-lenses is arranged within the objective in addition to a group of (100)-lenses.

[0036] The compensation is possible because the birefringence has not only an absolute value but also a direction. The compensation of the undesirable influence of the birefringence is optimal, if the distribution of the optical path differences  $\Delta OPL_1(\alpha_R, \theta_R)$  that is caused by the lenses or lens parts of all groups with (100)-lenses has maximum values of similar magnitude as the distribution of the optical path differences  $\Delta OPL_2(\alpha_R, \theta_R)$  that is caused by the lenses or lens parts of all groups with (111)- or (110)-lenses.

[0037] The preferred material to use for the lenses in projection objectives is calcium fluoride, because when used together with quartz at an operating wavelength of 193 nm, calcium fluoride is particularly well suited for the color correction, and with an operating wavelength of 157 nm, it still has a sufficient transmissivity. However, the foregoing statements are likewise applicable to the fluoride crystals strontium fluoride and barium fluoride, as they are crystals of the same type of cubic crystal structure.

[0038] The undesirable influence of intrinsic birefringence becomes particularly noticeable if the light rays inside the lenses have large aperture angles. This is the case in projection objectives with an image-side numerical aperture larger than 0.7, in particular larger than 0.8.

[0039] The intrinsic birefringence becomes noticeably stronger with decreasing working wavelength. Thus, the intrinsic birefringence at a wavelength of 193 nm is more than twice as strong, and at a wavelength of 157 nm it is more than five times as strong as it is at a wavelength of 248 nm. The invention can therefore be used to particular advantage if the light rays have wavelengths shorter than 200 nm, in particular shorter than 160 nm.

[0040] The objective in the present context can be a purely refractive projection objective that consists of a multitude of lenses arranged with rotational symmetry about the optical axis, or it can be a projection objective of the catadioptric type of objectives.

[0041] Projection objectives of this kind can be used advantageously in microlithography projection exposure apparatus which include a light source followed by an

illumination system, a mask-positioning system, a structure-carrying mask, a projection objective, an object-positioning system, and a light-sensitive substrate.

[0042] This microlithography projection exposure apparatus can be used to produce micro-structured semiconductor elements.

[0043] The invention also provides a suitable method for the manufacture of objectives. According to the method, lenses or lens parts of fluoride crystal wherein the lens axes are oriented in a principal crystallographic direction are arranged with a rotation about the lens axes such that the values of the distribution  $\Delta OPL(\alpha_R, \theta_R)$  are significantly reduced in comparison to a lens arrangement in which the lens axes of the fluoride crystal lenses point in the same principal crystallographic direction and where the lenses have a uniform orientation.

[0044] The method further includes the concept of forming groups of (100)-lenses and groups of (111)-lenses or (110)-lenses and to use the groups in parallel. The method is in this case applied, e.g., in a projection objective that has at least two fluoride crystal lenses in <100>-orientation and at least two lenses in <111>-orientation, where the orientation of the reference directions is known for these lenses. The method makes use of the inventive observation that the maximum values of the distribution  $\Delta OPL(\alpha_R, \theta_R)$  of the optical path differences can be significantly reduced by rotating the fluoride crystal lenses about the optical axis. Using suitable simulation methods, a bundle of light rays originating from an object point is propagated through a projection objective, and the distribution  $\Delta OPL(\alpha_R, \theta_R)$  in the image plane is calculated on the basis of the known optical

properties of the fluoride crystal lenses. In an optimizing step of the method, the angles of rotation between the fluoride crystal lenses are varied until the birefringence values are within tolerance. It is possible to take further boundary constraints into account in the optimizing step, such as for example the compensation of rotationally non-symmetric lens errors by rotating the lenses. This optimizing step can reduce the maximum value of the distribution  $\Delta OPL(\alpha_R, \theta_R)$  by up to 30%, in particular cases up to 50%, in comparison to a projection objective in which the fluoride crystal lenses are arranged with uniform orientation. The optimizing routine can also contain an intermediate step in which groups are formed among the fluoride crystal lenses, where the lenses in each group, when arranged with uniform orientation of the lenses, produce a similar optical path difference between two mutually orthogonal states of linear polarization in an outermost aperture ray. In the subsequent optimizing step, the lenses are rotated only within the groups in order to reduce the optical path differences. Thus, the (100)-lenses can first be rotated so that the optical path differences caused by the (100)-lenses are reduced, and subsequently the (111)-lenses are rotated so that the optical path differences caused by them are reduced. The allocation of the fluoride crystal lenses to lenses with (100)-orientation and (111)-orientation, respectively, has to be made in such a manner in the optimization that the resultant (100)-distribution  $\Delta OPL_{100}(\alpha_R, \theta_R)$  and the resultant (111)-distribution  $\Delta OPL_{111}(\alpha_R, \theta_R)$  compensate each other to a large extent. An analogous statement also applies to arrangements where (100)-lenses and (110)-lenses are used in parallel.

[0045] The invention further relates to a method for the manufacture of a lens, where in a first step a plurality of fluoride crystal plates are joined in an optically seamless

manner to form a blank, and in a second step the lens is formed out of the blank through state-of-the-art manufacturing methods. The plates are arranged with a rotation relative to each other about the normal axes of the plate surfaces, analogous to the foregoing description for lenses or lens parts.

[0046] It is advantageous if plates in which the normal vectors of the surfaces are oriented in one and the same or an equivalent principal crystallographic direction are of equal axial thickness.

[0047] If (100)-plates are joined with (111)-plates in an optically seamless manner, the sum of the thicknesses of the (111)-plates in relation to the sum of the thicknesses of the (100)-plates should be in a ratio of  $1.5 \pm 0.2$ .

[0048] If (100)-plates are joined with (110)-plates in an optically seamless manner, the sum of the thicknesses of the (110)-plates in relation to the sum of the thicknesses of the (100)-plates should be in a ratio of  $4.0 \pm 0.4$ .

[0049] The invention will be explained in more detail with reference to the drawings.

[0050] Figure 1 illustrates a cross-section of a fluoride crystal block perpendicular to the crystallographic {100}-planes together with a lens of a projection objective in a schematic representation;

[0051] Figures 2A-C show, respectively, a planar-parallel lens with (100)-orientation, a planar-parallel lens with (111)-orientation, and a planar-parallel lens with (110)-orientation in a schematic three-dimensional representation;

[0052] Figure 3 shows a coordinate system for the definition of the aperture angle and the azimuth angle;

[0053] Figures 4A-F illustrate the birefringence distributions of (100)-lenses in different representations as well as the birefringence distribution for two (100)-lenses that are rotated relative to each other by 45°;

[0054] Figures 5A-F illustrate the birefringence distributions of (111)-lenses in different representations as well as the birefringence distribution for two (111)-lenses that are rotated relative to each other by 60°;

[0055] Figures 6A-G illustrate the birefringence distributions of (111)-lenses in different representations as well as the birefringence distribution for two (110)-lenses that are rotated relative to each other by 90° and four (110)-lenses that are rotated relative to each other by 45°;

[0056] Figure 7 represents the lens section of a refractive projection objective;

[0057] Figure 8 represents the lens section of a catadioptric projection objective; and

[0058] Figure 9 illustrates a microlithography projection exposure apparatus in a schematic representation.

[0059] Figure 1 schematically illustrates a section through a fluoride crystal block 3. The section is selected so that the crystallographic {100}-planes 5 can be seen as individual lines, i.e., the crystallographic {100}-planes 5 are oriented perpendicular to the plane of the paper. The fluoride crystal

block 3 serves as a blank or raw material for the (100)-lens 1. In the illustrated example, the (100)-lens 1 is a bi-convex lens with the lens axis EA which is at the same time the symmetry axis of the lens. The lens 1 is now formed out of the fluoride crystal block in such a manner that the lens axis EA stands perpendicular to the crystallographic {100}-planes.

[0060] Figure 2A visualizes in a three-dimensional representation how the intrinsic birefringence is related to the crystallographic directions in the case where the lens axis EA points in the crystallographic <100>-direction. The lens shown in Figure 2A is a circular planar-parallel plate 201 of calcium fluoride. The lens axis EA points in the crystallographic <100>-direction. Besides the crystallographic <100>-direction, the crystallographic <101>-, <1 $\bar{1}$ 0>-, <10 $\bar{1}$ >-, and <110>-directions are likewise represented as arrows. The intrinsic birefringence is represented schematically by four lobes 203, whose surface areas represent the amount of the intrinsic birefringence for the respective ray direction of a light ray. The maxima for the intrinsic birefringence occur, respectively, in the crystallographic <101>-, <1 $\bar{1}$ 0>-, <10 $\bar{1}$ >-, and <110>-directions, i.e., for light rays with an aperture angle of 45° and an azimuth angle of 0°, 90°, 180° and 270° inside the lens. The minima of the intrinsic birefringence are associated with azimuth angles of 45°, 135°, 225° and 315°. The intrinsic birefringence vanishes at an aperture angle of 0°.

[0061] Figure 2B visualizes in a three-dimensional representation how the intrinsic birefringence is related to the crystallographic directions in the case where the lens axis EA points in the crystallographic <111>-direction. The lens shown in Figure 2B is a circular planar-parallel plate

205 of calcium fluoride. The lens axis EA points in the crystallographic  $\langle 111 \rangle$ -direction. Besides the crystallographic  $\langle 111 \rangle$ -direction, the crystallographic  $\langle 011 \rangle$ -,  $\langle 101 \rangle$ -, and  $\langle 110 \rangle$ -directions are likewise represented as arrows. The intrinsic birefringence is represented schematically by three lobes 207, whose surface areas represent the amount of the intrinsic birefringence for the respective ray directions of a light ray. The maxima for the intrinsic birefringence occur, respectively, in the crystallographic  $\langle 011 \rangle$ -,  $\langle 101 \rangle$ -, and  $\langle 110 \rangle$ -directions, i.e., for light rays with an aperture angle of  $35^\circ$  and an azimuth angle of  $0^\circ$ ,  $120^\circ$ , and  $240^\circ$  inside the lens. The minima of the intrinsic birefringence are associated with azimuth angles of  $60^\circ$ ,  $180^\circ$ , and  $300^\circ$ . The intrinsic birefringence vanishes at an aperture angle of  $0^\circ$ .

[0062] Figure 2C visualizes in a three-dimensional representation how the intrinsic birefringence is related to the crystallographic directions in the case where the lens axis EA points in the crystallographic  $\langle 110 \rangle$ -direction. The lens shown in Figure 2C is a circular planar-parallel plate 209 of calcium fluoride. The lens axis EA points in the crystallographic  $\langle 110 \rangle$ -direction. Besides the crystallographic  $\langle 110 \rangle$ -direction, the crystallographic  $\langle 01\bar{1} \rangle$ -,  $\langle 10\bar{1} \rangle$ -,  $\langle 101 \rangle$ -, and  $\langle 011 \rangle$ -directions are likewise represented as arrows. The intrinsic birefringence is represented schematically by five lobes 211, whose surface areas represent the amount of the intrinsic birefringence for the respective ray direction of a light ray. The respective maxima for the intrinsic birefringence occur on the one hand in the direction of the lens axis EA and on the other hand in the crystallographic  $\langle 01\bar{1} \rangle$ -,  $\langle 10\bar{1} \rangle$ -,  $\langle 101 \rangle$ -, and  $\langle 011 \rangle$ -directions, i.e., for light rays with an aperture angle of  $0^\circ$ , and for light rays with an aperture angle of  $60^\circ$  and the four

azimuth angles that are obtained as a result of projecting the crystallographic  $\langle 01\bar{1} \rangle$ -,  $\langle 10\bar{1} \rangle$ -,  $\langle 101 \rangle$ -, and  $\langle 011 \rangle$ -directions into the crystallographic {110}-plane. However, aperture angles of such a high magnitude do not occur in crystal material, because the maximum aperture angles are limited to a value of less than 45° by the refractive index of the crystal.

[0063] The definition of aperture angle  $\theta$  and azimuth angle  $\alpha$  is illustrated in Figure 3. For the (100)-lens of Figure 2, the z-axis points in the crystallographic  $\langle 100 \rangle$ -direction, and the x-axis points in the crystallographic direction that is obtained by projecting the crystallographic  $\langle 110 \rangle$ -direction into the crystallographic {100}-plane. In this representation, the z-axis equals the lens axis and the x-axis equals the reference direction.

[0064] As disclosed in the Internet publication cited hereinabove, in measurements with a light ray propagation in the crystallographic  $\langle 110 \rangle$ -direction, a birefringence of  $(6.5 \pm 0.4) \text{ nm/cm}$  was found at a wavelength of  $\lambda = 156.1 \text{ nm}$  in calcium fluoride. Taking this measured value as a normative factor, it is possible to theoretically derive the birefringence distribution  $\Delta n(\theta, \alpha)$  of a calcium fluoride lens dependent on the crystal orientation. The computations are based on the formalisms known from crystal optics for the calculation of the index ellipsoids dependent on the direction of the light ray. The theoretical basis can be found, e.g., in "Lexikon der Optik", Spektrum Akademischer Verlag Heidelberg Berlin 1999 under the term "Kristalloptik".

[0065] Represented in Figure 4A is the amount of the intrinsic birefringence as a function of the aperture angle  $\theta$  for the azimuth angle  $\alpha = 0^\circ$  in a (100)-lens. The value of  $6.5 \text{ nm/cm}$  for the intrinsic birefringence at an aperture angle

of  $\theta = 45^\circ$  represents the measured value. The curve profile was determined according to the formulae that are known from crystal optics.

[0066] Figure 4B illustrates the intrinsic birefringence as a function of the azimuth angle  $\alpha$  for the aperture angle  $\theta = 45^\circ$  in a (100)-lens. The fourfold symmetry is evident.

[0067] Figure 4C illustrates the birefringence distribution  $\Delta n(\theta, \alpha)$  for individual ray directions in a  $(\theta, \alpha)$  coordinate space for a (100)-lens. Each line represents the amount and the direction for a ray direction that is defined by the aperture angle  $\theta$  and the azimuth angle  $\alpha$ . The length of the lines is proportional to the amount of the birefringence or the length difference between the principal axes of the elliptical section, while the direction of the lines indicates the orientation of the longer principal axis of the elliptical section. The elliptical section is obtained by intersecting the index ellipsoid for the ray of the direction  $(\theta, \alpha)$  with a plane that is perpendicular to the ray direction and passes through the center point of the index ellipsoid. The directions as well as the lengths of the lines indicate the fourfold structure of the distribution. The length of the lines, and thus the amount of the birefringence, has its maxima at the azimuth angles of  $0^\circ$ ,  $90^\circ$ ,  $180^\circ$ , and  $270^\circ$ .

[0068] Figure 4D illustrates the birefringence distribution  $\Delta n(\theta, \alpha)$  that is obtained by arranging two adjacent planar-parallel (100)-lenses of equal thickness with a rotation of  $45^\circ$ . The resultant birefringence distribution  $\Delta n(\theta, \alpha)$  is independent of the azimuth angle  $\alpha$ . The longer principal axes of the elliptical sections run in the tangential direction. The resultant optical path differences between two mutually orthogonal states of polarization are obtained by multiplying

the birefringence values with the physical path lengths of the rays inside the planar-parallel (100)-lenses. Rotationally symmetric birefringence distributions are obtained by arranging n planar-parallel (100)-lenses of equal thickness in such a manner that the angle of rotation  $\beta$  between each two lenses conforms to the equation:

$$\beta = \frac{90^\circ}{n} + m \cdot 90^\circ \pm 5^\circ$$

wherein n stands for the number of planar-parallel (100)-lenses and m represents an integer number. In comparison to an arrangement of uniformly oriented lenses, the maximum value of the birefringence for the aperture angle  $\theta = 30^\circ$  can be reduced by 30%. A rotationally near-symmetric distribution of the optical path differences for two mutually orthogonal states of linear polarization is also obtained for arbitrary lenses if all rays of a bundle have respective aperture angles of similar magnitude in the lenses and cover similar path lengths inside the lenses. The lenses should therefore be combined into groups where the rays conform as much as possible to the foregoing condition.

[0069] Figure 4E represents the amount of the intrinsic birefringence as a function of the aperture angle  $\theta$  for the azimuth angle  $\alpha=0^\circ$  for the two adjacent planar-parallel (100)-lenses of equal thickness that are shown in Figure 4D. The maximum value for the intrinsic birefringence at the aperture angle  $\theta=41^\circ$  amounts to 4.2 nm/cm and is thus reduced by 35% in comparison to the maximum value of 6.5 nm/cm of Figure 4A.

[0070] Figure 4F represents the amount of the intrinsic birefringence as a function of the azimuth angle  $\alpha$  with the aperture angle  $\theta=41^\circ$  for the two adjacent planar-parallel (100)-lenses of equal thickness that are shown in Figure 4D.

The intrinsic birefringence is independent of the azimuth angle  $\alpha$ .

[0071] Figure 5A represents the intrinsic birefringence as a function of the aperture angle  $\theta$  for the azimuth angle  $\alpha = 0^\circ$  in a (111)-lens. The value of 6.5 nm/cm for the intrinsic birefringence at an aperture angle of  $\theta = 35^\circ$  represents the measured value. The curve profile was determined according to the formulae that are known from crystal optics.

[0072] Figure 5B illustrates the intrinsic birefringence as a function of the azimuth angle  $\alpha$  for the aperture angle  $\theta = 35^\circ$  for a (111)-lens. The threefold azimuthal symmetry is evident.

[0073] Figure 5C illustrates the birefringence distribution  $\Delta n(\theta, \alpha)$  for individual ray directions in the  $(\theta, \alpha)$  coordinate space for a (111)-lens in an analogous representation as was introduced already in Figure 4C. The directions as well as the lengths of the lines indicate the threefold structure of the distribution. The length of the lines, and thus the birefringence, has its maxima at the azimuth angles of  $0^\circ$ ,  $120^\circ$ , and  $240^\circ$ . In contrast to a (100)-lens, the orientation of the birefringence rotates by  $90^\circ$  if a ray passes through the lens with an azimuth angle of  $180^\circ$  instead of with an azimuth angle of  $0^\circ$ . Thus, the birefringence can be compensated, e.g., by two (111)-lenses of equal orientation, if the ray angles of a ray bundle change signs between the two lenses.

[0074] Figure 5D illustrates the birefringence distribution  $\Delta n(\theta, \alpha)$  that is obtained by arranging two adjacent planar-parallel (111)-lenses of equal thickness with a rotation of  $60^\circ$ . The resultant birefringence distribution  $\Delta n(\theta, \alpha)$  is

independent of the azimuth angle  $\alpha$ . However, in contrast to Figure 4C, the longer principal axes of the elliptical sections run in the radial direction. The resultant optical path differences between two mutually orthogonal states of polarization are obtained by multiplying the birefringence values with the physical path lengths inside the (111)-lenses. Rotationally symmetric birefringence distributions are likewise obtained by arranging  $n$  planar-parallel (111)-lenses of equal thickness in such a manner that the angle of rotation between each two lenses conforms to the equation:

$$\gamma = \frac{120^\circ}{k} + l \cdot 120^\circ \pm 5^\circ$$

wherein  $k$  stands for the number of planar-parallel (111)-lenses and  $l$  represents an integer number. In comparison to an arrangement of uniformly oriented lenses, the value of the birefringence for the aperture angle  $\theta = 30^\circ$  can be reduced by 68%. A rotationally near-symmetric distribution of the optical path differences for two mutually orthogonal states of linear polarization is also obtained for arbitrary lenses if all rays of a bundle have aperture angles of similar magnitude in the lenses and cover similar path lengths inside the lenses. Therefore, the lenses should be combined into groups where the rays conform as much as possible to the foregoing condition.

[0075] Figure 5E represents the amount of the intrinsic birefringence as a function of the aperture angle  $\theta$  for the azimuth angle  $\alpha=0^\circ$  for the two adjacent planar-parallel (111)-lenses of equal thickness that are shown in Figure 5D. The maximum value for the intrinsic birefringence at the aperture angle  $\theta=41^\circ$  amounts to 2.8 nm/cm and is thus reduced by 57% in comparison to the maximum value of 6.5 nm/cm of Figure 5A.

[0076] Figure 5F represents the amount of the intrinsic birefringence as a function of the azimuth angle  $\alpha$  for the aperture angle  $\theta=41^\circ$  in the two adjacent planar-parallel (111)-lenses of equal thickness that are shown in Figure 5D. The intrinsic birefringence is independent of the azimuth angle  $\alpha$ .

[0077] Now, if one combines groups of (100)-lenses and groups of (111)-lenses within a projection objective, it is possible to compensate to a large extent the contributions of these lenses to the optical path differences for two mutually orthogonal states of linear polarization. To accomplish this, it is first necessary that within these groups a distribution of the optical path differences close to rotational symmetry is obtained by rotating the lenses, and then that by combining a group of (100)-lenses with a group of (111)-lenses, their respective distributions of the optical path differences will compensate each other. To achieve this result, one makes use of the fact that the orientations of the longer principal axes of the elliptical sections for the birefringence distribution of a group of rotated (100)-lenses are perpendicular to the orientations of the longer principal axes of the elliptical sections of the birefringence distribution of a group of rotated (111)-lenses, as can be concluded from Figures 4D and 5D. In this respect, it is of critical importance that on the one hand the individual groups produce a distribution of the optical path differences close to rotational symmetry and on the other hand the sum of the contributions of the groups of (100)-lenses closely matches the sum of the contributions of the groups of (111)-lenses in regard to the absolute amounts.

[0078] Figure 6A represents the amount of intrinsic birefringence as a function of the aperture angle  $\theta$  for the azimuth angle  $\alpha = 0^\circ$  in a (110)-lens. The value of 6.5 nm/cm

for the intrinsic birefringence at the aperture angle of  $\theta = 0^\circ$  represents the measured value. The curve profile was determined according to the formulae that are known from crystal optics.

[0079] Figure 6B represents the amount of the intrinsic birefringence as a function of the azimuth angle  $\alpha$  for the aperture angle  $\theta = 35^\circ$  for a (110)-lens. The twofold azimuthal symmetry is evident.

[0080] Figure 6C illustrates the birefringence distribution  $\Delta n(\theta, \alpha)$  for individual ray directions in the  $(\theta, \alpha)$  coordinate space for a (110)-lens in an analogous representation as was introduced already in Figure 4C. The directions as well as the lengths of the lines indicate the twofold structure of the distribution. The line of maximum length, and thus the maximum amount of birefringence, occurs at an aperture angle  $\theta=0^\circ$ .

[0081] Figure 6D illustrates the birefringence distribution  $\Delta n(\theta, \alpha)$  that is obtained by arranging two adjacent planar-parallel (110)-lenses of equal thickness with a rotation of  $90^\circ$ . The resultant birefringence distribution  $\Delta n(\theta, \alpha)$  in this case has a fourfold azimuthal symmetry. Birefringence maxima occur at the azimuth angles  $\alpha=45^\circ, 135^\circ, 225^\circ$ , and  $315^\circ$ , where the birefringence at an aperture angle of  $\theta=40^\circ$  amounts to 2.6 nm/cm.

[0082] Figure 6E represents the birefringence distribution  $\Delta n(\theta, \alpha)$  that is obtained if the two planar-parallel (110)-lenses of equal thickness in Figure 6C are combined with two further planar-parallel (110)-lenses of equal thickness. The angle of rotation between each two of the (110)-lenses is  $45^\circ$ . The resultant birefringence distribution  $\Delta n(\theta, \alpha)$  is

independent of the azimuth angle  $\alpha$ . However, in contrast to Figure 4C, the longer principal axes of the elliptical sections are now oriented radially, i.e., similar to the distribution of Figure 5C. The resultant optical path differences between two mutually orthogonal states of polarization are obtained by multiplying the birefringence values with the physical path lengths of the rays inside the (110)-lenses. Rotationally symmetric birefringence distributions are likewise obtained by arranging  $4 \cdot n$  planar-parallel (110)-lenses of equal thickness in such a manner that the angle of rotation  $\beta$  between each two lenses conforms to the equation:

$$\beta = \frac{45^\circ}{n} + m \cdot 90^\circ \pm 5^\circ$$

wherein  $4 \cdot n$  stands for the number of planar-parallel (100)-lenses and  $m$  represents an integer number. A rotationally near-symmetric distribution of the optical path differences for two mutually orthogonal states of linear polarization is also obtained for arbitrary lenses if all rays of a bundle have respective aperture angles of similar magnitude in the lenses and cover similar path lengths inside the lenses. The lenses should therefore be combined into groups where the rays conform as much as possible to the foregoing condition.

[0083] Figure 6F represents the amount of the intrinsic birefringence as a function of the aperture angle  $\theta$  with the azimuth angle  $\alpha=0^\circ$  for the four adjacent planar-parallel (110)-lenses of equal thickness that are shown in Figure 6E. The value of the intrinsic birefringence at the aperture angle  $\theta=41^\circ$  amounts to 1.0 nm/cm which represents a reduction by 84% in relation to the maximum value of 6.5 nm/cm in Figure 5A.

[0084] Figure 6G represents the amount of the intrinsic birefringence as a function of the azimuth angle  $\alpha$  with the

aperture angle  $\theta=41^\circ$  for the four adjacent planar-parallel (110)-lenses of equal thickness that are shown in Figure 6E. The intrinsic birefringence is independent of the azimuth angle  $\alpha$ .

[0085] Now, if one combines groups of (110)-lenses and groups of (100)-lenses within a projection objective, it is possible to compensate to a large extent the contributions of these lenses to the optical path differences for two mutually orthogonal states of linear polarization. To accomplish this, it is first necessary that within these groups a distribution of the optical path differences close to rotational symmetry is obtained by rotating the lenses, and then that by combining a group of (110)-lenses with a group of (100)-lenses, the two distributions of the optical path differences will compensate each other. To achieve this result, one makes use of the fact that the orientations of the longer principal axes of the elliptical sections for the birefringence distribution of a group of rotated (110)-lenses are perpendicular to the orientations of the longer principal axes of the elliptical sections of the birefringence distribution of a group of rotated (100)-lenses, as can be concluded from Figures 4D and 6E. In this respect, it is of critical importance that on the one hand the individual groups produce a distribution of the optical path differences close to rotational symmetry and on the other hand the sum of the contributions of the groups of (110)-lenses are closely matched in their amounts to the sum of the contributions of the groups of (100)-lenses.

[0086] Figure 7 represents the lens section of a refractive projection objective 611 for the wavelength of 157 nm. The optical data for this objective are listed in Table 1. This example is taken from the applicant's patent application PCT/EP00/13184 where it corresponds to Figure 7 and Table 6.

For a detailed description of the function of the objective, see PCT/EP00/13184. All lenses of this objective consist of calcium fluoride crystal. The image-side numerical aperture of the objective is 0.9. The imaging performance of the objective is corrected so well that the deviation from a wave front of an ideal spherical wave is smaller than  $1.8 \text{ m}\lambda$  at  $\lambda = 157 \text{ nm}$ . Especially with these high-performance objectives, it is necessary for undesirable effects such as those of intrinsic birefringence to be reduced to the farthest extent possible.

[0087] For the embodiment of Figure 6, a calculation was made of the aperture angles  $\theta$  and ray paths  $RL_L$  of the outermost aperture ray 609 for the individual lenses L601 to L630. The outermost aperture ray 609 originates from the object point with the coordinates  $x = 0 \text{ mm}$  and  $y = 0 \text{ mm}$  and in the image plane has an angle relative to the optical axis that corresponds to the image-side numerical aperture. The reason why the outermost aperture ray 609 is selected is that it is associated with close to the maximum aperture angles inside the lenses.

Table 2

Lens	Aperture angle $\theta$ [°]	Ray path $R_{L_L}$ [mm]	Optical path difference [nm] (111)-Lens $\alpha_L = 0^\circ$	Optical path difference [nm] (111)-Lens $\alpha_L = 60^\circ$	Optical path difference [nm] (100)-Lens $\alpha_L = 0^\circ$	Optical path difference [nm] (100)-Lens $\alpha_L = 45^\circ$	Optical path difference [nm] (110)-Lens $\alpha_L = 0^\circ$	Optical path difference [nm] (110)-Lens $\alpha_L = 45^\circ$	Optical path difference [nm] (110)-Lens $\alpha_L = 90^\circ$	Optical path difference [nm] (110)-Lens $\alpha_L = 135^\circ$
L601	8.1	15.1	2.9	-2.2	-0.8	-0.4	-9.0	-9.0	-9.1	-9.0
L602	8.7	8.2	1.7	-1.2	-0.5	-0.2	-4.9	-4.8	-4.9	-4.8
L603	7.8	9.5	1.7	-1.3	-0.4	-0.2	-5.7	-5.7	-5.7	-5.7
L604	10.7	7.2	1.9	-1.3	-0.6	-0.3	-4.1	-4.1	-4.1	-4.1
L605	9.4	6.5	1.5	-1.0	-0.4	-0.2	-3.8	-3.8	-3.8	-3.8
L606	10.3	8.5	2.1	-1.4	-0.7	-0.3	-4.8	-4.8	-4.8	-4.8
L607	21.8	12.7	6.6	-2.7	-3.9	-1.8	-4.2	-4.2	-4.3	-4.2
L608	25.4	22.2	12.8	-4.4	-8.7	-3.9	-5.3	-5.7	-5.8	-5.7
L609	16.3	36.1	14.3	-7.6	-6.8	-3.3	-16.5	-16.5	-16.7	-16.5
L610	12.2	15.2	4.5	-2.9	-1.7	-0.8	-8.2	-8.2	-8.2	-8.2
L611	2.3	26.6	1.4	-1.3	-0.1	-0.1	-17.2	-17.2	-17.2	-17.2
L612	2.3	32.2	1.6	-1.5	-0.1	-0.1	-20.8	-20.8	-20.8	-20.8
L613	-18.3	30.4	-6.6	13.5	-7.0	-3.3	-12.5	-12.6	-12.7	-12.6
L614	-18.7	22.0	-4.8	10.0	-5.3	-2.5	-8.9	-8.9	-9.0	-8.9
L615	-14.0	10.2	-2.0	3.5	-1.5	-0.7	-5.1	-5.1	-5.2	-5.1
L616	-1.3	29.8	-0.8	0.9	0.0	0.0	-19.3	-19.3	-19.3	-19.3
L617	26.4	31.6	18.6	-6.1	-13.0	-5.7	-6.7	-7.6	-7.5	-7.6
L618	33.5	14.3	9.3	-2.0	-7.9	-3.1	-0.6	3.2	-1.4	3.2
L619	26.5	7.5	4.4	-1.4	-3.1	-1.4	-1.6	-1.8	-1.8	-1.8
L620	19.3	6.4	3.0	-1.4	-1.6	-0.8	-2.5	-2.5	-2.5	-2.5
L621	6.7	8.0	1.3	-1.0	-0.3	-0.1	-4.9	-4.9	-4.9	-4.9
L622	-10.3	7.7	-1.3	1.9	-0.6	-0.3	-4.4	-4.4	-4.4	-4.4
L623	-11.9	9.6	-1.8	2.8	-1.0	-0.5	-5.2	-5.2	-5.2	-5.2
L624	0.3	17.8	0.1	-0.1	0.0	0.0	-11.6	-11.6	-11.6	-11.6
L625	6.0	16.3	2.3	-1.8	-0.5	-0.2	-9.9	-9.9	-10.0	-9.9
L626	-24.0	9.0	-1.9	5.0	-3.2	-1.5	-2.5	-2.6	-2.6	-2.6
L627	-35.6	8.0	-0.9	5.2	-4.7	-1.7	0.1	2.1	-0.5	2.1
L628	-39.4	12.0	-1.0	7.6	-7.5	-2.5	1.0	4.0	-0.3	4.0
L629	-35.3	27.3	-3.3	17.7	-15.7	-5.9	0.5	6.9	-1.9	6.9
L630	-35.3	26.0	-3.1	16.9	-15.0	-5.6	0.4	6.5	-1.9	6.5
Sum			64,5	42,3	112,9	47,4	-198.2	-178.7	-208.0	-178.8

[0088] In addition to the aperture angles  $\theta$  and the path lengths  $R_{L_L}$  for the outermost aperture ray, Table 2 also lists the optical path differences between two mutually orthogonal states of linear polarization for different lens orientations. The optical path differences are shown for (111)-lenses as

well as for (100)-lenses and (110)-lenses, where the respective azimuth angle  $\alpha_L$  of the outermost marginal ray inside the lenses is  $0^\circ$  and  $60^\circ$  for a (111)-lens, and  $0^\circ$  and  $45^\circ$  for a (100)-lens, and  $0^\circ$ ,  $45^\circ$ ,  $90^\circ$ ,  $135^\circ$  for a (110)-lens.

[0089] As can be seen in Table 2, the aperture angles  $\theta$  for the lenses L608, L617, L618, L619, L627, L628, L629 and L630 are larger than  $25^\circ$ , and for the lenses L618, L627, L628, L629 and L630 even larger than  $30^\circ$ . Particularly affected by the large aperture angles are the lenses L627 to L630, which are closest to the image plane.

[0090] The projection objective was designed so that the maximum aperture angle of all light rays is smaller than  $45^\circ$ . The maximum aperture angle for the outermost aperture ray is  $39.4^\circ$  for the lens L628. Also helpful was the use of two thick planar lenses L629 and L630 immediately ahead of the image plane.

[0091] The diameter of the aperture stop located between the lenses L621 and L622 is 270 mm. The diameter of the lens L618 is 207 mm and the diameters of the lenses L627 to L630 are all smaller than 190 mm. Thus, the diameters of these lenses, which are associated with large aperture angles, are smaller than 80% of the aperture stop diameter.

[0092] As can be concluded from Table 2, it is advantageous to orient the individual lenses with large aperture angles in the (100)-direction, as the birefringence values will overall be lower. The reason for this lies in the fact that in (100)-lenses the influence of the crystallographic <110>-direction begins to manifest itself only at larger angles than it does in (111)-lenses. As an example the optical path differences for the lenses L608, L609 and L617 are more than 30% smaller.

[0093] The example of the two planar-parallel lenses L629 and L630 provides a good way of demonstrating how the birefringence can be noticeably reduced by rotating the lenses in relation to each other.

[0094] Both lenses have equal aperture angles of 35.3° for the outermost aperture ray and similar ray paths of 27.3 and 26.0 mm, respectively. If the two lenses were installed as (100)-lenses with equal orientation, there would be a resultant path difference of 30.7 nm. However, if the two (100)-lenses are rotated relative to each other by 45°, the optical path difference is reduced to 20.9 nm, i.e., by 32%. If the two lenses were installed as (111)-lenses with equal orientation, there would be a resultant optical path difference of 34.6 nm; but if the two (111)-lenses are rotated relative to each other by 60°, the optical path difference is reduced to 13.6 nm, i.e., by 61%.

[0095] A near-perfect compensation of the optical path differences for two mutually orthogonal states of linear polarization caused by intrinsic birefringence for the lenses L629 and L630 can be achieved if the lens L629 is split up into the lenses L6291 and L6292, and the lens L630 is split up into the lenses L6301 and L6302, wherein the lens L6291 is a (100)-lens with a thickness of 9.15 mm, the lens L6292 is a (111)-lens with a thickness of 13.11 mm, the lens L6301 is a (100)-lens with a thickness of 8.33 mm and the lens L6302 is a (111)-lens with a thickness of 12.9 mm. The lenses L6291 and L6301 are rotated against each other by 45°, and the lenses L6292 and L6302 are rotated against each other by 60°. The resultant maximum for the optical path difference in this case amounts to 0.2 nm. The lenses L6291 and L6292, as well as the lenses L6301 and L6302 can be joined together with an

optically seamless connection, e.g., by wringing. This concept is also applicable if the projection objective has only one crystal lens. In this case, the crystal lens is split into at least two lenses that are arranged with a rotation relative to each other. The joining can be accomplished by wringing. As another possibility, individual plates of the desired crystallographic orientation are joined through an optically seamless connection in a first step, and the lens is fabricated from the combined plates in a further process step.

[0096] As a further possibility to reduce the undesirable influence of the intrinsic birefringence caused by the lenses L629 and L630, the lens L629 is split up into the lenses L6293 and L6294, and the lens L630 is split up into the lenses L6303 and L6304, wherein the lens L6293 is a (110)-lens with a thickness of 11.13 mm, the lens 6294 is a (110)-lens with a thickness of 11.13 mm, the lens L6303 is a (110)-lens with a thickness of 10.62 mm, and the lens L6304 is a (110)-lens with a thickness of 10.62 mm. The lenses L6293 and 6294 as well as the lenses L6303 and L6304 are rotated against each other by 90°, wherein the angle of rotation between the lens L6293 and the lens L6303 amounts to 45°. The resultant maximum for the optical path difference in this case amounts to 4.2 nm. The lenses L6293 and L6294, as well as the lenses L6303 and L6304 can be joined together as lens parts with an optically seamless connection, e.g., by wringing.

[0097] A compensation of the optical path differences for two mutually orthogonal states of linear polarization that is caused by the strongly affected lenses L629 and L630 is accomplished with near-total success, if each lens is split up into three lens parts, i.e., L6295, L6296, L6297, and L6305, L6306, L6307, wherein the lens L6295 is a (100)-lens with a

thickness of 4.45 mm, the lenses L6296 and L6297 are (110)-lenses with a thickness of 8.90 mm, the lens L6305 is a (100)-lens with a thickness of 4.25 mm and the lenses L6306 and L6307 are (110)-lenses with a thickness of 8.49 mm. The lenses L6294 and L6304 are rotated relative to each other by 45°, and each two of the lenses L6295, L6297, L6306 and L6307 are rotated by 45°. With this combination, the resultant maximum optical path difference is reduced to less than 0.1 nm. The lenses L6295 to L6297 as well as the lenses L6305 to L6307 can be joined together as lens parts with an optically seamless connection, e.g., by wringing.

[0098] As a further possibility to reduce the undesirable influence of the intrinsic birefringence that is caused by the lenses L629 and L630, two (110)-lenses can be combined with a (100)-lens. In this case, the two (110)-lenses need to be installed with a rotation of 90° relative to each other, while the angle of rotation between the (100)-lens and the (110)-lenses is  $45^\circ + m \cdot 90^\circ$ , wherein  $m$  represents an integer number. In this case, the lens L629 is split up into the lenses L6298 and L6299, and the lens L630 is split up into the lenses L6308 and L6309, wherein the lens L6298 is a (110)-lens with a thickness of 17.40 mm, the lens L6299 is a (110)-lens with a thickness of 4.87 mm, the lens L6308 is a (110)-lens with a thickness of 12.53 mm and the lens L6309 is a (100)-lens with a thickness of 8.70 mm. The resultant maximum optical path difference is 3.1 nm. The lenses L6298 and L6299 as well as the lenses L6308 and L6309 can be joined together as lens parts with an optically seamless connection, e.g., by wringing.

[0099] Figure 8 represents the lens section of a catadioptric projection objective 711 for the wavelength of 157 nm. The optical data for this objective are listed in Table 3. This

embodiment is taken from the applicant's patent application PCT/EP00/13184 where it corresponds to Figure 9 and Table 8. For a detailed description of the function of the objective, see PCT/EP00/13184. All lenses of this objective consist of calcium fluoride crystal. The image-side numerical aperture of the objective is 0.8.

[0100] For the embodiment of Figure 8, a calculation was made of the aperture angles  $\theta$  and the ray paths  $RL_L$  of the upper outermost aperture ray 713 and the lower outermost aperture ray 715 for the individual lenses L801 to L817. In this case, the outermost aperture rays 713 and 715 originate from the object point with the coordinates  $x = 0$  mm and  $y = -82.15$  mm, and in the image plane have angles relative to the optical axis that correspond to the image-side numerical aperture. The calculation was made for the upper and lower outermost aperture rays because the object field in this case is an off-axis object field, so that the aperture rays are not symmetric in relation to the optical axis as was the case for the outermost aperture ray of the embodiment of Figure 7.

[0101] The data for the upper outermost aperture ray are listed in Table 4 and for the lower outermost aperture ray in Table 5. In addition to the aperture angles  $\theta$  and the path lengths  $RL_L$  for the outermost aperture ray, Tables 4 and 5 also list the optical path differences for two mutually orthogonal states of linear polarization for different lens orientations, specifically for (111)-lenses, (100)-lenses and (110)-lenses, wherein the azimuth angles  $\alpha_L$  of the outermost marginal ray inside the lenses are  $0^\circ$  and  $60^\circ$  for a (111)-lens,  $0^\circ$  and  $45^\circ$  for a (100)-lens, and  $0^\circ$ ,  $45^\circ$ ,  $90^\circ$ ,  $135^\circ$  for a (110)-lens.

Table 4

Lens	Aperture angle $\theta$ [°]	Ray path $RL_L$ [mm]	Optical path difference [nm] (111)-Lens $\alpha_L = 0^\circ$		Optical path difference [nm] (111)-Lens $\alpha_L = 60^\circ$		Optical path difference [nm] (100)-Lens $\alpha_L = 0^\circ$		Optical path difference [nm] (100)-Lens $\alpha_L = 45^\circ$		Optical path difference [nm] (110)-Lens $\alpha_L = 0^\circ$		Optical path difference [nm] (110)-Lens $\alpha_L = 45^\circ$		Optical path difference [nm] (110)-Lens $\alpha_L = 90^\circ$		Optical path difference [nm] (110)-Lens $\alpha_L = 135^\circ$	
801	1.4	28.1	0.8	-0.8	0.0	0.0	-18.2	-18.2	-18.2	-18.2	-18.2	-18.2	-18.2	-18.2	-18.2	-18.2	-18.2	-18.2
802	-10.8	30.7	-5.3	8.0	-2.7	-1.3	-17.2	-17.2	-17.2	-17.3	-17.3	-17.2	-17.2	-17.2	-17.2	-17.2	-17.2	-17.2
803	-15.6	32.4	-6.8	12.4	-5.7	-2.7	-15.3	-15.3	-15.3	-15.4	-15.4	-15.3	-15.3	-15.3	-15.3	-15.3	-15.3	-15.3
803	-24.4	31.8	-6.5	17.8	-11.7	-5.2	-8.4	-8.4	-8.4	-9.0	-9.0	-8.8	-8.8	-8.8	-8.8	-8.8	-8.8	-8.8
802	-19.5	26.6	-5.8	12.4	-6.8	-3.2	-10.2	-10.2	-10.2	-10.4	-10.4	-10.3	-10.3	-10.3	-10.3	-10.3	-10.3	-10.3
804	6.4	20.1	3.0	-2.4	-0.6	-0.3	-12.4	-12.4	-12.4	-12.4	-12.4	-12.4	-12.4	-12.4	-12.4	-12.4	-12.4	-12.4
805	10.8	34.4	9.0	-6.0	-3.0	-1.5	-19.3	-19.3	-19.3	-19.3	-19.3	-19.3	-19.3	-19.3	-19.3	-19.3	-19.3	-19.3
806	0.2	10.0	0.1	-0.1	0.0	0.0	-6.5	-6.5	-6.5	-6.5	-6.5	-6.5	-6.5	-6.5	-6.5	-6.5	-6.5	-6.5
807	-11.1	22.0	-3.9	5.9	-2.1	-1.0	-12.2	-12.2	-12.2	-12.3	-12.3	-12.2	-12.2	-12.2	-12.2	-12.2	-12.2	-12.2
808	0.1	18.5	0.0	0.0	0.0	0.0	-12.0	-12.0	-12.0	-12.0	-12.0	-12.0	-12.0	-12.0	-12.0	-12.0	-12.0	-12.0
809	-0.8	9.0	-0.1	0.2	0.0	0.0	-5.8	-5.8	-5.8	-5.8	-5.8	-5.8	-5.8	-5.8	-5.8	-5.8	-5.8	-5.8
810	1.1	12.4	0.3	-0.3	0.0	0.0	-8.0	-8.0	-8.0	-8.0	-8.0	-8.0	-8.0	-8.0	-8.0	-8.0	-8.0	-8.0
811	-16.8	9.4	-2.0	3.8	-1.9	-0.9	-4.2	-4.2	-4.2	-4.2	-4.2	-4.2	-4.2	-4.2	-4.2	-4.2	-4.2	-4.2
812	-10.4	29.8	-5.0	7.5	-2.4	-1.2	-16.9	-16.9	-16.9	-16.9	-16.9	-16.9	-16.9	-16.9	-16.9	-16.9	-16.9	-16.9
813	-8.8	34.7	-5.2	7.3	-2.1	-1.0	-20.5	-20.5	-20.5	-20.5	-20.5	-20.5	-20.5	-20.5	-20.5	-20.5	-20.5	-20.5
814	-9.4	17.5	-2.8	4.0	-1.2	-0.6	-10.2	-10.2	-10.2	-10.2	-10.2	-10.2	-10.2	-10.2	-10.2	-10.2	-10.2	-10.2
815	-27.4	28.1	-5.3	16.9	-12.2	-5.3	-5.2	-6.4	-6.4	-6.1	-6.1	-6.4	-6.4	-6.4	-6.4	-6.4	-6.4	-6.4
816	-28.7	40.2	-7.1	24.8	-18.6	-7.9	-6.2	-8.5	-8.5	-7.6	-7.6	-8.5	-8.5	-8.5	-8.5	-8.5	-8.5	-8.5
817	-30.8	39.0	-6.3	24.7	-19.6	-8.1	-3.9	-8.0	-8.0	-5.7	-5.7	-8.0	-8.0	-8.0	-8.0	-8.0	-8.0	-8.0
Sum			-48.9	136.1	-90.9	-40.3	-212.9	-220.9	-220.9	-218.0	-220.9	-220.9	-220.9	-220.9	-220.9	-220.9	-220.9	-220.9

Table 5

Lens	Aperture angle $\theta$ [°]	Ray path $RL_L$ [mm]	Optical path difference [nm] (111)-Lens $\alpha_L = 0^\circ$	Optical path difference [nm] (111)-Lens $\alpha_L = 60^\circ$	Optical path difference [nm] (100)-Lens $\alpha_L = 0^\circ$	Optical path difference [nm] (100)-Lens $\alpha_L = 45^\circ$	Optical path difference [nm] (110)-Lens $\alpha_L = 0^\circ$	Optical path difference [nm] (110)-Lens $\alpha_L = 45^\circ$	Optical path difference [nm] (110)-Lens $\alpha_L = 90^\circ$	Optical path difference [nm] (110)-Lens $\alpha_L = 135^\circ$
801	-11.6	32.1	-5.8	9.0	-3.2	-1.6	-17.6	-17.6	-17.6	-17.6
802	19.5	28.3	13.3	-6.1	-7.3	-3.4	-10.9	-10.9	-11.1	-10.9
803	24.7	33.8	19.1	-6.9	-12.7	-5.7	-8.6	-9.2	-9.3	-9.2
803	17.7	34.3	14.7	-7.4	-7.5	-3.6	-14.6	-14.6	-14.8	-14.6
802	12.7	31.6	9.7	-6.0	-3.8	-1.8	-16.7	-16.7	-16.8	-16.7
804	-5.2	27.7	-2.7	3.3	-0.6	-0.3	-17.4	-17.4	-17.4	-17.4
805	-4.5	34.6	-3.0	3.5	-0.5	-0.3	-21.9	-21.9	-21.9	-21.9
806	-8.6	19.5	-2.9	4.0	-1.1	-0.6	-11.6	-11.6	-11.6	-11.6
807	-0.5	16.5	-0.2	0.2	0.0	0.0	-10.7	-10.7	-10.7	-10.7
808	-8.2	25.6	-3.7	5.0	-1.3	-0.7	-15.3	-15.3	-15.3	-15.3
809	-7.5	10.1	-1.3	1.8	-0.4	-0.2	-6.1	-6.1	-6.1	-6.1
810	-9.1	13.1	-2.0	2.9	-0.8	-0.4	-7.7	-7.7	-7.7	-7.7
811	9.0	9.9	2.1	-1.5	-0.6	-0.3	-5.8	-5.8	-5.8	-5.8
812	2.6	30.7	1.8	-1.6	-0.2	-0.1	-19.8	-19.8	-19.8	-19.8
813	0.9	34.0	0.6	-0.6	0.0	0.0	-22.1	-22.1	-22.1	-22.1
814	1.3	10.4	0.3	-0.3	0.0	0.0	-6.7	-6.7	-6.7	-6.7
815	23.5	16.3	8.9	-3.4	-5.7	-2.6	-4.7	-4.8	-4.9	-4.8
816	24.6	37.2	21.0	-7.6	-13.9	-6.2	-9.6	-10.2	-10.3	-10.2
817	29.4	29.6	18.5	-5.1	-14.1	-5.9	-4.0	-6.2	-5.2	-6.2
Sum			88.3	-16.8	-73.7	-33.5	-231.9	-235.4	-235.2	-235.4

[0102] As can be seen in Tables 4 and 5, the aperture angles  $\theta$  for the lenses L815 to L817 are larger than  $25^\circ$ . In this embodiment, too, the lenses L815 and L817 which are closest to the image plane have large aperture angles. The lenses L815 to L817 were designed so that the maximum aperture angle is

smaller than  $\arcsin\left(\frac{NA}{n_{FK}}\right) = \arcsin\left(\frac{0.8}{1.5597}\right) = 30.9^\circ$ . The maximum

aperture angle for the outermost aperture ray is  $30.8^\circ$  for the lens L817.

[0103] The aperture stop that is located between the lenses L811 and L812 has a diameter of 193 mm. All of the lenses

L815 to L817 have diameters of less than 162 mm. Thus, the diameters of these lenses, which are associated with large aperture angles, are smaller than 85% of the aperture stop diameter.

[0104] Tables 4 and 5 lead to the conclusion that it is advantageous if lenses with large aperture angles are oriented in the (100)-direction, as the birefringence values are lower overall. For example for the lenses L815 to L817, the optical path differences are smaller by more than 20%.

[0105] The embodiment of Figure 8 will now be used to demonstrate how the intrinsic birefringence can be compensated to a large extent by using groups of (100)-lenses that are rotated relative to each other in parallel with groups of (111)-lenses that are rotated relative to each other.

[0106] At the beginning, all calcium fluoride lenses of (111)-orientation are installed without rotating the (111)-lenses relative to each other. As a result, there will be a maximum optical path difference between two mutually orthogonal states of linear polarization of 136 nm. By rotating the (111)-lenses, the maximum optical path difference can be reduced to about 38 nm. This is achieved by combining the lenses L801 and L804 in a group and the lenses L802 and L804 in a further group, wherein the angle of rotation between the lenses is in each case 60°. The lenses L808, L809 and L810 are combined into a group of three, and so are the lenses L815, L816 and L817, wherein the angle of rotation between each two lenses is 40°. The lenses L811, L812, L813 and L814 are combined into a group of four with an angle of rotation of 30° relative to each other.

[0107] If all calcium fluoride lenses of (100)-orientation are installed without rotating the (100)-lenses in relation to each other, the resultant maximum optical path difference between two mutually orthogonal states of linear polarization will be 90.6 nm. By rotating the (100)-lenses, the maximum optical path difference can be reduced to about 40 nm. This is achieved by combining the lenses L801 and L804 in a group and the lenses L802 and L803 in a further group, wherein the angle of rotation between the lenses is in each case 45°. The lenses L808, L809 and L810 are combined into a group of three, and so are the lenses L815, L816 and L817, wherein the angle of rotation between each two lenses is 30°. The lenses L811, L812, L813 and L814 are combined into a group of four with an angle of rotation of 22.5° relative to each other.

[0108] A maximum of 7 nm is obtained in the optical path difference for two mutually orthogonal states of linear polarization, if groups of (100)-lenses are combined with groups of (111)-lenses. For this purpose, the lenses L801 and L804 are combined into a group of (111)-lenses where the angle of rotation between the lenses is 60°. The lenses L802 and L803 are combined into a group of (100)-lenses where the angle of rotation between the lenses is 45°. A group of three (100)-lenses is formed of the lenses L808, L809 and L810, wherein the angle of rotation between each two of these lenses is 30°. A group of three (111)-lenses is formed of the lenses L815, L816 and L817, wherein the angle of rotation between each two of these lenses is 40°. The lenses L811, L812, L813 and L814 are combined into a group of four (100)-lenses with an angle of rotation of 22.5°. The lens axes of the lenses L805 and L807 which are not combined in a group are oriented in the crystallographic <111>-direction, while the lens axis of the lens L806 is oriented in the crystallographic <100>-direction. The groups can be oriented in relation to each

other at arbitrary angles of rotation about the optical axis. These rotational degrees of freedom can be used for the compensation of aberrations that are not rotationally symmetric and which can be caused, e.g., by the lens mount.

[0109] As described above, birefringence in crystals for light in the UV range can be compensated by arranging crystal elements following each other with different orientations of the crystallographic axes. If one arranges lenses following each other with different crystallographic directions in an optical system, one encounters the problem that lenses are in many cases traversed by a light ray at different angles, in which case a compensation may be possible only to a limited extent. In optical systems that contain only one crystal lens, this kind of compensation is not possible at all.

[0110] As a possible solution, a lens can in the design be split into two lenses that are wrung together with a rotation relative to each other. In practice, this procedure suffers from the drawback that stresses deform the joint surface and also that the two halves have to be positioned with an accuracy of micrometers in the lateral direction.

[0111] It is proposed to make blanks from individual plates that are wrung together and are rotated relative to each other with respect to the orientation of their crystallographic axes and which are then made into lenses by milling and polishing. Everything that was said hereinabove in regard to the orientation is likewise applicable to this concept. In addition to the traditional technique of wringing in the optical manufacturing process, any other joining techniques that produce an intimate contact and minimize the occurrence of stress represent possible solutions and are encompassed within the scope of the invention. The wringing can be

supported in particular by layers consisting, e.g., of quartz glass. It is important that no refraction or reflection occurs at the joining interface, as this would be detrimental.

[0112] The selection of the orientations is made according to the rules described above.

[0113] Embodiments of the foregoing concept include blanks from which, e.g., the lens L816 for the projection objective of Figure 8 can be produced. The lens L816 has a convex aspherical front surface with a crown radius of 342.13 mm and a concave spherical rear surface with a crown radius of 449.26 mm. The axial thickness is 37.3 mm. The lens material is calcium fluoride. The lens diameter is 141 mm. The blank from which the lens is to be formed needs to have a minimum overall thickness of 45 mm and a diameter of 150 mm. The blank can consist of two (100)-plates of 9.0 mm thickness that are rotated relative to each other by 45° and two (111)-plates of 13.5 mm thickness that are rotated relative to each other by 60°, which are joined together in an optically seamless manner. The (100)-plates and the (111)-plates should in this case be arranged respectively adjacent to each other.

[0114] In a further embodiment, six (100)-plates of 3.0 mm thickness that are rotated by 45° relative to each other and six (111)-plates of 4.5 mm thickness that are rotated by 60° relative to each other are joined in an optically seamless manner, where in each case two (100)-plates are followed by two (111)-plates.

[0115] In a further embodiment, four (110)-plates of 9.0 mm thickness that are rotated by 45° relative to each other and two (100)-plates of 4.5 thickness that are rotated by 45° relative to each other are joined in an optically seamless

manner, where the two (100)-plates are following the four (110)-plates.

[0116] In a further embodiment, eight (110)-plates of 4.5 mm thickness that are rotated by 45° relative to each other and four (100)-plates of 2.25 thickness that are rotated by 45° relative to each other are joined in an optically seamless manner, where in each case four (110)-plates are followed by two (100)-plates.

[0117] The following description of the principal configuration of a microlithography projection exposure apparatus is based on Figure 9. The projection exposure apparatus 81 has an illumination device 83 and a projection objective 85. The projection objective 85 includes a lens arrangement 819 with an aperture stop AP, wherein an optical axis 87 is defined by the lens arrangement 89. Embodiments for the lens arrangement 89 are presented in Figure 6 and Figure 7. Arranged between the illumination device 83 and the projection objective 85 is a mask 89 which is held in the light path by means of a mask holder 811. Masks 89 of this type, which are used in microlithography, have a micrometer-nanometer structure, which is projected into the image plane 813 by means of the projection objective 85, reduced for example by a factor of 4 or 5. In the image plane 813, a light-sensitive substrate 815, more specifically a wafer positioned by a substrate holder 817, is held in place.

[0118] The smallest structure that can still be resolved depend on the wavelength  $\lambda$  of the light that is used for the illumination and they also depend on the image-side numerical aperture of the projection objective 85, i.e., the maximally achievable resolution of the projection exposure apparatus 81 increases with decreasing wavelength  $\lambda$  of the illumination

device 83 and with increasing image-side numerical aperture of the projection objective 85. With the embodiments shown in Figures 6 and 7, it is possible to realize resolutions smaller than 150 nm. This is also the reason why effects such as the intrinsic birefringence need to be minimized. The invention has been successful in strongly reducing the undesirable influence of the intrinsic birefringence in particular in projection objectives with large image-side numerical aperture values.

M1587a

TABLE 1

LENSES	RADI	THICKNESS VALUES	GLASSES	REFR. INDEX AT 157.629nm	1/2 FREE DIAMETER
0	0.000000000	27.171475840 0.000000000	N2 N2	1.00031429 1.00031429	46.200 52.673
L601	900.198243311AS -235.121108435	15.151284556 9.531971079	CaF2 CaF2	1.55929035 1.00031429	53.454 54.049
L602	-167.185917779 -132.673519510	8.294716452 14.020355779	CaF2 CaF2	1.55929035 1.00031429	54.178 54.901
L603	-333.194588652 -155.450516203	9.893809820 15.930502944	CaF2 N2	1.55929035 1.00031429	53.988 54.132
L604	-73.572316296 -68.248613899AS	7.641977580 2.881720302	CaF2 N2	1.55929035 1.00031429	53.748 55.167
L605	-86.993585564AS -238.150965327	5.094651720 5.379130780	CaF2 N2	1.55929035 1.00031429	52.580 53.729
L606	-165.613920870 153.417884485	5.094651720 34.150169591	CaF2 CaF2	1.55929035 1.00031429	53.730 56.762
L607	-92.061009990 8491.086261873AS	5.094651720 19.673523795	CaF2 N2	1.55929035 1.00031429	58.081 74.689
L608	-407.131300451 -140.620317156	30.380807138 0.761662684	CaF2 N2	1.55929035 1.00031429	87.291 91.858
L609	-4831.804853654AS -192.197373609	50.269660218 1.688916911	CaF2 N2	1.55929035 1.00031429	117.436 121.408
L610	-367.718684892 -233.628547894	21.227715500 2.224071019	CaF2 N2	1.55929035 1.00031429	127.704 129.305
L611	709.585855080 1238.859445357	28.736922725 9.120684720	CaF2 N2	1.55929035 1.00031429	137.016 137.428
L612	1205.457051945 -285.321880705	49.281218258 1.625271224	CaF2 N2	1.55929035 1.00031429	138.288 138.379
L613	137.549591710 -4380.301012978AS	56.718543740 0.623523902	CaF2 N2	1.55929035 1.00031429	108.652 106.138
L614	2663.880214408 149.184979730	6.792868960 15.779049257	CaF2 N2	1.55929035 1.00031429	103.602 84.589
L615	281.093108064 184.030288413	6.792868960 32.341552355	CaF2 N2	1.55929035 1.00031429	83.373 77.968
L616	-222.157416308 101.254238115AS	5.094651720 56.792834221	CaF2 N2	1.55929035 1.00031429	77.463 71.826
L617	-106.980638018 1612.305471130	5.094651720 20.581065398	CaF2 N2	1.55929035 1.00031429	72.237 89.760
L618	-415.596135628 -204.680044631	26.398111993 0.713343960	CaF2 N2	1.55929035 1.00031429	96.803 103.409
L619	-646.696622394 -231.917626896	25.867340760 0.766268682	CaF2 N2	1.55929035 1.00031429	116.636 118.569
L620	-790.657607677 -294.872053725	23.400482872 0.721402031	CaF2 N2	1.55929035 1.00031429	128.806 130.074
L621	786.625567756 -431.247283013	40.932308205 12.736629300	CaF2 N2	1.55929035 1.00031429	141.705 142.089
L622	0.000000000 295.022653593AS	0.000000000 -8.491086200	CaF2 N2	1.00031429 1.00031429	134.586 139.341
L623	449.912291916 358.934076212	0.619840486 48.662890509	N2 CaF2	1.00031429 1.55929035	137.916 136.936
L624	-622.662988878 -224.404889753	30.955714157 12.736629300	N2 CaF2	1.00031429 1.55929035	135.288 134.760
L625	-251.154571510AS -193.582989843AS	16.079850229 16.510083506	N2 CaF2	1.00031429 1.55929035	134.853 134.101
L626	-198.077570749 206.241795157	0.880353872 19.927993542	N2 CaF2	1.00031429 1.55929035	136.109 101.240
L627	338.140581666 111.017549581	0.925956949 24.580089962	N2 CaF2	1.00031429 1.55929035	97.594 85.023
L628	169.576109839 117.982165264	0.777849447 31.161065630	N2 CaF2	1.00031429 1.55929035	81.164 75.464
L629	921.219058213AS 0.000000000	6.934980174 22.260797322	N2 CaF2	1.00031429 1.55929035	69.501 63.637
L630	0.000000000 0.000000000	4.245543100 21.227715500	N2 CaF2	1.00031429 1.00031429	48.606 41.032
	0.000000000 0.000000000	8.491086200 0.000000000	N2	1.00031429 1.000000000	26.698 11.550

---

Wavelength and refractive index are stated relative to vacuum.

ASPHERIC CONSTANTS

Asphere of lens L601

K	0.0000
C1	1.28594437e-007
C2	8.50731836e-013
C3	1.16375620e-016
C4	2.28674275e-019
C5	-1.23202729e-022
C6	3.32056239e-026
C7	-4.28323389e-030
C8	0.00000000e+000
C9	0.00000000e+000

Asphere of lens L604

K	-1.3312
C1	-4.03355456e-007
C2	2.25776586e-011
C3	-2.19259878e-014
C4	4.32573397e-018
C5	-7.92477159e-022
C6	7.57618874e-026
C7	-7.14962797e-030
C8	0.00000000e+000
C9	0.00000000e+000

Asphere of lens L605

K	-1.1417
C1	1.33637337e-007
C2	1.56787758e-011
C3	-1.64362484e-014
C4	3.59793786e-018
C5	-5.11312568e-022
C6	1.70636633e-026
C7	1.82384731e-030
C8	0.00000000e+000
C9	0.00000000e+000

Asphere of lens L607

K	0.0000
C1	1.34745120e-007
C2	-2.19807543e-011
C3	1.20275881e-015
C4	4.39597377e-020
C5	-2.37132819e-023
C6	2.87510939e-027
C7	-1.42065162e-031
C8	0.00000000e+000
C9	0.00000000e+000

## Asphere of lens L609

K	0.0000
C1	6.85760526e-009
C2	-4.84524868e-013
C3	-6.28751350e-018
C4	-3.72607209e-022
C5	3.25276841e-026
C6	-4.05509974e-033
C7	-3.98843079e-035
C8	0.00000000e+000
C9	0.00000000e+000

## Asphere of lens L613

K	0.0000
C1	2.24737416e-008
C2	-4.45043770e-013
C3	-4.10272049e-017
C4	4.31632628e-021
C5	-3.27538237e-025
C6	1.44053025e-029
C7	-2.76858490e-034
C8	0.00000000e+000
C9	0.00000000e+000

## Asphere of lens L616

K	0.0000
C1	-2.83553693e-008
C2	-1.12122261e-011
C3	-2.05192812e-016
C4	-1.55525080e-020
C5	-4.77093112e-024
C6	8.39331135e-028
C7	-8.97313681e-032
C8	0.00000000e+000
C9	0.00000000e+000

## Asphere of lens L622

K	0.0421
C1	7.07310826e-010
C2	-2.00157185e-014
C3	-9.33825109e-020
C4	1.27125854e-024
C5	1.94008709e-027
C6	-6.11989858e-032
C7	2.92367322e-036
C8	0.00000000e+000
C9	0.00000000e+000

## Asphere of lens L624

K	0.0000
C1	3.02835805e-010
C2	-2.40484062e-014
C3	-3.22339189e-019
C4	1.64516979e-022
C5	-8.51268614e-027
C6	2.09276792e-031
C7	-4.74605669e-036
C8	0.00000000e+000
C9	0.00000000e+000

## Asphere of lens L625

K	0.0000
C1	-3.99248993e-010
C2	5.79276562e-014
C3	3.53241478e-018
C4	-4.57872308e-023
C5	-6.29695208e-027
C6	1.57844931e-031
C7	-2.19266130e-036
C8	0.00000000e+000
C9	0.00000000e+000

## Asphere of lens L628

K	0.0000
C1	4.40737732e-008
C2	1.52385268e-012
C3	-5.44510329e-016
C4	6.32549789e-020
C5	-4.58358203e-024
C6	1.92230388e-028
C7	-3.11311258e-033
C8	0.00000000e+000
C9	0.00000000e+000

TABLE 3

L61

LENSES	RADI	THICKNESS VALUES	GLASSES	REFR. INDEX AT 157.629nm	1/2 FREE DIAMETER
0	0.000000000	34.000000000		1.00000000	82.150
	0.000000000	0.100000000		1.00000000	87.654
L801	276.724757380	40.000000000	CaF2	1.55970990	90.112
	1413.944109416AS	95.000000000		1.00000000	89.442
<u>SP1</u>	0.000000000	11.000000000		1.00000000	90.034
	0.000000000	433.237005445		1.00000000	90.104
L802	-195.924336384	17.295305525	CaF2	1.55970990	92.746
	-467.658808527	40.841112468		1.00000000	98.732
L803	-241.385736441	15.977235467	CaF2	1.55970990	105.512
	-857.211727400AS	21.649331094		1.00000000	118.786
SP2	0.000000000	0.000010000		1.00000000	139.325
	253.074839896	21.649331094		1.00000000	119.350
L803'	857.211727400AS	15.977235467	CaF2	1.55970990	118.986
	241.385736441	40.841112468		1.00000000	108.546
L802'	467.658808527	17.295305525	CaF2	1.55970990	102.615
	195.924336384	419.981357165		1.00000000	95.689
SP3	0.000000000	6.255658280		1.00000000	76.370
	0.000000000	42.609155219		1.00000000	76.064
Z1	0.000000000	67.449547115		1.00000000	73.981
L804	432.544479547	37.784311058	CaF2	1.55970990	90.274
	-522.188532471	113.756133662		1.00000000	92.507
L805	-263.167605725	33.768525968	CaF2	1.55970990	100.053
	-291.940616829AS	14.536591424		1.00000000	106.516
L806	589.642961222AS	20.449887046	CaF2	1.55970990	110.482
	-5539.698828792	443.944079795		1.00000000	110.523
L807	221.780582003	9.000000000	CaF2	1.55970990	108.311
	153.071443064	22.790060084		1.00000000	104.062
L808	309.446967518	38.542735318	CaF2	1.55970990	104.062
	-2660.227900099	0.100022286		1.00000000	104.098
L809	23655.354584194	12.899131182	CaF2	1.55970990	104.054
	-1473.189213176	9.318886362		1.00000000	103.931
L810	-652.136459374	16.359499814	CaF2	1.55970990	103.644
	-446.489459129	0.100000000		1.00000000	103.877
L811	174.593507050	25.900313780	CaF2	1.55970990	99.267
	392.239615259AS	14.064505431		1.00000000	96.610
	0.000000000	2.045119392		1.00000000	96.552
L812	7497.306838492	16.759051656	CaF2	1.55970990	96.383
	318.210831711	8.891640764		1.00000000	94.998
L813	428.724465129	41.295806263	CaF2	1.55970990	95.548
	3290.097860119AS	7.377912006		1.00000000	95.040
L814	721.012739719	33.927118706	CaF2	1.55970990	95.443
	-272.650872353	6.871397517		1.00000000	95.207
L815	131.257556743	38.826450065	CaF2	1.55970990	81.345
	632.112566477AS	4.409527396		1.00000000	74.847
L816	342.127616157AS	37.346293509	CaF2	1.55970990	70.394
	449.261078744	4.859754445		1.00000000	54.895
L817	144.034814702	34.792179308	CaF2	1.55970990	48.040
	-751.263321098AS	11.999872684		1.00000000	33.475
0'	0.000000000	0.000127776		1.00000000	16.430

## ASPHERIC CONSTANTS

Asphere of lens L801

K	0.0000
C1	4.90231706e-009
C2	3.08634889e-014
C3	-9.53005325e-019
C4	-6.06316417e-024
C5	6.11462814e-028
C6	-8.64346302e-032
C7	0.00000000e+000
C8	0.00000000e+000
C9	0.00000000e+000

Asphere of lens L803

K	0.0000
C1	-5.33460884e-009
C2	9.73867225e-014
C3	-3.28422058e-018
C4	1.50550421e-022
C5	0.00000000e+000
C6	0.00000000e+000
C7	0.00000000e+000
C8	0.00000000e+000
C9	0.00000000e+000

Asphere of lens L803'

K	0.0000
C1	5.33460884e-009
C2	-9.73867225e-014
C3	3.28422058e-018
C4	-1.50550421e-022
C5	0.00000000e+000
C6	0.00000000e+000
C7	0.00000000e+000
C8	0.00000000e+000
C9	0.00000000e+000

Asphere of lens L805

K	0.0000
C1	2.42569449e-009
C2	3.96137865e-014
C3	-2.47855149e-018
C4	7.95092779e-023
C5	0.00000000e+000
C6	0.00000000e+000
C7	0.00000000e+000
C8	0.00000000e+000
C9	0.00000000e+000

## Asphere of lens L806

K	0.0000
C1	-6.74111232e-009
C2	-2.57289693e-014
C3	-2.81309020e-018
C4	6.70057831e-023
C5	5.06272344e-028
C6	-4.81282974e-032
C7	0.00000000e+000
C8	0.00000000e+000
C9	0.00000000e+000

## Asphere of lens L811

K	0.0000
C1	2.28889624e-008
C2	-1.88390559e-014
C3	2.86010656e-017
C4	-3.18575336e-021
C5	1.45886017e-025
C6	-1.08492931e-029
C7	0.00000000e+000
C8	0.00000000e+000
C9	0.00000000e+000

## Asphere of lens L813

K	0.0000
C1	3.40212872e-008
C2	-1.08008877e-012
C3	4.33814531e-017
C4	-7.40125614e-021
C5	5.66856812e-025
C6	0.00000000e+000
C7	0.00000000e+000
C8	0.00000000e+000
C9	0.00000000e+000

## Asphere of lens L815

K	0.0000
C1	-3.15395039e-008
C2	4.30010133e-012
C3	3.11663337e-016
C4	-3.64089769e-020
C5	1.06073268e-024
C6	0.00000000e+000
C7	0.00000000e+000
C8	0.00000000e+000
C9	0.00000000e+000

## Asphere of lens L816

K	0.0000
C1	-2.16574623e-008
C2	-6.67182801e-013
C3	4.46519932e-016
C4	-3.71571535e-020
C5	0.00000000e+000
C6	0.00000000e+000
C7	0.00000000e+000
C8	0.00000000e+000
C9	0.00000000e+000

## Asphere of lens L817

K	0.0000
C1	2.15121397e-008
C2	-1.65301726e-011
C3	-5.03883747e-015
C4	1.03441815e-017
C5	-6.29122773e-021
C6	1.44097714e-024
C7	0.00000000e+000
C8	0.00000000e+000
C9	0.00000000e+000

## Patent Claims:

1. Objective (611, 711), in particular a projection objective for a microlithography projection exposure apparatus (81) with a plurality of lenses (L601-L630, L801-L817), with at least one fluoride crystal lens (1), characterized in that the at least one lens (1) is a (100)-lens with a lens axis (EA) that is oriented approximately perpendicular to the crystallographic {100}-planes or to the crystallographic planes of the fluoride crystal that are equivalent to the {100}-planes.
2. Objective according to claim 1, wherein the (100)-lens is a rotationally symmetric lens with a symmetry axis and wherein the symmetry axis coincides with the lens axis of the (100)-lens.
3. Objective according to one of the claims 1 to 2, with an optical axis (OA), wherein the lens axis of the (100)-lens coincides with the optical axis of the objective.
4. Objective according to one of the claims 1 to 3, wherein light rays run inside the objective from an object plane (O) to an image plane (O') and at least one light ray (609, 713, 715) inside the (100)-lens has a ray angle larger than 25°, in particular larger than 30°, relative to the lens axis.
5. Objective according to one of the claims 1 to 4, wherein light rays run inside the objective from an object plane to an image plane and all light rays inside the (100)-lens have ray angles of maximally 45°, in particular maximally  $\arcsin\left(\frac{NA}{n_{FK}}\right)$  in relation to the lens axis, wherein NA stands

for the image-side numerical aperture and  $n_{FK}$  stands for the refractive index of the fluoride crystal.

6. Objective according to one of the claims 1 to 5, with an aperture stop plane, wherein the aperture stop plane has an aperture stop diameter, wherein the (100)-lens has a lens diameter, and wherein the lens diameter is smaller than 85%, in particular smaller than 80%, of the aperture stop diameter.
7. Objective according to one of the claims 1 to 6 with an image plane, wherein the (100)-lens (L630, L817) is the lens nearest to the image plane.
8. Objective (611, 711), in particular a projection objective for a microlithography projection exposure apparatus, with at least two lenses or lens parts consisting of fluoride crystal,  
wherein the lenses or the lens parts have lens axes that point approximately in a principal crystallographic direction,  
wherein a bundle of light rays falls on an image point in an image plane, each of said rays having an azimuth angle  $\alpha_R$ , an aperture angle  $\theta_R$ , and an optical path difference  $\Delta OPL$  for two mutually orthogonal states of linear polarization,  
characterized in that the lenses or the lens parts are rotated relative to each other about the lens axes in such a manner that the distribution of the optical path differences  $\Delta OPL(\alpha_R, \theta_R)$  of the ray bundle as a function of the azimuth angle  $\alpha_R$  and the aperture angle  $\theta_R$  has significantly reduced values in comparison to lenses or lens parts in which the lens axes are oriented in the same

principal crystallographic direction and which are not rotated relative to each other about the lens axes.

9. Objective according to claim 8, wherein the optical path differences  $\Delta OPL$  as a function of the azimuth angle  $\alpha_R$  for a given aperture angle  $\theta_0$  vary by less than 30%, in particular by less than 20%.
10. Objective according to one of the claims 8 or 9, wherein each of the lenses or lens parts has a birefringence distribution  $\Delta n(\alpha_L, \theta_L)$  whose birefringence values  $\Delta n$  depend on azimuth angles  $\alpha_L$  relative to a reference direction that is perpendicular to the lens axis and on aperture angles  $\theta_R$  relative to the lens axis,  
wherein the birefringence distribution  $\Delta n(\alpha_L, \theta_L)$  has a k-fold azimuthal symmetry,  
wherein respective rotation angles  $\gamma$  are defined between the reference directions of the individual lenses or lens parts,  
wherein a number of n lenses or n lens parts form a group within which the lens axes point in one and the same or an equivalent principal crystallographic direction and within which the birefringence distributions  $\Delta n(\alpha_L, \theta_L)$  have the same azimuthal profile relative to the reference directions,  
wherein the rotation angle  $\gamma$  between each two lenses or lens parts of a group conforms to the equation:
$$\gamma = \frac{360^\circ}{k \cdot n} + m \cdot \frac{360^\circ}{k} \pm 10^\circ,$$
wherein m represents an integer number.
11. Objective according to claim 10, wherein an outermost aperture ray (609, 713, 715) of the bundle of rays has

inside each of the lenses or lens parts a respective aperture angle  $\theta_L$  and wherein the aperture angles  $\theta_L$  within the lenses or lens parts of the group vary by no more than 30%, in particular no more than 20%.

12. Objective according to one of the claims 10 or 11, wherein an outermost aperture ray (609, 713, 715) of the bundle of rays covers inside each of the lenses or lens parts a respective ray path  $RP_L$  and wherein the ray paths  $RP_L$  within the lenses or lens parts of the group vary by no more than 30%, in particular no more than 20%.
13. Objective according to one of the claims 10 to 12, wherein the respective optical path differences  $\Delta OPL$  for an outermost aperture ray (609, 713, 715) of the bundle of rays determined at a rotation angle  $\gamma=0^\circ$  for the lenses or lens parts of a group vary by no more than 30%, in particular no more than 20%.
14. Objective according to one of the claims 10 to 13, wherein the group comprises two to four lenses or lens parts.
15. Objective according to claim 14, wherein the lenses (L629, L630) or lens parts are arranged adjacent to each other and are, in particular, joined to each other by wringing.
16. Objective according to one of the claims 10 to 15, wherein the objective has at least two groups, in each of which the lenses or lens parts are rotated relative to each other.
17. Objective according to one of the claims 8 to 16, wherein the lens axes point in the crystallographic <111>-direction or in equivalent principal crystallographic

- directions and the birefringence distribution  $\Delta n(\alpha_L, \theta_L)$  of the lenses or lens parts has a threefold azimuthal symmetry.
18. Objective according to one of the claims 8 to 16, wherein the lens axes point in the crystallographic <100>-direction or in equivalent principal crystallographic directions and the birefringence distribution  $\Delta n(\alpha_L, \theta_L)$  of the lenses or lens parts has a fourfold azimuthal symmetry.
19. Objective according to one of the claims 8 to 16, wherein the lens axes point in the crystallographic <110>-direction or in equivalent principal crystallographic directions and the birefringence distribution  $\Delta n(\alpha_L, \theta_L)$  of the lenses or lens parts has a twofold azimuthal symmetry.
20. Objective according to one of the claims 8 to 19, wherein the lens axes of the lenses or lens parts of a first group point in the crystallographic <100>-direction or an equivalent principal crystallographic direction and the lens axes of the lenses or lens parts of a second group point in the crystallographic <111>-direction or an equivalent principal crystallographic direction.
21. Objective according to one of the claims 8 to 19, wherein the lens axes of the lenses or lens parts of a first group point in the crystallographic <100>-direction or an equivalent principal crystallographic direction and the lens axes of the lenses or lens parts of a second group point in the crystallographic <110>-direction or an equivalent principal crystallographic direction.

22. Objective according to claim 20 or 21, wherein the distribution  $\Delta OPL(\alpha_R, \theta_R)$  of the optical path differences is composed of a first distribution  $\Delta OPL_1(\alpha_R, \theta_R)$  of the optical path differences that is due to the lenses or lens parts of all first groups and a second distribution  $\Delta OPL_2(\alpha_R, \theta_R)$  of the optical path differences that is due to the lenses or lens parts of all second groups and wherein the amount of the maximum value of the first distribution  $\Delta OPL_1(\alpha_R, \theta_R)$  of the optical path differences differs by no more than 30%, in particular no more than 20%, from the amount of the maximum value of the second distribution  $\Delta OPL_2(\alpha_R, \theta_R)$  of the optical path differences.
23. Objective according to one of the claims 1 to 22, wherein the fluoride crystal is a calcium fluoride crystal, a strontium fluoride crystal or a barium fluoride crystal.
24. Objective according to one of the claims 1 to 23, wherein the objective has an image-side numerical aperture NA, and wherein the image-side numerical aperture NA is larger than 0.7, in particular larger than 0.8.
25. Objective according to one of the claims 1 to 24, wherein the light rays have wavelengths shorter than 200 nm.
26. Objective according to one of the claims 1 to 25, wherein the light rays have wavelengths shorter than 160 nm.
27. Objective according to one of the claims 1 to 26, wherein the Objective (611) is a refractive objective.
28. Objective according to one of the claims 1 to 27, wherein the objective is a catadioptric objective (711) with lenses and with at least one mirror (Sp2).

29. Objective according to one of the claims 1 to 28, wherein all of the lenses are of calcium fluoride.
30. Microlithography projection exposure apparatus (81), comprising
  - an illumination system (83),
  - an objective (85) according to one of the claims 1 to 29 which projects a structure-carrying mask (89) onto a light-sensitive substrate (815).
31. Method for the manufacture of semiconductor components by means of a microlithography projection exposure apparatus (81) according to claim 30.
32. Method for the manufacture of objectives, in particular projection objectives for a microlithography projection exposure apparatus,  
with at least two lenses or lens parts consisting of fluoride crystal,  
wherein the lenses or the lens parts have lens axes pointing approximately in a respective principal crystallographic direction,  
characterized in that  
for a ray bundle wherein each of the rays of the bundle has a respective azimuth angle  $\alpha_R$ , a respective aperture angle  $\theta_R$ , and a respective optical path difference  $\Delta OPL$  for two mutually orthogonal states of linear polarization in an image plane, the distribution  $\Delta OPL(\theta_R, \alpha_R)$  of the optical path differences is determined for lenses or lens parts, and  
the lenses or lens parts are arranged with a rotation relative to each other about the lens axes such that the distribution of the optical path differences  $\Delta OPL(\theta_R, \alpha_R)$

of the ray bundle has significantly reduced values in comparison to lenses or lens parts in which the lens axes point in the same principal crystallographic direction and which are not arranged with a rotation relative to each other about the lens axes.

33. Method according to claim 32, wherein the objective comprises a first group with lenses or lens parts and a second group with lenses or lens parts, wherein the lens axes of the lenses or lens parts of the first group point in the crystallographic <100>-direction or an equivalent principal crystallographic direction, and wherein the lens axes of the lenses or lens parts of the second group point in the crystallographic <111>-direction or an equivalent principal crystallographic direction.
34. Method according to claim 32, wherein the objective comprises a first group with lenses or lens parts and a second group with lenses or lens parts, wherein the lens axes of the lenses or lens parts of the first group point in the crystallographic <100>-direction or an equivalent principal crystallographic direction, and wherein the lens axes of the lenses or lens parts of the second group point in the crystallographic <110>-direction or an equivalent principal crystallographic direction.
35. Method for the manufacture of lenses, characterized in that a plurality of plates of a crystal material, preferably fluoride crystal and in particular calcium fluoride, which are rotated relative to each other in regard to their respective crystallographic orientations of the crystal material, are joined together in an optically seamless manner, in particular by wringing, and are subsequently shaped and polished as a unitary blank.

36. Method for the manufacture of lenses according to claim 35, wherein each of the plates has a birefringence distribution  $\Delta n(\alpha_L, \theta_L)$  with birefringence values  $\Delta n$  dependent on azimuth angles  $\alpha_L$  relative to a reference direction that is perpendicular to the lens axis and further dependent on aperture angles  $\theta_L$  relative to the lens axis, and wherein said birefringence distribution has a k-fold azimuthal symmetry,  
wherein for a number of N plates the surface normal vectors point in one and the same or an equivalent principal crystallographic direction and the birefringence distributions  $\Delta n(\alpha_L, \theta_L)$  have the same azimuthal profile relative to the reference directions,  
wherein angles of rotation  $\gamma$  are defined between the reference directions of the individual plates, and wherein the rotation angle  $\gamma$  between each two plates conforms to the equation:

$$\gamma = \frac{360^\circ}{k \cdot n} + m \cdot \frac{360^\circ}{k} \pm 10^\circ, \text{ wherein } m \text{ is an integer number.}$$

37. Method for the manufacture of lenses according to claim 36, wherein two plates are seamlessly joined.

38. Method for the manufacture of lenses according to one of the claims 36 and 37, wherein the plates are of approximately equal thickness.

39. Method for the manufacture of lenses according to one of the claims 35 to 38, wherein in first plates the normal vectors of the plate surfaces point in the crystallographic <111>-direction or an equivalent principal crystallographic direction, and wherein in second plates the normal vectors of the plate surfaces

point in the crystallographic <100>-direction or an equivalent principal crystallographic direction.

40. Method for the manufacture of lenses according to claim 39, wherein the first plates have an approximately equal first thickness and the second plates have an approximately equal second thickness, and wherein the ratio between the sum of the first thicknesses and the sum of the second thicknesses is  $1.5 \pm 0.2$ .
41. Method for the manufacture of lenses according to one of the claims 35 to 38, wherein in first plates the normal vectors of the plate surfaces point in the crystallographic <110>-direction or an equivalent principal crystallographic direction, and wherein in second plates the normal vectors of the plate surfaces point in the crystallographic <100>-direction or an equivalent principal crystallographic direction.
42. Method for the manufacture of lenses according to claim 41, wherein the first plates have an approximately equal first thickness and the second plates have an approximately equal second thickness, and wherein the ratio between the sum of the first thicknesses and the sum of the second thicknesses is  $4.0 \pm 0.4$ .
43. Method for the manufacture of lenses according to one of the claims 41 and 42, wherein two first plates are seamlessly joined with a second plate.
44. Method for the manufacture of lenses according to one of the claims 41 and 42, wherein four first plates are seamlessly joined with two second plates.

- 
45. Lens, characterized by the manufacture according to one of the claims 35 to 44.
  46. Objective, in particular a projection objective (611, 711) for a microlithography projection exposure apparatus (81), characterized in that the objective comprises a lens according to claim 45.
  47. Objective according to at least one of the claims 1 to 29, characterized in that it comprises a lens according to claim 45.

---

Attached hereto: 27 page(s) of drawings

---

**Summary:****Objective with Fluoride Crystal Lenses**

(Fig. 1)

Objective, in particular a projection objective for a microlithography projection exposure apparatus with at least one fluoride crystal lens. A reduction of the undesirable influence of birefringence is achieved if this lens is a (100)-lens with a lens axis that is oriented approximately perpendicular to the crystallographic {100}-planes or equivalent crystallographic planes of the fluoride crystal. In objectives with at least two fluoride crystal lenses, it is advantageous if the fluoride crystal lenses are arranged with a rotation relative to each other. In addition to the crystallographic <100>-direction, the lens axes of the fluoride crystal lenses can also be oriented in the crystallographic <111>- or <110>-direction. A further reduction in the undesirable influence of birefringence is achieved by using groups of mutually rotated (100)-lenses in simultaneous combination with groups of mutually rotated (111)-lenses or (110)-lenses.

**DR. WALTER E. KUPPER**

65 Barnsdale Road  
Madison, NJ. 07940

Telephone: 973 301-1989 Fax: 973 822-9096 E-mail: wekupper@att.net

July 27, 2005

TO WHOM IT MAY CONCERN:

**TRANSLATOR'S CERTIFICATE**

The undersigned hereby certifies that he is bilingually proficient in German and English,  
that he has personally prepared the attached translation

**"Objective with Crystal Lenses"**

of the published German Patent Application

**"Offenlegungsschrift DE 102 10 782 A1,  
Objektiv mit Kristall-Linsen "**

and that the translation is accurate.



Walter Kupper

Description

Objective with Crystal Lenses

[0001] The invention relates to an objective in accordance with the introductory part of claim 1.

[0002] Projection objectives of this kind are known from U.S. Patent 6,201,634 which discloses that, ideally, in the manufacture of fluoride crystal lenses the lens axes are aligned perpendicularly to the crystallographic {111}-planes of the fluoride crystals in order to minimize the stress-related birefringence. The implied assumption in U.S. Patent 6,201,634 is that fluoride crystals have no intrinsic birefringence.

[0003] However, as is known from the Internet publication "Preliminary Determination of an Intrinsic Birefringence in CaF<sub>2</sub>" by John H. Burnett, Eric L. Shirley, and Zachary H. Levine, NIST, Gaithersburg, MD 20899, USA (posted May 7, 2001), calcium fluoride single crystals also exhibit birefringence that is not stress-induced, i.e., intrinsic birefringence. The measurements presented in that reference demonstrate that with a ray propagation in the crystallographic <110>-direction, the birefringence in calcium fluoride amounts to  $(6.5 \pm 0.4)$  nm/cm at a wavelength of  $\lambda=156.1$  nm,  $(3.6 \pm 0.2)$  nm/cm at a wavelength of  $\lambda=193.09$  nm, and  $(1.2 \pm 0.1)$  nm/cm at a wavelength of  $\lambda=253.65$  nm. However, with a ray propagation in the crystallographic <100>-direction and in the crystallographic <111>-direction, no intrinsic birefringence occurs in calcium fluoride, as is also predicted by theory. Thus, the intrinsic birefringence is strongly direction-dependent and becomes noticeably more pronounced as the wavelength decreases.

[0004] The indices for the crystallographic directions will hereinafter be bracketed between the symbols "<" and ">", while the indices for the crystallographic planes will be bracketed between the symbols "{" and "}". The crystallographic direction always indicates the direction of the normal vector of the corresponding crystallographic plane. Thus, the crystallographic direction  $\langle 100 \rangle$  points in the direction of the normal vector of the crystallographic plane  $\{100\}$ . The cubic crystals, to which the fluoride crystals belong, have the principal crystallographic directions  $\langle 110 \rangle$ ,  $\langle \bar{1}10 \rangle$ ,  $\langle \bar{1}\bar{1}0 \rangle$ ,  $\langle 101 \rangle$ ,  $\langle 10\bar{1} \rangle$ ,  $\langle \bar{1}01 \rangle$ ,  $\langle \bar{1}0\bar{1} \rangle$ ,  $\langle 011 \rangle$ ,  $\langle 0\bar{1}1 \rangle$ ,  $\langle 01\bar{1} \rangle$ ,  $\langle 111 \rangle$ ,  $\langle \bar{1}\bar{1}\bar{1} \rangle$ ,  $\langle \bar{1}\bar{1}1 \rangle$ ,  $\langle \bar{1}1\bar{1} \rangle$ ,  $\langle 1\bar{1}\bar{1} \rangle$ ,  $\langle \bar{1}11 \rangle$ ,  $\langle 1\bar{1}1 \rangle$ ,  $\langle 100 \rangle$ ,  $\langle 010 \rangle$ ,  $\langle 001 \rangle$ ,  $\langle \bar{1}00 \rangle$ ,  $\langle 0\bar{1}0 \rangle$ , and  $\langle 00\bar{1} \rangle$ . Because of the symmetry properties of cubic crystals, the principal crystallographic directions  $\langle 100 \rangle$ ,  $\langle 010 \rangle$ ,  $\langle 001 \rangle$ ,  $\langle \bar{1}00 \rangle$ ,  $\langle 0\bar{1}0 \rangle$ , and  $\langle 00\bar{1} \rangle$  are equivalent to each other, so that crystallographic directions that point in one of these principal crystallographic directions will hereinafter be identified with the prefix "(100)-". Crystallographic planes that are perpendicular to one of these principal crystallographic directions are accordingly identified by the prefix "(100)-". The principal crystallographic directions  $\langle 110 \rangle$ ,  $\langle \bar{1}10 \rangle$ ,  $\langle \bar{1}\bar{1}0 \rangle$ ,  $\langle \bar{1}\bar{1}\bar{1}0 \rangle$ ,  $\langle 101 \rangle$ ,  $\langle 10\bar{1} \rangle$ ,  $\langle \bar{1}01 \rangle$ ,  $\langle \bar{1}0\bar{1} \rangle$ ,  $\langle 011 \rangle$ ,  $\langle 0\bar{1}1 \rangle$ ,  $\langle 01\bar{1} \rangle$  and  $\langle 0\bar{1}\bar{1} \rangle$  are likewise equivalent to each other, so that crystallographic directions that point in one of these principal crystallographic directions will hereinafter be identified with the prefix "(110)-". Crystallographic planes that are perpendicular to one of the principal crystallographic directions are accordingly identified by the prefix "(110)-". The principal crystallographic directions  $\langle 111 \rangle$ ,  $\langle \bar{1}\bar{1}\bar{1} \rangle$ ,  $\langle \bar{1}\bar{1}1 \rangle$ ,  $\langle \bar{1}1\bar{1} \rangle$ ,  $\langle 1\bar{1}\bar{1} \rangle$ ,  $\langle \bar{1}11 \rangle$ ,  $\langle 1\bar{1}1 \rangle$  and

<11̄1> are likewise equivalent to each other, so that crystallographic directions that point in one of these principal crystallographic directions will hereinafter be identified with the prefix "(111)-". Crystallographic planes that are perpendicular to one of these principal crystallographic directions are accordingly identified by the prefix "(111)-". Hereinafter, statements made in reference to one of the aforementioned principal crystallographic directions will always be applicable likewise to the equivalent principal crystallographic directions.

[0005] Projection objectives and microlithography projection exposure apparatus are known, e.g., from this applicant's patent application PCT/EP00/13184 and the references cited therein. The embodiments given in that application illustrate suitable purely refractive and catadioptric projection objectives with numerical aperture values of 0.8 and 0.9 at an operating wavelength of 193 nm as well as 157 nm.

[0006] The concept of rotating lens elements in order to compensate birefringence effects is also described in the patent application "Microlithography Projection Exposure Apparatus, Optical System and Manufacturing Method" (DE 10123725.1) identified by applicant's file reference 01055P, with a filing date of May 15, 2001. The content of that application is hereby incorporated by reference in the present application.

[0007] The present invention has the object to propose projection objectives for a microlithography projection exposure apparatus, wherein the influence of birefringence, in particular intrinsic birefringence, is significantly reduced.

[0008] The object just described is solved by an objective according to claim 1, 8 and 31, a microlithography projection exposure apparatus according to claim 47, a method for the manufacture of semiconductor components according to claim 48, a method for the manufacture of objectives according to claim 49, a method of compensating birefringence effects according to claim 53, and a method for the manufacture of lenses according to claim 54.

[0009] Advantageous embodiments of the invention are presented in the features of the dependent claims.

[0010] As a means for reducing the influence of intrinsic birefringence, claim 1 proposes to align the lens axes of lenses made of a fluoride crystal so that they coincide with the crystallographic <100>-direction. The lens axes are considered to be coinciding with a principal crystallographic direction, if the maximum deviation between lens axis and principal crystallographic direction is smaller than 5°. In this arrangement, it is not necessary for all of the fluoride crystal lenses of the objective to have the aforementioned orientation of the crystallographic planes. Those lenses in which the lens axes are oriented perpendicular to the crystallographic {100}-planes will hereinafter also be referred to as (100)-lenses. Orienting the lens axis in the crystallographic <100>-direction has the advantage that the aperture angles of the light rays where the undesirable influence of the intrinsic birefringence associated with a light propagation in the crystallographic <110>-direction becomes noticeable are larger than with an orientation of the lens axis in the crystallographic <111>-direction. The term aperture angle in the present context refers to the angle between a light ray and the optical axis outside of a lens and between a light ray and the lens axis inside a lens. Only as

the aperture angles enter into the angular range between the crystallographic  $<100>-$  and  $<110>-$  directions does the influence of birefringence manifest itself in the respective light rays. The angle between the crystallographic  $<110>-$  and  $<100>-$  directions amounts to  $45^\circ$ . If the lens axis were, on the other hand, oriented in the crystallographic  $<111>-$  direction, the undesirable influence of intrinsic birefringence would be noticeable already at smaller aperture angles, as the angle between the crystallographic  $<110>-$  and  $<111>-$  directions is only  $35^\circ$ .

[0011] If the angle-dependence of the birefringence is caused, e.g., by the manufacturing process of the fluoride crystal or by mechanical stress applied to the lens, in particular stress-induced birefringence, the conceptual solutions disclosed herein can, of course, be used as well to lessen the undesirable influence of the birefringence.

[0012] The lens axis is constituted, e.g., by a symmetry axis of a rotationally symmetrical lens. If the lens has no symmetry axis, the lens axis can be defined by the center of an incident bundle of light rays or by a straight line in relation to which the ray angles of all light rays inside the lens are minimal. The lenses can be, e.g., refractive or diffractive lenses as well as corrective plates with free-form corrective surfaces. Planar-parallel plates, too, are considered as lenses, if they are arranged in the light path of the objective. The lens axis of a planar-parallel plate is perpendicular to the plane lens surfaces.

[0013] With preference, however, the lenses are rotationally symmetric lenses.

[0014] Objectives have an optical axis that runs from the object plane to the image plane. With preference, the (100)-lenses are arranged in centered alignment relative to this optical axis, so that the lens axes also coincide with the optical axis.

[0015] The invention can be used to good advantage in projection objectives for a microlithography projection exposure apparatus, because the requirements in regard to resolution are extremely high for these objectives. But in test objectives, too, which are used for example to test lenses for projection objectives through measurements of wave fronts with large aperture, the influence of birefringence has a detrimental effect.

[0016] In objectives with large numerical aperture values on the image side, in particular larger than 0.7, aperture angles larger than  $25^\circ$  and in particular larger than  $30^\circ$  will occur inside the (100)-lenses. It is especially at these large aperture angles that the inventive concept of orienting the lens axes in the crystallographic <100>-direction proves to be useful. If the lens axes were oriented in the crystallographic <111>-direction, the undesirable influence of the birefringence would manifest itself more noticeably at aperture angles larger than  $25^\circ$  and in particular larger than  $30^\circ$ , unless one of the corrective measures described below is applied.

[0017] Since on the other hand the undesirable influence of intrinsic birefringence can have a maximum at an aperture angle of  $45^\circ$ , it is advantageous to design the projection objective in such a way that all aperture angles of the light rays are smaller than  $45^\circ$ , in particular smaller than or equal

to  $\arcsin\left(\frac{NA}{n_{FK}}\right)$ , wherein NA stands for the image-side numerical aperture and  $n_{FK}$  stands for the refractive index of the fluoride crystal. The expression  $\arcsin\left(\frac{NA}{n_{FK}}\right)$  represents in this case the aperture angle that corresponds to the image-side numerical aperture inside a fluoride crystal lens if the light beam is refracted at a planar boundary surface. This is achieved by a design in which the lenses that are arranged near the image plane have light-collecting lens surfaces, planar lens surfaces or at most slightly dispersing lens surfaces, if in the direction of the light the light-dispersing lens surface is followed by a lens surface of a stronger light-collecting power.

[0018] Large aperture angles occur primarily in lenses near field planes, in particular near the image plane. The (100)-lenses should therefore be used with preference in the vicinity of the field planes. The range where the (100)-lenses should be used can be determined by way of the ratio between the lens diameter and the diameter of the aperture stop. Thus, the lens diameter of the (100)-lenses is preferably at most 85%, in particular at most 80% of the aperture stop diameter.

[0019] In projection objectives, the largest aperture angles occur as a rule in the lens closest to the image plane. It is therefore preferred to align the lens axis of this lens in the crystallographic <100>-direction.

[0020] The intrinsic birefringence of a fluoride crystal lens in this case depends not only on the aperture angle of a light ray, but also on the azimuth angle of the light ray. Thus, every fluoride crystal lens can be characterized by a

birefringence distribution  $\Delta n(\alpha_L, \theta_L)$  that is on the one hand a function of the aperture angle  $\theta_L$  and on the other hand a function of the azimuth angle  $\alpha_L$ . For a ray direction that is defined by the aperture angle  $\theta_L$  and the azimuth angle  $\alpha_L$ , the value of the birefringence  $\Delta n$  indicates the ratio - in the unit [nm/cm] - between the optical path difference for two mutually orthogonal states of linear polarization and the physical path length covered in the fluoride crystal. Thus, the intrinsic birefringence is independent of the ray paths and the lens shape. The optical path difference for a ray is obtained accordingly by multiplying the birefringence with the ray path covered by the ray. The aperture angle  $\theta_L$  is determined between the ray direction and the lens axis, the azimuth angle  $\alpha_L$  between the projection of the ray direction into the crystallographic plane perpendicular to the lens axis and a reference direction that is physically fixed in the lens.

[0021] Because of the angle-dependence of the birefringence distributions of the individual fluoride crystal lenses, the rays of a bundle which merges in an image point in the image plane of the objective are subject to angle-dependent optical path differences  $\Delta OPL(\alpha_R, \theta_R)$  for two mutually orthogonal states of linear polarization. The optical path differences  $\Delta OPL$  in this expression are stated as a function of the aperture angle  $\theta_R$  and the azimuth angle  $\alpha_R$ . The aperture angle  $\theta_R$  of a ray is determined as the angle between the ray direction and the optical axis in the image plane, and the azimuth angle  $\alpha_R$  is determined as the angle between the projection of the ray direction into the image plane and a fixed reference direction in the image plane. If the objective has at least two lenses or lens parts of fluoride crystal, it is advantageous, if the lens axes of these lenses or lens parts point in a principal

crystallographic direction and the lenses or lens parts are arranged with a rotation relative to each other such that the distribution  $\Delta OPL(\alpha_R, \theta_R)$  of the optical path differences has significantly reduced values in comparison to an arrangement in which the lens axes point in the same principal crystallographic direction and the lenses or lens parts are installed with the same orientation. As the birefringence distributions of the lenses are azimuth-dependent, the rotated arrangement of the lenses can result in lowering the maximum value of the distribution  $\Delta OPL(\alpha_R, \theta_R)$  by as much as 20%, in particular by as much as 25%, in comparison to an installation with the same orientation of the lenses.

[0022] Lens parts can for example refer to individual lenses that are combined into a single lens by wringing, so that they have an optically seamless joint surface. In the most general sense, lens parts are defined as the components of a single lens, wherein the lens axes of each of the lens parts point in the direction of the lens axis of the single lens.

[0023] The rotated installation of the fluoride crystal lenses can in particular lead to a noticeable reduction of the dependence of the distribution  $\Delta OPL(\alpha_R, \theta_R)$  on the azimuth angle  $\alpha_R$ , resulting in a distribution  $\Delta OPL(\alpha_R, \theta_R)$  that is close to rotational symmetry.

[0024] If the lens axis is oriented in a principal crystallographic direction, the birefringence distribution  $\Delta n(\alpha_L, \theta_L)$  of the lens will have a k-fold azimuthal symmetry. For example, the birefringence distribution of a (100)-lens whose lens axis points in the crystallographic <100>-direction, has a fourfold azimuthal symmetry, while the birefringence distribution of a (111)-lens whose lens axis points in the crystallographic <111>-direction, has a

threefold azimuthal symmetry, and the birefringence distribution of a (110)-lens whose lens axis points in the crystallographic <110>-direction, has a twofold azimuthal symmetry. Depending on the rank of the azimuthal symmetry, the individual lenses or lens parts of a group are arranged with a rotation about the lens axis by a given angle  $\gamma$  relative to each other. The rotation angle  $\gamma$  is measured between the respective reference directions of two lenses or lens parts. The lens axes of the lenses in a group are oriented in one and the same or an equivalent principal crystallographic direction. The reference directions of the lenses in a group are fixed in the lenses in such a way that the birefringence distributions  $\Delta n(\alpha_L, \theta_0)$  for a given aperture angle  $\theta_0$  have the same azimuthal profile. Thus, the azimuthal locations where the birefringence has its maxima occur at the same azimuth angles in all lenses of a group. In a group of  $n$  lenses, the angles of rotation between each two of the lenses are determined as follows:

$$\gamma = \frac{360^\circ}{k \cdot n} + m \cdot \frac{360^\circ}{k} \pm 10^\circ$$

where  $k$  indicates the rank of the azimuthal symmetry,  $n$  stands for the number of lenses in a group, and  $m$  stands for an arbitrary integer number. The tolerance of  $\pm 10^\circ$  allows for the fact that the angles of rotation may deviate from the theoretically ideal angles, so that other boundary constraints can be taken into account in the adjustment of the objective. A deviation from the ideal angle of rotation leads to a non-optimized azimuthal equalization of the optical path differences for the lenses in a group. However, this can be tolerated within certain limits.

[0025] Accordingly, the angles of rotation for (100)-lenses are determined as follows:

$$\gamma = \frac{90^\circ}{n} + m \cdot 90^\circ \pm 10^\circ.$$

[0026] If the group has two (100)-lenses, the ideal angle of rotation between the two lenses is  $45^\circ$ , or  $135^\circ$ ,  $225^\circ$  ...

[0027] Accordingly, the angles of rotation for (111)-lenses are determined as follows:

$$\gamma = \frac{120^\circ}{n} + m \cdot 120^\circ \pm 10^\circ.$$

[0028] The angles of rotation for (110)-lenses are determined as follows:

$$\gamma = \frac{180^\circ}{n} + m \cdot 180^\circ \pm 10^\circ.$$

[0029] The distribution of the optical path differences  $\Delta OPL_G(\alpha_R, \theta_R)$  can also be stated for the influence of an individual group of lenses, if only these lenses are considered in the evaluation of the birefringence and the other lenses are assumed to be not birefringent.

[0030] The lenses of a group are determined, e.g., according to the criterion that an outermost aperture ray of a bundle of rays has similar respective aperture angles inside these lenses. It is of advantage if the aperture angles of the outermost aperture ray are larger than  $15^\circ$  in these lenses, in particular if they are larger than  $20^\circ$ . The term "outermost aperture ray" refers to a ray that originates from an object point and whose ray height in the aperture stop plane equals the radius of the aperture stop, so that in the image plane this ray has an angle corresponding to the image-side numerical aperture. The reason why the outermost aperture rays are used to define the groups is that they normally have

the largest aperture angles inside the lenses and are thus affected the most by the undesirable effects of the birefringence. By determining the optical path difference for two mutually orthogonal states of linear polarization for the outermost aperture rays, one can therefore arrive at conclusions about the maximum irregularity of a wave front due to birefringence.

[0031] It is further advantageous if the outermost aperture ray in each of these lenses has an equal ray path. These measures have the result of a good compensation of the azimuthal contributions to the distribution of the optical path differences that are caused by the individual lenses of a group, so that the resultant distribution of the optical path differences is close to rotationally symmetric.

[0032] It is further advantageous if with uniform orientation of the lenses, the outermost aperture ray in each lens of a group is subjected to an optical path difference of similar magnitude between two mutually orthogonal states of linear polarization. If this condition is met, the rotated arrangement of these lenses will lead to an optimized balancing of the azimuthal contributions.

[0033] In the case of adjacent planar-parallel (100)- or (111)-lenses of equal thickness, or four adjacent planar-parallel (110)-lenses of equal thickness, the rotation of the lenses in accordance with the foregoing formulae produces a rotationally symmetric distribution of the optical path differences  $\Delta OPL$ . In lenses with curved surfaces, it is likewise possible through a judicious selection of the lenses of a group or through an appropriate choice of the thicknesses and radii of the lenses to achieve an approximately rotation-symmetric birefringence distribution already by rotating two

lenses. In the case of (100)-lenses or (111)-lenses, it is advantageous if a group has two lenses. In (110)-lenses, a distribution of the optical path differences with approximate rotational symmetry is obtained with four lenses in a group.

[0034] The concept of rotating the lenses relative to each other is particularly effective if the lenses are arranged adjacent to each other. It is particularly advantageous to split a lens into two parts and to combine the lens parts in rotated positions with an optically seamless joint, for example by wringing.

[0035] In a projection objective with a multitude of lenses it is advantageous to form a plurality of groups of lenses. The lenses of a group are arranged with a rotation about the lens axes such that the resultant distribution  $\Delta OPL(\alpha_R, \theta_R)$  is nearly independent of the azimuth angle.

[0036] While the rotation of the lenses in a group relative to each other has the effect that the distributions  $\Delta OPL_g(\alpha_R, \theta_R)$  that are caused by the individual groups are nearly independent of the azimuth angle, the maximum value of the overall distribution  $\Delta OPL(\alpha_R, \theta_R)$  for the entire objective can be noticeably reduced by using at least one group of (100)-lenses as well as at least one group of (111)-lenses in the projection objective. A good compensation is also possible, if a group of (110)-lenses is arranged within the objective in addition to a group of (100)-lenses.

[0037] The compensation is possible because the birefringence has not only an absolute value but also a direction. The compensation of the undesirable influence of the birefringence is optimal, if the distribution of the optical path differences  $\Delta OPL_1(\alpha_R, \theta_R)$  that is caused by the lenses or lens

parts of all groups with (100)-lenses has maximum values of similar magnitude as the distribution of the optical path differences  $\Delta OPL_2(\alpha_R, \theta_R)$  that is caused by the lenses or lens parts of all groups with (111)- or (110)-lenses.

[0038] As a further advantageous possibility to reduce the undesirable influence of the birefringence, a compensation coating can be applied to an optical element of the projection objective. The basis for pursuing this possibility lies in the observation that any optical coating, e.g., an anti-reflex coating or a mirror coating, always involves optical path differences for two mutually orthogonal states of linear polarization in addition to the reflective and transmissive properties. These are different for s- and p-polarized light and depend in addition on the angle of incidence of the ray on the coating. In other words, one observes a birefringence that is dependent on the angle of incidence. For a ray bundle wherein the central ray meets the compensation coating at an incident angle of  $0^\circ$ , the values and directions of the birefringence are rotationally symmetric relative to the central ray. The compensation coating is now designed for specified properties in regard to the amount of birefringence as a function of the aperture angle of the rays of a light bundle.

[0039] As a first step, one determines the distribution of the optical path differences  $\Delta OPL(\alpha_R, \theta_R)$  for two mutually orthogonal states of linear polarization for a ray bundle in the image plane of the projection objective. The aperture angle  $\theta_R$  of a ray is measured between the ray direction and the optical axis in the image plane, while the azimuth angle  $\alpha_R$  is measured between the projection of the ray direction into the image plane and a fixed reference direction in the image plane. The distribution of the optical path differences

$\Delta OPL(\alpha_R, \theta_R)$  for two mutually orthogonal states of linear polarization describes the overall resultant influence of birefringence, intrinsic birefringence of fluoride crystal lenses, stress-induced birefringence, coatings of optical elements with anti-reflex layers of lenses, or mirror coatings.

[0040] Based on the distribution of the optical path differences  $\Delta OPL(\alpha_R, \theta_R)$ , one determines the effective birefringence distribution of the compensation coating that is to be applied to an optical element with an element axis. Optical elements include, e.g., refractive or diffractive lenses, planar plates, or mirrors. The optical surfaces of the optical element are defined as the optically used surface areas, i.e., normally the front and back surface. The element axis is constituted, e.g., by a symmetry axis of a rotationally symmetric lens. If the lens has no symmetry axis, the element axis can be constituted by the center of an incident ray bundle or by a straight line in relation to which the ray angles of all light rays inside the lens are minimal. The effective birefringence values depend on azimuth angles  $\alpha_F$  which are defined relative to a reference direction that is perpendicular to the element axis, and they further depend on aperture angles  $\theta_F$  that are referenced against the element axis.

[0041] A value pair  $(\alpha_R, \theta_R)$  of a ray in the image plane correlates to a value pair  $(\alpha_F, \theta_F)$  in the optical element.

[0042] The effective birefringence distribution of the compensation coating is now determined in such a manner that the distribution of the optical path differences for two mutually orthogonal states of linear polarization for the overall system inclusive of the compensation coating is

significantly reduced in comparison to the distribution that would exist without the compensation coating.

[0043] The effective birefringence distribution can be influenced through the choice of material, the thickness profiles, and the vapor-deposition angles of the individual layers of the compensation coating. The design of the layers and the process parameters are obtained by using computer programs for coating design which determine the thickness profiles for the individual layers and the process parameters based on the effective birefringence distribution, the given materials and the geometry of the optical element.

[0044] It is also possible to apply the compensation coating to a plurality of optical elements. This increases the degrees of freedom in the determination of the compensation layers which in addition to their compensating function should also ensure a high transmissivity of the coating.

[0045] Typical distributions of the optical path differences  $\Delta OPL(\alpha_R, \theta_R)$  for two mutually orthogonal states of linear polarization have small path differences at the aperture angle  $\theta_R=0^\circ$ . It is therefore advantageous if the birefringent effect of the compensation coating is of a nearly vanishing magnitude at the aperture angle  $\theta_R=0^\circ$ . This is achieved if no large vapor-deposition angles are used in the manufacturing process of the compensation coating. It is therefore of advantage if the curvature of the respective optical surface of the optical element where the compensation coating is applied is as weak as possible.

[0046] As described above, as a result of rotating lenses of (100)- or (111)-orientation relative to each other, one obtains an approximately rotation-symmetric distribution

$\Delta OPL(\alpha_R, \theta_R)$  of the optical path differences in the image plane, which depends only on the aperture angle  $\theta_R$ . The optical path differences can be further reduced by applying to an optical element a compensation coating with an effective birefringence distribution which depends primarily on the aperture angle  $\theta_R$  alone. This property of the coating is achieved in a design where the layer thicknesses of the individual layers of the compensation coating are homogeneous over the optical element and don't have tapered thickness profiles.

[0047] The invention can be used advantageously if the optical element with the compensation coating is an interchangeable element.

[0048] It is of advantage to use the optical element closest to the image plane.

[0049] As a first step of the inventive method, the distribution of the optical path differences  $\Delta OPL(\alpha_R, \theta_R)$  for two mutually orthogonal states of linear polarization is determined for a bundle of rays in the image plane. In this determination, the influence of all optical elements of the objective inclusive of coatings is taken into account. The optical element, to which the compensation coating is applied in a subsequent step, is likewise included in the ray path of the light bundle.

[0050] As a second step of the method described above, the effective birefringence distribution of a compensation coating is determined along with the resultant thickness profiles of the individual layers as well as the process parameters for producing the individual layers.

[0051] In a third step, the optical element is removed from the ray path and the compensation coating is applied to it. In case the optical surface of the optical element was already coated, the existing coating is removed prior to applying the new coating.

[0052] In a fourth step, the optical element with the compensation coating is put back into its original place inside the objective.

[0053] The preferred material to use for the lenses in projection objectives is calcium fluoride, because when used together with quartz at an operating wavelength of 193 nm, calcium fluoride is particularly well suited for the color correction, and with an operating wavelength of 157 nm, it still has a sufficient transmissivity. However, the foregoing statements are likewise applicable to the fluoride crystals strontium fluoride and barium fluoride, as they are crystals of the same type of cubic crystal structure.

[0054] The undesirable influence of intrinsic birefringence becomes particularly noticeable if the light rays inside the lenses have large aperture angles. This is the case in projection objectives with an image-side numerical aperture larger than 0.7, in particular larger than 0.8.

[0055] The intrinsic birefringence becomes noticeably stronger with decreasing working wavelength. Thus, the intrinsic birefringence at a wavelength of 193 nm is more than twice as strong, and at a wavelength of 157 nm it is more than five times as strong as it is at a wavelength of 248 nm. The invention can therefore be used to particular advantage if the light rays have wavelengths shorter than 200 nm, in particular shorter than 160 nm.

[0056] The projection objective in the present context can be a purely refractive objective that consists of a multitude of lenses arranged with rotational symmetry about the optical axis, or it can be a projection objective of the catadioptric type of objectives.

[0057] Projection objectives of this kind can be used advantageously in microlithography projection exposure apparatus which include a light source followed by an illumination system, a mask-positioning system, a structure-carrying mask, a projection objective, an object-positioning system, and a light-sensitive substrate.

[0058] This microlithography projection exposure apparatus can be used to produce micro-structured semiconductor elements.

[0059] The invention also provides a suitable method for the manufacture of objectives. According to the method, lenses or lens parts of fluoride crystal wherein the lens axes are oriented in a principal crystallographic direction are arranged with a rotation about the lens axes such that the values of the distribution  $\Delta OPL(\alpha_r, \theta_r)$  are significantly reduced in comparison to a lens arrangement in which the lens axes of the fluoride crystal lenses point in the same principal crystallographic direction and where the lenses are arranged with the same orientation.

[0060] The method further includes the concept of forming groups of (100)-lenses and groups of (111)-lenses or (110)-lenses and to use the groups in parallel. The method is in this case applied, e.g., in a projection objective that has at least two fluoride crystal lenses in <100>-orientation and at

least two lenses in <111>-orientation, where the orientation of the reference directions is known for these lenses. The method makes use of the inventive observation, that the maximum values of the distribution  $\Delta OPL(\alpha_R, \theta_R)$  of the optical path differences can be significantly reduced by rotating the fluoride crystal lenses about the optical axis. Using suitable simulation methods, a bundle of light rays originating from an object point is propagated through a projection objective, and the distribution  $\Delta OPL(\alpha_R, \theta_R)$  in the image plane is calculated on the basis of the known optical properties of the fluoride crystal lenses. In an optimizing step, the angles of rotation between the fluoride crystal lenses are varied until the birefringence values are within tolerance. It is possible to take further boundary constraints into account in the optimizing step, such as for example the compensation of rotationally non-symmetric lens errors by rotating the lenses. This optimizing step can reduce the maximum value of the distribution  $\Delta OPL(\alpha_R, \theta_R)$  by up to 30%, in particular cases up to 50%, in comparison to a projection objective in which the fluoride crystal lenses are arranged with the same orientation. The optimizing routine can also include an intermediate step in which groups are formed among the fluoride crystal lenses, where the lenses in a group, when arranged with the same orientation of the lenses, produce similar optical path differences between two mutually orthogonal states of linear polarization in an outermost aperture ray. In the subsequent optimizing step, the lenses are rotated only within the groups in order to reduce the optical path differences. Thus, the (100)-lenses can first be rotated so that the optical path differences caused by the (100)-lenses are reduced, and subsequently the (111)-lenses are rotated so that the optical path differences caused by the (111)-lenses are reduced. The allocation of the fluoride crystal lenses to lenses with (100)-orientation and

(111)-orientation, respectively, has to be made in such a manner in the optimization that the resultant (100)-distribution  $\Delta OPL_{100}(\alpha_R, \theta_R)$  and the resultant (111)-distribution  $\Delta OPL_{111}(\alpha_R, \theta_R)$  compensate each other to a large extent. An analogous condition applies also to the parallel use of (100)-lenses and (110)-lenses.

[0061] The invention further relates to a method for the manufacture of a lens, where in a first step a plurality of fluoride crystal plates are joined in an optically seamless manner to form a blank, and in a second step the lens is formed out of the blank through state-of-the-art manufacturing methods. The plates are arranged with a rotation relative to each other about the normal axes of the plate surfaces, analogous to the foregoing description for lenses or lens parts.

[0062] It is advantageous if plates in which the normal vectors of the surfaces are oriented in one and the same or an equivalent principal crystallographic direction are of equal axial thickness.

[0063] If (100)-plates are joined with (111)-plates in an optically seamless manner, the sum of the thicknesses of the (111)-plates in relation to the sum of the thicknesses of the (100)-plates should be in a ratio of  $1.5 \pm 0.2$ .

[0064] If (100)-plates are joined with (110)-plates in an optically seamless manner, the sum of the thicknesses of the (110)-plates in relation to the sum of the thicknesses of the (100)-plates should be in a ratio of  $4.0 \pm 0.4$ .

[0065] The invention will be explained in more detail with reference to the drawings.

[0066] Figure 1 illustrates a cross-section of a fluoride crystal block perpendicular to the crystallographic {100}-planes together with a lens of a projection objective in a schematic representation;

[0067] Figures 2A-C show, respectively, a planar-parallel (100)-, (111)-, and (110)-lens in a schematic three-dimensional representation;

[0068] Figure 3 shows a coordinate system for the definition of the aperture angle and the azimuth angle;

[0069] Figures 4A-F represent the birefringence distributions of (100)-lenses in different representations as well as the birefringence distribution for two (100)-lenses that are rotated relative to each other by 45°;

[0070] Figures 5A-F represent the birefringence distribution of (111)-lenses in different representations as well as the birefringence distribution for two (111)-lenses that are rotated relative to each other by 60°;

[0071] Figures 6A-G represent the birefringence distributions of (111)-lenses in different representations as well as the birefringence distribution for two (110)-lenses that are rotated relative to each other by 90°, and four (110)-lenses that are rotated relative to each other by 45°;

[0072] Figure 7 represents the lens section of a refractive projection objective;

[0073] Figure 8 represents the lens section of a catadioptric projection objective; and

[0074] Figure 9 illustrates a microlithography projection exposure apparatus in a schematic representation.

[0075] Figure 1 schematically illustrates a section through a fluoride crystal block 3. The section is selected so that the crystallographic {100}-planes 5 can be seen as individual lines, i.e., the crystallographic {100}-planes 5 are oriented perpendicular to the plane of the paper. The fluoride crystal block 3 serves as a blank or raw material for the (100)-lens 1. In the illustrated example, the (100)-lens 1 is a bi-convex lens with the lens axis EA which is at the same time the symmetry axis of the lens. The lens 1 is now formed out of the fluoride crystal block in such a manner that the lens axis EA stands perpendicular to the crystallographic {100}-planes.

[0076] Figure 2A visualizes in a three-dimensional representation how the intrinsic birefringence is related to the crystallographic directions in the case where the lens axis EA points in the crystallographic <100>-direction. The lens shown is a circular planar-parallel plate 201 of calcium fluoride. The lens axis EA points in the crystallographic <100>-direction. Besides the crystallographic <100>-direction, the <101>-, <1 $\bar{1}$ 0>-, <10 $\bar{1}$ >-, and <110>-directions are likewise represented as arrows. The intrinsic birefringence is represented schematically by four lobes 203, whose surface areas represent the amount of the intrinsic birefringence for the respective ray direction of a light ray. The maxima for the intrinsic birefringence occur, respectively, in the crystallographic <101>-, <1 $\bar{1}$ 0>-, <10 $\bar{1}$ >-, and <110>-directions, i.e., for light rays with an aperture angle of 45° and an azimuth angle of 0°, 90°, 180° and 270° inside the lens. The minima of the intrinsic birefringence

are associated with azimuth angles of  $45^\circ$ ,  $135^\circ$ ,  $225^\circ$  and  $315^\circ$ . The intrinsic birefringence vanishes at an aperture angle of  $0^\circ$ .

[0077] Figure 2B visualizes in a three-dimensional representation how the intrinsic birefringence is related to the crystallographic directions in the case where the lens axis EA points in the crystallographic  $\langle 111 \rangle$ -direction. The lens shown is a circular planar-parallel plate 205 of calcium fluoride. The lens axis EA points in the crystallographic  $\langle 111 \rangle$ -direction. Besides the crystallographic  $\langle 111 \rangle$ -direction, the  $\langle 011 \rangle$ -,  $\langle 101 \rangle$ -, and  $\langle 110 \rangle$ -directions are likewise represented as arrows. The intrinsic birefringence is represented schematically by three lobes 207, whose surface areas represent the amount of the intrinsic birefringence for the respective ray direction of a light ray. The maxima for the intrinsic birefringence occur, respectively, in the crystallographic  $\langle 011 \rangle$ -,  $\langle 101 \rangle$ -, and  $\langle 110 \rangle$ -directions, i.e., for light rays with an aperture angle of  $35^\circ$  and an azimuth angle of  $0^\circ$ ,  $120^\circ$ , and  $240^\circ$  inside the lens. The minima of the intrinsic birefringence are associated, respectively, with azimuth angles of  $60^\circ$ ,  $180^\circ$ , and  $300^\circ$ . The intrinsic birefringence vanishes at an aperture angle of  $0^\circ$ .

[0078] Figure 2C visualizes in a three-dimensional representation how the intrinsic birefringence is related to the crystallographic directions in the case where the lens axis EA points in the crystallographic  $\langle 110 \rangle$ -direction. The lens shown is a circular planar-parallel plate 209 of calcium fluoride. The lens axis EA points in the crystallographic  $\langle 110 \rangle$ -direction. Besides the crystallographic  $\langle 110 \rangle$ -direction, the  $\langle 01\bar{1} \rangle$ -,  $\langle 10\bar{1} \rangle$ -,  $\langle 101 \rangle$ -, and  $\langle 011 \rangle$ -directions are likewise represented as arrows. The intrinsic birefringence is represented schematically by five lobes 211,

whose surface areas represent the amount of the intrinsic birefringence for the respective ray direction of a light ray. The respective maxima for the intrinsic birefringence occur on the one hand in the direction of the lens axis EA and on the other hand in each of the crystallographic directions  $\langle 01\bar{1} \rangle$ ,  $\langle 10\bar{1} \rangle$ ,  $\langle 101 \rangle$ , and  $\langle 011 \rangle$ , i.e., for light rays with an aperture angle of  $0^\circ$ , and for light rays with an aperture angle of  $60^\circ$  and the four azimuth angles that are obtained as a result of projecting the crystallographic  $\langle 01\bar{1} \rangle$ -,  $\langle 10\bar{1} \rangle$ -,  $\langle 101 \rangle$ -, and  $\langle 011 \rangle$ -directions into the crystallographic  $\{110\}$ -plane. However, such high aperture angles do not occur in crystal material, because the maximum aperture angles are limited to a value of less than  $45^\circ$  by the refractive index of the crystal.

[0079] The definition of aperture angle  $\theta$  and azimuth angle  $\alpha$  is illustrated in Figure 3. In the case of the  $(100)$ -lens of Figure 2, the z-axis indicates the crystallographic  $\langle 100 \rangle$ -direction, and the x-axis represents the direction that is obtained by projecting the crystallographic  $\langle 110 \rangle$ -direction into the crystallographic  $\{100\}$ -plane. In this representation, the z-axis equals the lens axis and the x-axis equals the reference direction.

[0080] As disclosed in the Internet publication cited hereinabove, in measurements with a light ray propagation in the crystallographic  $\langle 110 \rangle$ -direction, a birefringence of  $(6.5 \pm 0.4) \text{ nm/cm}$  was found at a wavelength of  $\lambda = 156.1 \text{ nm}$  in calcium fluoride. Taking this measured value as a normative factor, it is possible to theoretically derive the birefringence distribution  $\Delta n(\theta, \alpha)$  of a calcium fluoride lens dependent on the crystal orientation. The derivations are based on the formalisms known from crystal optics for the calculation of the index ellipsoids dependent on the direction of the light ray. The theoretical basis can be found, e.g.,

in "Lexikon der Optik", Spektrum Akademischer Verlag Heidelberg Berlin 1999 under the term "Kristalloptik".

[0081] More recent measurements by the present applicant have led to the result that with a ray propagation in the crystallographic <110>-direction the intrinsic birefringence in calcium fluoride crystal at a wavelength of  $\lambda$  of 156.1 nm amounts to 11 nm/cm. While the statements made below relate to  $\Delta n_{\max} = 6.5$  nm/cm as the normative factor, they can be converted without difficulty to  $\Delta n_{\max} = 11$  nm/cm as the normative factor.

[0082] Represented in Figure 4A is the amount of the intrinsic birefringence as a function of the aperture angle  $\theta$  with the azimuth angle  $\alpha = 0^\circ$  for a (100)-lens. The value of 6.5 nm/cm for the intrinsic birefringence at an aperture angle of  $\theta = 45^\circ$  represents the measured value. The curve profile was determined according to the formulae that are known from crystal optics.

[0083] Figure 4B illustrates the intrinsic birefringence as a function of the azimuth angle  $\alpha$  with the aperture angle  $\theta = 45^\circ$  for a (100)-lens. The fourfold azimuthal symmetry is evident.

[0084] Figure 4C illustrates the birefringence distribution  $\Delta n(\theta, \alpha)$  for individual ray directions in the  $(\theta, \alpha)$  coordinate space for a (100)-lens. Each line represents the amount and the direction for a ray direction that is defined by the aperture angle  $\theta$  and the azimuth angle  $\alpha$ . The length of each line is proportional to the amount of the birefringence or to the length difference between the principal axes of the elliptical section, while the direction of the line indicates the orientation of the longer principal axis of the elliptical

section. The elliptical section is obtained by intersecting the index ellipsoid for the ray of the direction  $(\theta, \alpha)$  with a plane that is perpendicular to the ray direction and passes through the center point of the index ellipsoid. The directions as well as the lengths of the lines indicate the fourfold structure of the distribution. The length of the lines, and thus the birefringence, has its maxima at the azimuth angles of  $0^\circ$ ,  $90^\circ$ ,  $180^\circ$ , and  $270^\circ$ .

[0085] Figure 4D illustrates the birefringence distribution  $\Delta n(\theta, \alpha)$  that is obtained by arranging two adjacent planar-parallel (100)-lenses of equal thickness with a rotation of  $45^\circ$ . The resultant birefringence distribution  $\Delta n(\theta, \alpha)$  is independent of the azimuth angle  $\alpha$ . The longer principal axes of the elliptical sections run in the tangential direction. The resultant optical path differences between two mutually orthogonal states of polarization are obtained by multiplying the birefringence values with the physical path lengths of the rays inside the planar-parallel (100)-lenses. Rotationally symmetric birefringence distributions are obtained by arranging  $n$  planar-parallel (100)-lenses of equal thickness in such a manner that the angle of rotation  $\beta$  between each two of the lenses conforms to the equation:

$$\beta = \frac{90^\circ}{n} + m \cdot 90^\circ \pm 5^\circ$$

wherein  $n$  stands for the number of planar-parallel (100)-lenses and  $m$  represents an integer number. In comparison to an arrangement of uniformly oriented lenses, the maximum value of the birefringence for the aperture angle  $\theta = 30^\circ$  can be reduced by 30%. A nearly rotation-symmetric birefringence distribution is also obtained for arbitrary lenses if all rays of a bundle have respective aperture angles of similar magnitude and cover similar path lengths inside the lenses.

The lenses should therefore be combined into groups where the rays conform as much as possible to the foregoing condition.

[0086] Figure 4E represents the amount of the intrinsic birefringence as a function of the aperture angle  $\theta$  for the azimuth angle  $\alpha=0^\circ$  for the two adjacent planar-parallel (100)-lenses of equal thickness that are shown in Figure 4D. The maximum value for the intrinsic birefringence at the aperture angle  $\theta=41^\circ$  amounts to 4.2 nm/cm and is thus reduced by 35% in comparison to the maximum value of 6.5 nm/cm of Figure 4A.

[0087] Figure 4F represents the amount of the intrinsic birefringence as a function of the azimuth angle  $\alpha$  with the aperture angle  $\theta=41^\circ$  for the two adjacent planar-parallel (100)-lenses of equal thickness that are shown in Figure 4D. The intrinsic birefringence is independent of the azimuth angle  $\alpha$ .

[0088] Figure 5A represents the intrinsic birefringence as a function of the aperture angle  $\theta$  for the azimuth angle  $\alpha = 0^\circ$  in a (111)-lens. The value of 6.5 nm/cm for the intrinsic birefringence at an aperture angle of  $\theta = 35^\circ$  represents the measured value. The curve profile was determined according to the formulae that are known from crystal optics.

[0089] Figure 5B illustrates the amount of intrinsic birefringence as a function of the azimuth angle  $\alpha$  for the aperture angle  $\theta = 35^\circ$  for a (111)-lens. The threefold azimuthal symmetry is evident.

[0090] Figure 5C illustrates the birefringence distribution  $\Delta n(\theta, \alpha)$  for individual ray directions in the  $(\theta, \alpha)$  coordinate space for a (111)-lens in an analogous representation as presented already in Figure 4C. The directions as well as the

lengths of the lines indicate the threefold structure of the distribution. The length of the lines, and thus the birefringence, has its maxima at the azimuth angles of  $0^\circ$ ,  $120^\circ$ , and  $240^\circ$ . In contrast to a (100)-lens, the orientation of the birefringence rotates by  $90^\circ$  if a ray passes through the lens with an azimuth angle of  $180^\circ$  instead of with an azimuth angle of  $0^\circ$ . Thus, the birefringence can be compensated, e.g., by two (111)-lenses of equal orientation, if the ray angles of a ray bundle change signs between the two lenses.

[0091] Figure 5D illustrates the birefringence distribution  $\Delta n(\theta, \alpha)$  that is obtained by arranging two adjacent planar-parallel (111)-lenses of equal thickness with a rotation of  $60^\circ$ . The resultant birefringence distribution  $\Delta n(\theta, \alpha)$  is independent of the azimuth angle  $\alpha$ . However, in contrast to Figure 4C, the longer principal axes of the elliptical sections run in the radial direction. The resultant optical path differences between two mutually orthogonal states of polarization are obtained by multiplying the birefringence values with the physical path lengths inside the (111)-lenses. Rotationally symmetric birefringence distributions are likewise obtained by arranging  $n$  planar-parallel (111)-lenses of equal thickness in such a manner that the angle of rotation between each two lenses conforms to the equation:

$$\gamma = \frac{120^\circ}{k} + l \cdot 120^\circ \pm 5^\circ$$

wherein  $k$  stands for the number of planar-parallel (111)-lenses and  $l$  represents an integer number. In comparison to an arrangement of uniformly oriented lenses, the value of the birefringence for the aperture angle  $\theta = 30^\circ$  can be reduced by 68%. A rotationally near-symmetric distribution of the optical path differences between two mutually orthogonal states of linear polarization is also obtained for arbitrary

lenses if all rays of a bundle have similar respective angles in the lenses and cover similar respective path lengths inside the lenses. Therefore, the lenses should be combined into groups where the rays conform as much as possible to the foregoing condition.

[0092] Figure 5E represents the amount of the intrinsic birefringence as a function of the aperture angle  $\theta$  for the azimuth angle  $\alpha=0^\circ$  for the two adjacent planar-parallel (111)-lenses of equal thickness that are shown in Figure 5D. The maximum value for the intrinsic birefringence at the aperture angle  $\theta=41^\circ$  amounts to 2.8 nm/cm and is thus reduced by 57% in comparison to the maximum value of 6.5 nm/cm of Figure 5A.

[0093] Figure 5F represents the amount of the intrinsic birefringence as a function of the azimuth angle  $\alpha$  with the aperture angle  $\theta=41^\circ$  for the two adjacent planar-parallel (111)-lenses of equal thickness that are shown in Figure 5D. The intrinsic birefringence is independent of the azimuth angle  $\alpha$ .

[0094] Now, if one combines groups of (100)-lenses and groups of (111)-lenses within a projection objective, it is possible to compensate to a large extent the contributions of these lenses to the optical path differences for two mutually orthogonal states of linear polarization. To accomplish this, it is first necessary that within the groups a distribution of the optical path differences close to rotational symmetry is obtained by rotating the lenses, and then that by combining a group of (100)-lenses with a group of (111)-lenses, the two distributions of the optical path differences will compensate each other. To achieve this result, one makes use of the fact that the orientations of the longer principal axes of the elliptical sections for the birefringence distribution of a

group of rotated (100)-lenses are perpendicular to the orientations of the longer principal axes of the elliptical sections of the birefringence distribution of a group of rotated (111)-lenses, as can be concluded from Figures 4D and 5D. In this respect, it is of critical importance that on the one hand the individual groups produce a distribution of the optical path differences close to rotational symmetry and that on the other hand the sum of the contributions of the groups of (100)-lenses and the sum of the contributions of the groups of (111)-lenses are closely matched in regard to their absolute amounts.

[0095] Figure 6A represents the intrinsic birefringence as a function of the aperture angle  $\theta$  for the azimuth angle  $\alpha = 0^\circ$  in a (110)-lens. The value of 6.5 nm/cm for the intrinsic birefringence at an aperture angle of  $\theta = 0^\circ$  represents the measured value. The curve profile was determined according to the formulae that are known from crystal optics.

[0096] Figure 6B represents the amount of the intrinsic birefringence as a function of the azimuth angle  $\alpha$  for the aperture angle  $\theta = 35^\circ$  for a (110)-lens. The twofold azimuthal symmetry is evident.

[0097] Figure 6C illustrates the birefringence distribution  $\Delta n(\theta, \alpha)$  for individual ray directions in the  $(\theta, \alpha)$  coordinate space for a (110)-lens in an analogous representation as introduced already in Figure 4C. The directions as well as the lengths of the lines indicate the twofold structure of the distribution. The line of maximum length, and thus the maximum birefringence, occurs at an aperture angle  $\theta=0^\circ$ .

[0098] Figure 6D illustrates the birefringence distribution  $\Delta n(\theta, \alpha)$  that is obtained by arranging two adjacent planar-

parallel (110)-lenses of equal thickness with a rotation of 90° relative to each other. The resultant birefringence distribution  $\Delta n(\theta, \alpha)$  in this case has a fourfold azimuthal symmetry. Maximum values of the birefringence occur at the azimuth angles  $\alpha=45^\circ$ ,  $135^\circ$ ,  $225^\circ$ , and  $315^\circ$ , where the value of the birefringence at an aperture angle of  $\theta=40^\circ$  amounts to 2.6 nm/cm.

[0099] Figure 6E represents the birefringence distribution  $\Delta n(\theta, \alpha)$  that is obtained if the two planar-parallel (110)-lenses of equal thickness in Figure 6C are combined with two further planar-parallel (110)-lenses of equal thickness. The angle of rotation between each two of the (110)-lenses is 45°. The resultant birefringence distribution  $\Delta n(\theta, \alpha)$  is independent of the azimuth angle  $\alpha$ . However, in contrast to Figure 4C, the longer principal axes of the elliptical sections are now oriented radially, i.e., similar to the distribution of Figure 5C. The resultant optical path differences between two mutually orthogonal states of polarization are obtained by multiplying the birefringence values with the physical path lengths of the rays inside the (110)-lenses. Rotationally symmetric birefringence distributions are likewise obtained by arranging  $4 \cdot n$  planar-parallel (110)-lenses of equal thickness in such a manner that the angle of rotation  $\beta$  between each two of the lenses conforms to the equation:

$$\beta = \frac{45^\circ}{n} + m \cdot 90^\circ \pm 5^\circ$$

wherein  $4 \cdot n$  stands for the number of planar-parallel (100)-lenses and  $m$  represents an integer number. A nearly rotation-symmetric distribution of the optical path differences for two mutually orthogonal states of linear polarization is also obtained for arbitrary lenses if all rays of a bundle have respective aperture angles of similar magnitude in the lenses

and cover similar path lengths inside the lenses. The lenses should therefore be combined into groups where the rays conform as much as possible to the foregoing condition.

[0100] Figure 6F represents the amount of the intrinsic birefringence as a function of the aperture angle  $\theta$  with the azimuth angle  $\alpha=0^\circ$  for the four adjacent planar-parallel (110)-lenses of equal thickness that are shown in Figure 6E. The value of the intrinsic birefringence at the aperture angle  $\theta=41^\circ$  amounts to 1.0 nm/cm which represents a reduction by 84% in relation to the maximum value of 6.5 nm/cm in Figure 5A.

(0101) Figure 6G represents the amount of the intrinsic birefringence as a function of the azimuth angle  $\alpha$  for the aperture angle  $\theta=41^\circ$  for the four adjacent planar-parallel (110)-lenses of equal thickness that are shown in Figure 6E. The intrinsic birefringence is independent of the azimuth angle  $\alpha$ .

[0102] Now, if one combines groups of (110)-lenses and groups of (100)-lenses within a projection objective, it is possible to compensate to a large extent the contributions of these lenses to the optical path differences for two mutually orthogonal states of linear polarization. To accomplish this, it is first necessary that within the groups a distribution of the optical path differences close to rotational symmetry is obtained by rotating the lenses, and then that by combining a group of (110)-lenses with a group of (100)-lenses the two distributions of the optical path differences will compensate each other. To achieve this result, one makes use of the fact that the orientations of the longer principal axes of the elliptical sections for the birefringence distribution of a group of rotated (110)-lenses are perpendicular to the orientations of the longer principal axes of the elliptical

sections of the birefringence distribution of a group of rotated (100)-lenses, as can be concluded from Figures 4D and 6E. In this respect, it is of critical importance that on the one hand the individual groups produce a distribution of the optical path differences close to rotational symmetry and on the other hand the sum of the contributions of the groups of (110)-lenses and the sum of the contributions of the groups of (100)-lenses are closely matched in regard to their absolute amounts.

[0103] Figure 7 represents the lens section of a refractive projection objective 611 for the wavelength of 157 nm. The optical data for this objective are listed in Table 1. This example is taken from the applicant's patent application PCT/EP00/13184 where it corresponds to Figure 7 and Table 6. For a detailed description of the function of the objective, see PCT/EP00/13184. All lenses of this objective consist of calcium fluoride crystal. The image-side numerical aperture of the objective is 0.9. The imaging performance of the objective is corrected so well that the deviation from a wave front of an ideal spherical wave is smaller than  $1.8 \text{ m}\lambda$  at  $\lambda = 157 \text{ nm}$ . Especially with these high-performance objectives, it is necessary for undesirable effects such as those of intrinsic birefringence to be reduced to the farthest extent possible.

[0104] For the embodiment of Figure 6, a calculation was made of the aperture angles  $\theta$  and ray paths  $RL_L$  of the outermost aperture ray 609 for the individual lenses L601 to L630. The outermost aperture ray 609 originates from the object point with the coordinates  $x = 0 \text{ mm}$  and  $y = 0 \text{ mm}$ , and in the image plane has an angle relative to the optical axis that corresponds to the image-side numerical aperture. The reason why the outermost aperture ray 609 is selected is that it is

associated with close to the maximum aperture angles inside the lenses.

Table 2

Lens	Aperture angle $\theta$ [°]	Ray path $RL_L$ [mm]	Optical path difference [nm] (111)-Lens $\alpha_t = 0^\circ$	Optical path difference [nm] (111)-Lens $\alpha_t = 60^\circ$	Optical path difference [nm] (100)-Lens $\alpha_t = 0^\circ$	Optical path difference [nm] (100)-Lens $\alpha_t = 45^\circ$	Optical path difference [nm] (110)-Lens $\alpha_t = 0^\circ$	Optical path difference [nm] (110)-Lens $\alpha_t = 45^\circ$	Optical path difference [nm] (110)-Lens $\alpha_t = 90^\circ$	Optical path difference [nm] (110)-Lens $\alpha_t = 135^\circ$
L601	8.1	15.1	2.9	-2.2	-0.8	-0.4	-9.0	-9.0	-9.1	-9.0
L602	8.7	8.2	1.7	-1.2	-0.5	-0.2	-4.9	-4.8	-4.9	-4.8
L603	7.8	9.5	1.7	-1.3	-0.4	-0.2	-5.7	-5.7	-5.7	-5.7
L604	10.7	7.2	1.9	-1.3	-0.6	-0.3	-4.1	-4.1	-4.1	-4.1
L605	9.4	6.5	1.5	-1.0	-0.4	-0.2	-3.8	-3.8	-3.8	-3.8
L606	10.3	8.5	2.1	-1.4	-0.7	-0.3	-4.8	-4.8	-4.8	-4.8
L607	21.8	12.7	6.6	-2.7	-3.9	-1.8	-4.2	-4.2	-4.3	-4.2
L608	25.4	22.2	12.8	-4.4	-8.7	-3.9	-5.3	-5.7	-5.8	-5.7
L609	16.3	36.1	14.3	-7.6	-6.8	-3.3	-16.5	-16.5	-16.7	-16.5
L610	12.2	15.2	4.5	-2.9	-1.7	-0.8	-8.2	-8.2	-8.2	-8.2
L611	2.3	26.6	1.4	-1.3	-0.1	-0.1	-17.2	-17.2	-17.2	-17.2
L612	2.3	32.2	1.6	-1.5	-0.1	-0.1	-20.8	-20.8	-20.8	-20.8
L613	-18.3	30.4	-6.6	13.5	-7.0	-3.3	-12.5	-12.6	-12.7	-12.6
L614	-18.7	22.0	-4.8	10.0	-5.3	-2.5	-8.9	-8.9	-9.0	-8.9
L615	-14.0	10.2	-2.0	3.5	-1.5	-0.7	-5.1	-5.1	-5.2	-5.1
L616	-1.3	29.8	-0.8	0.9	0.0	0.0	-19.3	-19.3	-19.3	-19.3
L617	26.4	31.6	18.6	-6.1	-13.0	-5.7	-6.7	-7.6	-7.5	-7.6
L618	33.5	14.3	9.3	-2.0	-7.9	-3.1	-0.6	3.2	-1.4	3.2
L619	26.5	7.5	4.4	-1.4	-3.1	-1.4	-1.6	-1.8	-1.8	-1.8
L620	19.3	6.4	3.0	-1.4	-1.6	-0.8	-2.5	-2.5	-2.5	-2.5
L621	6.7	8.0	1.3	-1.0	-0.3	-0.1	-4.9	-4.9	-4.9	-4.9
L622	-10.3	7.7	-1.3	1.9	-0.6	-0.3	-4.4	-4.4	-4.4	-4.4
L623	-11.9	9.6	-1.8	2.8	-1.0	-0.5	-5.2	-5.2	-5.2	-5.2
L624	0.3	17.8	0.1	-0.1	0.0	0.0	-11.6	-11.6	-11.6	-11.6
L625	6.0	16.3	2.3	-1.8	-0.5	-0.2	-9.9	-9.9	-10.0	-9.9
L626	-24.0	9.0	-1.9	5.0	-3.2	-1.5	-2.5	-2.6	-2.6	-2.6
L627	-35.6	8.0	-0.9	5.2	-4.7	-1.7	0.1	2.1	-0.5	2.1
L628	-39.4	12.0	-1.0	7.6	-7.5	-2.5	1.0	4.0	-0.3	4.0
L629	-35.3	27.3	-3.3	17.7	-15.7	-5.9	0.5	6.9	-1.9	6.9
L630	-35.3	26.0	-3.1	16.9	-15.0	-5.6	0.4	6.5	-1.9	6.5
Sum			64,5	42,3	112,9	47,4	-198.2	-178.7	-208.0	-178.8

[0105] In addition to the aperture angles  $\theta$  and the path lengths  $RL_L$  for the outermost aperture ray, Table 2 also lists the optical path differences between two mutually orthogonal

states of linear polarization for different lens orientations. The optical path differences are shown for (111)-lenses as well as for (100)-lenses and (110)-lenses, where the azimuth angle  $\alpha_L$  of the outermost aperture ray inside the lenses are  $0^\circ$  and  $60^\circ$  for a (111)-lens,  $0^\circ$  and  $45^\circ$  for a (100)-lens, and  $0^\circ$ ,  $45^\circ$ ,  $90^\circ$ ,  $135^\circ$  for a (110)-lens.

[0106] As can be seen in Table 2, the aperture angles  $\theta$  for the lenses L608, L617, L618, L619, L627, L628, L629 and L630 are larger than  $25^\circ$ , and for the lenses L618, L627, L628, L629 and L630 even larger than  $30^\circ$ . Particularly affected by the large aperture angles are the lenses L627 to L630, which are closest to the image plane.

[0107] The projection objective was designed so that the maximum aperture angle of all light rays is smaller than  $45^\circ$ . The maximum aperture angle for the outermost aperture ray is  $39.4^\circ$  for the lens L628. Helpful was the use of two thick planar lenses L629 and L630 immediately ahead of the image plane.

[0108] The diameter of the aperture stop located between the lenses L621 and L622 is 270 mm. The diameter of the lens L618 is 207 mm and the diameters of the lenses L627 to L630 are all smaller than 190 mm. Thus, the diameters of these lenses, which are associated with large aperture angles, are smaller than 80% of the aperture stop diameter.

[0109] As can be concluded from Table 2, it is advantageous to orient individual lenses with large aperture angles in the (100)-direction, as the birefringence values will overall be lower. The reason for this lies in the fact that in (100)-lenses the influence of the crystallographic <110>-direction begins to manifest itself at larger angles than it does in

(111)-lenses. As an example the optical path differences for the lenses L608, L609 and L617 are more than 30% smaller.

[0110] The example of the two planar-parallel lenses L629 and L630 provides a good way of demonstrating how the birefringence can be noticeably reduced by rotating the lenses in relation to each other. Both lenses have equal aperture angles of 35.3° for the outermost aperture ray and similar ray paths of 27.3 mm and 26.0 mm, respectively. If the two lenses were installed as (100)-lenses with equal orientation, there would be a resultant optical path difference of 30.7 nm. However, if the two (100)-lenses are rotated relative to each other by 45°, the optical path difference is reduced to 20.9 nm, i.e., by 32%. If the two lenses were installed as (111)-lenses with equal orientation, there would be a resultant optical path difference of 34.6 nm; but if the two (111)-lenses are rotated relative to each other by 60°, the optical path difference is reduced to 13.6 nm, i.e., by 61%.

[0111] A near-perfect compensation of the optical path differences for two mutually orthogonal states of linear polarization caused intrinsic birefringence in the lenses L629 and L630 can be achieved if the lens L629 is split up into the lenses L6291 and L6292, and the lens L630 is split up into the lenses L6301 and L6302, wherein the lens L6291 is a (100)-lens with a thickness of 9.15 mm, the lens L6292 is a (111)-lens with a thickness of 13.11 mm, the lens L6301 is a (100)-lens with a thickness of 8.33 mm and the lens L6302 is a (111)-lens with a thickness of 12.9 mm. The lenses L6291 and L6301 are rotated against each other by 45°, and the lenses L6292 and L6302 are rotated against each other by 60°. The resultant maximum for the optical path difference in this case amounts to 0.2 nm. The lenses L6291 and L6292, as well as the lenses L6301 and L6302 can be joined together with an optically

seamless connection, e.g., by wringing. This concept is also applicable if the projection objective has only one crystal lens. In this case, the crystal lens is split into at least two lenses that are arranged with a rotation relative to each other. The joining can be accomplished by wringing. As another possibility, individual plates of the desired crystallographic orientation are joined through an optically seamless connection in a first step, and the lens is fabricated from the combined plates in a further process step.

[0112] As a further possibility to reduce the undesirable influence of the intrinsic birefringence caused by the lenses L629 and L630, the lens L629 is split up into the lenses L6293 and L6294, and the lens L630 is split up into the lenses L6303 and L6304, wherein the lens L6293 is a (110)-lens with a thickness of 11.13 mm, the lens L6294 is a (110)-lens with a thickness of 11.13 mm, the lens L6303 is a (110)-lens with a thickness of 10.62 mm and the lens L6304 is a (110)-lens with a thickness of 10.62 mm. The lenses L6293 and L6294 are rotated against each other by 90°, as are the lenses L6303 and L6304, wherein the angle of rotation between the lens L6293 and the lens L6303 amounts to 45°. The resultant maximum for the optical path difference in this case amounts to 4.2 nm. The lenses L6293 and L6294, as well as the lenses L6303 and L6304 can be joined together as lens parts with an optically seamless connection, e.g., by wringing.

[0113] A compensation of the optical path differences for two mutually orthogonal states of linear polarization that is caused by the strongly affected lenses L629 and L630 is accomplished with near-total success, if each lens is split up into three lens parts, i.e., L6295, L6296, L6297, and L6305, L6306, L6307, wherein the lens L6295 is a (100)-lens with a thickness of 4.45 mm, the lenses L6296 and L6297 are (110)-

lenses with a thickness of 8.90 mm, the lens L6305 is a (100)-lens with a thickness of 4.25 mm and the lenses L6306 and L6307 are (110)-lenses with a thickness of 8.49 mm. The lenses L6294 and 6304 are rotated relative to each other by 45°, and each two of the lenses L6295, L6297, L6306 and L6307 are rotated by 45°. With this combination, the resultant maximum optical path difference is reduced to less than 0.1 nm. The lenses L6295 to L6297 as well as the lenses L6305 to L6307 can be joined together as lens parts with an optically seamless connection, e.g., by wringing.

[0114] As a further possibility to reduce the undesirable influence of the intrinsic birefringence that is caused by the lenses L629 and L630, two (110)-lenses can be combined with a (100)-lens. In this arrangement, the two (110)-lenses need to be installed with a rotation of 90° relative to each other, while the angle of rotation between the (100)-lens and the (110)-lenses is  $45^\circ + m \cdot 90^\circ$ , wherein m represents an integer number. In this case, the lens L629 is split up into the lenses L6298 and L6299, and the lens L630 is split up into the lenses L6308 and L6309, wherein the lens L6298 is a (110)-lens with a thickness of 17.4 mm, the lens L6299 is a (110)-lens with a thickness of 4.87 mm, the lens L6308 is a (110)-lens with a thickness of 12.53 mm, and the lens L6309 is a (100)-lens with a thickness of 8.7 mm. The resultant maximum optical path difference is around 3.1 nm. The lenses L6298 and 6299 as well as the lenses L6308 and L6309 can be joined together as lens parts with an optically seamless connection, e.g., by wringing.

[0115] Figure 8 represents the lens section of a catadioptric projection objective 711 for the wavelength of 157 nm. The optical data for this objective are listed in Table 3. This embodiment is taken from the applicant's patent application

PCT/EP00/13184 where it corresponds to Figure 9 and Table 8. For a detailed description of the function of the objective, see PCT/EP00/13184. All lenses of this objective consist of calcium fluoride crystal. The image-side numerical aperture of the objective is 0.8.

[0116] For the embodiment of Figure 8, a calculation was made of the aperture angles  $\theta$  and the ray paths  $RL_L$  of the upper outermost aperture ray 713 and the lower outermost aperture ray 715 for the individual lenses L801 to L817. The outermost aperture rays 713 and 715 originate here from the object point with the coordinates  $x = 0$  mm and  $y = -82.15$  mm, and in the image plane have angles relative to the optical axis that correspond to the image-side numerical aperture. The calculation was made for the upper and lower outermost aperture rays because this embodiment has an off-axis object field, so that the aperture rays are not symmetric in relation to the optical axis as was the case for the outermost aperture ray of the embodiment of Figure 7.

[0117] The data for the upper outermost aperture ray are listed in Table 4 and for the lower outermost aperture ray in Table 5. In addition to the aperture angles  $\theta$  and the path lengths  $RL_L$  for the outermost aperture ray, Tables 4 and 5 also list the optical path differences for two mutually orthogonal states of linear polarization for different lens orientations, specifically for (111)-lenses, (100)-lenses and (110)-lenses, wherein the azimuth angles  $\alpha_L$  of the outermost marginal ray inside the lenses are  $0^\circ$  and  $60^\circ$  for a (111)-lens,  $0^\circ$  and  $45^\circ$  for a (100)-lens, and  $0^\circ$ ,  $45^\circ$ ,  $90^\circ$ ,  $135^\circ$  for a (110)-lens.

Table 4

Lens	Aperture angle $\theta$ [°]	Ray path RL [mm]	Optical path difference [nm] (111)-Lens $\alpha_L = 0^\circ$	Optical path difference [nm] (111)-Lens $\alpha_L = 60^\circ$	Optical path difference [nm] (100)-Lens $\alpha_L = 0^\circ$	Optical path difference [nm] (100)-Lens $\alpha_L = 45^\circ$	Optical path difference [nm] (110)-Lens $\alpha_L = 0^\circ$	Optical path difference [nm] (110)-Lens $\alpha_L = 45^\circ$	Optical path difference [nm] (110)-Lens $\alpha_L = 90^\circ$	Optical path difference [nm] (110)-Lens $\alpha_L = 135^\circ$
801	1.4	28.1	0.8	-0.8	0.0	0.0	-18.2	-18.2	-18.2	-18.2
802	-10.8	30.7	-5.3	8.0	-2.7	-1.3	-17.2	-17.2	-17.3	-17.2
803	-15.6	32.4	-6.8	12.4	-5.7	-2.7	-15.3	-15.3	-15.4	-15.3
803	-24.4	31.8	-6.5	17.8	-11.7	-5.2	-8.4	-8.8	-9.0	-8.8
802	-19.5	26.6	-5.8	12.4	-6.8	-3.2	-10.2	-10.3	-10.4	-10.3
804	6.4	20.1	3.0	-2.4	-0.6	-0.3	-12.4	-12.4	-12.4	-12.4
805	10.8	34.4	9.0	-6.0	-3.0	-1.5	-19.3	-19.3	-19.3	-19.3
806	0.2	10.0	0.1	-0.1	0.0	0.0	-6.5	-6.5	-6.5	-6.5
807	-11.1	22.0	-3.9	5.9	-2.1	-1.0	-12.2	-12.2	-12.3	-12.2
808	0.1	18.5	0.0	0.0	0.0	0.0	-12.0	-12.0	-12.0	-12.0
809	-0.8	9.0	-0.1	0.2	0.0	0.0	-5.8	-5.8	-5.8	-5.8
810	1.1	12.4	0.3	-0.3	0.0	0.0	-8.0	-8.0	-8.0	-8.0
811	-16.8	9.4	-2.0	3.8	-1.9	-0.9	-4.2	-4.2	-4.2	-4.2
812	-10.4	29.8	-5.0	7.5	-2.4	-1.2	-16.9	-16.9	-16.9	-16.9
813	-8.8	34.7	-5.2	7.3	-2.1	-1.0	-20.5	-20.5	-20.5	-20.5
814	-9.4	17.5	-2.8	4.0	-1.2	-0.6	-10.2	-10.2	-10.2	-10.2
815	-27.4	28.1	-5.3	16.9	-12.2	-5.3	-5.2	-6.4	-6.1	-6.4
816	-28.7	40.2	-7.1	24.8	-18.6	-7.9	-6.2	-8.5	-7.6	-8.5
817	-30.8	39.0	-6.3	24.7	-19.6	-8.1	-3.9	-8.0	-5.7	-8.0
Sum			-48.9	136.1	-90.9	-40.3	-212.9	-220.9	-218.0	-220.9

Table 5

Lens	Aperture angle $\theta$ [°]	Ray path RL <sub>L</sub> [nm]	Optical path difference [nm] (111)-Lens $\alpha_L = 0^\circ$	Optical path difference [nm] (111)-Lens $\alpha_L = 60^\circ$	Optical path difference [nm] (100)-Lens $\alpha_L = 0^\circ$	Optical path difference [nm] (100)-Lens $\alpha_L = 45^\circ$	Optical path difference [nm] (110)-Lens $\alpha_L = 0^\circ$	Optical path difference [nm] (110)-Lens $\alpha_L = 45^\circ$	Optical path difference [nm] (110)-Lens $\alpha_L = 90^\circ$	Optical path difference [nm] (110)-Lens $\alpha_L = 135^\circ$
801	-11.6	32.1	-5.8	9.0	-3.2	-1.6	-17.6	-17.6	-17.6	-17.6
802	19.5	28.3	13.3	-6.1	-7.3	-3.4	-10.9	-10.9	-11.1	-10.9
803	24.7	33.8	19.1	-6.9	-12.7	-5.7	-8.6	-9.2	-9.3	-9.2
803	17.7	34.3	14.7	-7.4	-7.5	-3.6	-14.6	-14.6	-14.8	-14.6
802	12.7	31.6	9.7	-6.0	-3.8	-1.8	-16.7	-16.7	-16.8	-16.7
804	-5.2	27.7	-2.7	3.3	-0.6	-0.3	-17.4	-17.4	-17.4	-17.4
805	-4.5	34.6	-3.0	3.5	-0.5	-0.3	-21.9	-21.9	-21.9	-21.9
806	-8.6	19.5	-2.9	4.0	-1.1	-0.6	-11.6	-11.6	-11.6	-11.6
807	-0.5	16.5	-0.2	0.2	0.0	0.0	-10.7	-10.7	-10.7	-10.7
808	-8.2	25.6	-3.7	5.0	-1.3	-0.7	-15.3	-15.3	-15.3	-15.3
809	-7.5	10.1	-1.3	1.8	-0.4	-0.2	-6.1	-6.1	-6.1	-6.1
810	-9.1	13.1	-2.0	2.9	-0.8	-0.4	-7.7	-7.7	-7.7	-7.7
811	9.0	9.9	2.1	-1.5	-0.6	-0.3	-5.8	-5.8	-5.8	-5.8
812	2.6	30.7	1.8	-1.6	-0.2	-0.1	-19.8	-19.8	-19.8	-19.8
813	0.9	34.0	0.6	-0.6	0.0	0.0	-22.1	-22.1	-22.1	-22.1
814	1.3	10.4	0.3	-0.3	0.0	0.0	-6.7	-6.7	-6.7	-6.7
815	23.5	16.3	8.9	-3.4	-5.7	-2.6	-4.7	-4.8	-4.9	-4.8
816	24.6	37.2	21.0	-7.6	-13.9	-6.2	-9.6	-10.2	-10.3	-10.2
817	29.4	29.6	18.5	-5.1	-14.1	-5.9	-4.0	-6.2	-5.2	-6.2
Sum			88.3	-16.8	-73.7	-33.5	-231.9	-235.4	-235.2	-235.4

[0118] As can be seen in Tables 4 and 5, the aperture angles  $\theta$  for the lenses L815 to L817 are larger than  $25^\circ$ . In this embodiment, too, the lenses L815 to L817 which are closest to the image plane have large aperture angles. The lenses L815 to L817 were designed so that the maximum aperture angle of all light rays is smaller than or equal to

$$\arcsin\left(\frac{NA}{n_{FK}}\right) = \arcsin\left(\frac{0.8}{1.5597}\right) = 30.9^\circ. \text{ The maximum aperture}$$

angle for the outermost aperture ray is  $30.8^\circ$  for the lens L817.

[0119] The aperture stop that is located between the lenses L811 and L812 has a diameter of 193 mm. All of the lenses L815 to L817 have diameters of less than 162 mm. Thus, the diameters of these lenses, which are associated with large aperture angles, are smaller than 85% of the aperture stop diameter.

[0120] Tables 4 and 5 lead to the conclusion that it is advantageous if lenses with large aperture angles are oriented in the (100)-direction, as the birefringence values are lower overall. For example in the lenses L815 to L817, the optical path differences are smaller by more than 20%.

[0121] The embodiment of Figure 8 will now be used to demonstrate how the intrinsic birefringence can be compensated to a large extent by using groups of (100)-lenses that are rotated relative to each other in parallel with groups of (111)-lenses that are rotated relative to each other.

[0122] To begin, all calcium fluoride lenses of (111)-orientation are installed without rotating the (111)-lenses. As a result, there will be a maximum optical path difference between two mutually orthogonal states of linear polarization of 136 nm. By rotating the (111)-lenses, the maximum optical path difference can be reduced to about 38 nm. This is achieved by combining the lenses L801 and L804 in a group and the lenses L802 and L803 in a further group, wherein the respective angle of rotation between the lenses is 60°. The lenses L808, L809 and L810 are combined into a group of three, and so are the lenses L815, L816 and L817, wherein the angle of rotation between each two of these lenses is 40°. The lenses L811, L812, L813 and L814 are combined into a group of four with an angle of rotation of 30° relative to each other.

[0123] If all calcium fluoride lenses of (100)-orientation are installed without rotating the (100)-lenses relative to each other, the resultant maximum optical path difference between two mutually orthogonal states of linear polarization will be 90.6 nm. By rotating the (100)-lenses, the maximum optical path difference can be reduced to about 40 nm. This is achieved by combining the lenses L801 and L804 in a group and the lenses L802 and L803 in a further group, wherein the angle of rotation between the lenses is 45°. The lenses L808, L809 and L810 are combined into a group of three, and so are the lenses L815, L816 and L817, wherein the angle of rotation between each two of these lenses is 30°. The lenses L811, L812, L813 and L814 are combined into a group of four with an angle of rotation of 22.5° relative to each other.

[0124] A maximum of 7 nm is obtained in the optical path difference for two mutually orthogonal states of linear polarization, if groups of (100)-lenses are combined with groups of (111)-lenses. The lenses L801 and L804 are combined into a group of (111)-lenses in which the angle of rotation between the lenses is 60°. The lenses L802 and L803 are combined into a group of (100)-lenses in which the angle of rotation between the lenses is 45°. A group of three (100)-lenses is formed of the lenses L808, L809 and L810, wherein the angle of rotation between each two of these lenses is 30°. A group of three (111)-lenses is formed of the lenses L815, L816 and L817, wherein the angle of rotation between each two of these lenses is 40°. The lenses L811, L812, L813 and L814 are combined into a group of four (100)-lenses with an angle of rotation of 22.5°. The lens axes of the lenses L805 and L807 which are not combined in a group are oriented in the crystallographic <111>-direction, while the lens axis of the lens L806 is oriented in the crystallographic <100>-direction. The groups can be oriented in relation to each other at

arbitrary angles of rotation about the optical axis. These rotational degrees of freedom can be used for the compensation of aberrations that are not rotationally symmetric and which can be caused, e.g., by the mounting of the lens.

[0125] Using the refractive objective 611 as an example, the following discussion aims to demonstrate how the undesirable influence of birefringence effects can be noticeably reduced by coating an optical element with a compensation coating 613. Only the birefringence contributions of the two lenses L629 and L630 will be considered, which lenses consist of calcium fluoride and thus exhibit intrinsic birefringence. The two lenses in the present embodiment have (111)-orientation and are rotated relative to each other by 60°. This results in a distribution of the optical path differences  $\Delta OPL$  that is close to rotational symmetry. The maximum optical path difference  $\Delta OPL$  for an outermost aperture ray lies between 13.6 nm and 14.6 nm depending on the azimuth angle  $\alpha_R$ . Now, the compensation coating 613 described in Table 6 is applied to the optical surface of the lens L630 that faces towards the image plane O'. The compensation coating 613 consists of 15 individual layers of the materials magnesium fluoride ( $MgF_2$ ) and lanthanum fluoride ( $LaF_3$ ). Under the headings n and k, Table 6 lists, respectively, the real and imaginary components of the refractive index. The layer thicknesses are homogenous and have no taper in their lateral thickness profiles. The vapor-deposition angles during the coating process are perpendicular to the optical surface of the lens L630. With the compensation coating, the resultant optical path difference amounts to 1.1 nm and is thus noticeably reduced in comparison to the same objective without compensation coating.

Table 6

Layer	Thickness [nm]	Material
	Substrate	CaF2
1	103.54	MgF2
2	41.54	LaF3
3	33.35	MgF2
4	30.8	LaF3
5	39.53	MgF2
6	35.34	LaF3
7	32.05	MgF2
8	27.25	LaF3
9	28.57	MgF2
10	26.48	LaF3
11	27.64	MgF2
12	26.17	LaF3
13	27.36	MgF2
14	26.11	LaF3
15	8.66	MgF2

Optical constants	n	k
LaF3	1.760026	0.00118471
MgF2	1.506675	0.00305275

[0126] An analogous procedure is also possible, if the entire objective is considered instead of the two last lenses.

Instead of compensating the birefringence with only one optical element with a compensation coating, one could also apply a compensation coating to several optical elements.

[0127] The process can also be used to compensate the birefringence in an overall system, wherein the sources for the birefringence can include stress-induced birefringence, intrinsic birefringence, and birefringence caused by the other coatings.

[0128] After the final adjustment of a system, the distribution of the optical path differences  $\Delta OPL$  is determined for one or more ray bundles in the image plane. By means of a program for the optimization of layers, the

required compensation coating is calculated and applied, e.g., to the system surface nearest to the image plane. It is advantageous if the optical element that is nearest to the image plane is interchangeable. This provides the possibility to correct birefringence effects that do not occur until the objective is in operation.

[0129] As described above, birefringence in crystals for light in the UV range can be compensated by arranging crystal elements with different orientations of the crystallographic axes following each other. If one arranges lenses with different crystallographic directions following each other in an optical system, one encounters the problem that lenses are in many cases traversed by a light ray at different angles, in which case a compensation may be possible only to a limited extent. In optical systems that contain only one crystal lens, this kind of compensation is not possible at all.

[0130] As a possible solution, a lens can in the design be split into two lenses that are wrung together with a rotation relative to each other. In practice, this procedure suffers from the drawback that stresses deform the joint surface and also that the two halves have to be positioned with an accuracy of micrometers in the lateral direction.

[0131] It is proposed to make blanks from individual plates that are wrung together and are rotated relative to each other with respect to the orientation of their crystallographic axes and which are then made into a lens by milling and polishing. Everything that was said hereinabove in regard to the orientation is likewise applicable to this concept. In addition to the traditional technique of wringing in the optical manufacturing process, any other joining techniques that produce an intimate contact and minimize the occurrence

of stress represent possible solutions and are encompassed within the scope of the invention. The wringing can be supported in particular by layers consisting, e.g., of quartz glass. It is important that no refraction or reflection occurs at the joining interface, as this would be detrimental.

[0132] The selection of the orientations is made according to the rules described above.

[0133] Embodiments of the foregoing concept include blanks from which, e.g., the lens L816 for the projection objective of Figure 8 can be produced. The lens L816 has a convex aspherical front surface with a crown radius of 342.13 mm and a concave spherical rear surface with a crown radius of 449.26 mm. The axial thickness is 37.3 mm. The lens material is calcium fluoride. The lens diameter is 141 mm. The blank from which the lens is to be formed needs to have a minimum overall thickness of 45 mm and a diameter of 150 mm. The blank can consist of two (100)-plates of 9.0 mm thickness that are rotated relative to each other by 45° and two (111)-plates of 13.5 mm thickness that are rotated relative to each other by 60° which are joined together in an optically seamless manner. In this arrangement, the (100)-plates and the (111)-plates should be arranged respectively adjacent to each other.

[0134] In a further embodiment, six (100)-plates of 3.0 mm thickness that are rotated by 45° relative to each other and six (111)-plates of 4.5 thickness that are rotated by 60° relative to each other are joined in an optically seamless manner, where after each two (100)-plates there are two (111)-plates following in the sequence.

[0135] In a further embodiment, four (110)-plates of 9.0 mm thickness that are rotated by 45° relative to each other and

two (100)-plates of 4.5 thickness that are rotated by 45° relative to each other are joined in an optically seamless manner, where the two (100)-plates are following the four (110)-plates.

[0136] In a further embodiment, eight (110)-plates of 4.5 thickness that are rotated by 45° relative to each other and four (100)-plates of 2.25 mm thickness that are rotated by 45° relative to each other are joined in an optically seamless manner, where after each four (110)-plates there are two (100)-plates following in the sequence.

[0137] The following description of the principal configuration of a microlithography projection exposure apparatus is based on Figure 9. The projection exposure apparatus 81 has an illumination device 83 and a projection objective 85. The projection objective 85 includes a lens arrangement 819 with an aperture stop AP, wherein an optical axis 87 is defined by the lens arrangement 89. Embodiments of the lens arrangement 89 are presented in Figure 6 and Figure 7. Arranged between the illumination device 83 and the projection objective 85 is a mask 89 which is held in the ray path by means of a mask holder 811. Masks 89 of this type, which are used in microlithography, have a micrometer-nanometer structure, which is projected into the image plane 813 by means of the projection objective 85, reduced for example by a factor of 4 or 5. In the image plane 813, a light-sensitive substrate 815, more specifically a wafer positioned by a substrate holder 817, is held in place.

[0138] The smallest structure that can still be resolved depend on the wavelength  $\lambda$  of the light that is used for the illumination and they also depend on the image-side numerical aperture of the projection objective 85, i.e., the maximally

---

achievable resolution of the projection exposure apparatus 81 increases with decreasing wavelength  $\lambda$  of the illumination device 83 and with increasing numerical aperture on the image side of the projection objective 85. With the embodiments shown in Figures 6 and 7, it is possible to realize resolutions smaller than 150 nm. This is also the reason why effects such as the intrinsic birefringence need to be minimized. The invention has been successful in strongly reducing the undesirable influence of the intrinsic birefringence in particular in projection objectives with large image-side numerical aperture values.

M1587a

TABLE 1

LENSES	RADI	THICKNESS VALUES	GLASSES	REFR. INDEX AT 157.629nm	1/2 FREE DIAMETER
0	0.000000000	27.171475840	N2	1.00031429	46.200
	0.000000000	0.602670797	N2	1.00031429	52.673
L601	900.198243311AS	15.151284556	CaF2	1.55929035	53.454
	-235.121108435	9.531971079	N2	1.00031429	54.049
L602	-167.185917779	8.294716452	CaF2	1.55929035	54.178
	-132.673519510	14.020355779	N2	1.00031429	54.901
L603	-333.194588652	9.893809820	CaF2	1.55929035	53.988
	-155.450516203	15.930502944	N2	1.00031429	54.132
L604	-73.572316296	7.641977580	CaF2	1.55929035	53.748
	-68.248613899AS	2.881720302	N2	1.00031429	55.167
L605	-86.993585564AS	5.094651720	CaF2	1.55929035	52.580
	-238.150965327	5.379130780	N2	1.00031429	53.729
L606	-165.613920870	5.094651720	CaF2	1.55929035	53.730
	153.417884485	34.150169591	N2	1.00031429	56.762
L607	-92.061009990	5.094651720	CaF2	1.55929035	58.081
	8491.086261873AS	19.673523795	N2	1.00031429	74.689
L608	-407.131300451	30.380807138	CaF2	1.55929035	87.291
	-140.620317156	0.761662684	N2	1.00031429	91.858
L609	-4831.804853654AS	50.269660218	CaF2	1.55929035	117.436
	-192.197373609	1.688916911	N2	1.00031429	121.408
L610	-367.718684892	21.227715500	CaF2	1.55929035	127.704
	-233.628547894	2.224071019	N2	1.00031429	129.305
L611	709.585855080	28.736922725	CaF2	1.55929035	137.016
	1238.859445357	9.120684720	N2	1.00031429	137.428
L612	1205.457051945	49.281218258	CaF2	1.55929035	138.288
	-285.321880705	1.625271224	N2	1.00031429	138.379
L613	137.549591710	56.718543740	CaF2	1.55929035	108.652
	-4380.301012978AS	0.623523902	N2	1.00031429	106.138
L614	2663.880214408	6.792868960	CaF2	1.55929035	103.602
	149.184979730	15.779049257	N2	1.00031429	84.589
L615	281.093108064	6.792868960	CaF2	1.55929035	83.373
	184.030288413	32.341552355	N2	1.00031429	77.968
L616	-222.157416308	5.094651720	CaF2	1.55929035	77.463
	101.254238115AS	56.792834221	N2	1.00031429	71.826
L617	-106.980638018	5.094651720	CaF2	1.55929035	72.237
	1612.305471130	20.581065398	N2	1.00031429	89.760
L618	-415.596135628	26.398111993	CaF2	1.55929035	96.803
	-204.680044631	0.713343960	N2	1.00031429	103.409
L619	-646.696622394	25.867340760	CaF2	1.55929035	116.636
	-231.917626896	0.766268682	N2	1.00031429	118.569
L620	-790.657607677	23.400482872	CaF2	1.55929035	128.806
	-294.872053725	0.721402031	N2	1.00031429	130.074
L621	786.625567756	40.932308205	CaF2	1.55929035	141.705
	-431.247283013	12.736629300	N2	1.00031429	142.089
	0.000000000	-8.491086200	N2	1.00031429	134.586
L622	295.022653593AS	20.185109438	CaF2	1.55929035	139.341
	449.912291916	0.619840486	N2	1.00031429	137.916
L623	358.934076212	48.662890509	CaF2	1.55929035	136.936
	-622.662988878	30.955714157	N2	1.00031429	135.288
L624	-224.404889753	12.736629300	CaF2	1.55929035	134.760
	-251.154571510AS	16.079850229	N2	1.00031429	134.853
L625	-193.582989843AS	16.510083506	CaF2	1.55929035	134.101
	-198.077570749	0.880353872	N2	1.00031429	136.109
L626	206.241795157	19.927993542	CaF2	1.55929035	101.240
	338.140581666	0.925956949	N2	1.00031429	97.594
L627	111.017549581	24.580089962	CaF2	1.55929035	85.023
	169.576109839	0.777849447	N2	1.00031429	81.164
L628	117.982165264	31.161065630	CaF2	1.55929035	75.464
	921.219058213AS	6.934980174	N2	1.00031429	69.501
L629	0.000000000	22.260797322	CaF2	1.55929035	63.637
	0.000000000	4.245543100	N2	1.00031429	48.606
L630	0.000000000	21.227715500	CaF2	1.55929035	41.032
	0.000000000	8.491086200	N2	1.00031429	26.698
	0.000000000	0.000000000		1.000000000	11.550

Wavelength and refractive index are stated relative to vacuum.

#### ASPHERIC CONSTANTS

##### Asphere of lens L601

K	0.0000
C1	1.28594437e-007
C2	8.50731836e-013
C3	1.16375620e-016
C4	2.28674275e-019
C5	-1.23202729e-022
C6	3.32056239e-026
C7	-4.28323389e-030
C8	0.00000000e+000
C9	0.00000000e+000

##### Asphere of lens L604

K	-1.3312
C1	-4.03355456e-007
C2	2.25776586e-011
C3	-2.19259878e-014
C4	4.32573397e-018
C5	-7.92477159e-022
C6	7.57618874e-026
C7	-7.14962797e-030
C8	0.00000000e+000
C9	0.00000000e+000

##### Asphere of lens L605

K	-1.1417
C1	1.33637337e-007
C2	1.56787758e-011
C3	-1.64362484e-014
C4	3.59793786e-018
C5	-5.11312568e-022
C6	1.70636633e-026
C7	1.82384731e-030
C8	0.00000000e+000
C9	0.00000000e+000

##### Asphere of lens L607

K	0.0000
C1	1.34745120e-007
C2	-2.19807543e-011
C3	1.20275881e-015
C4	4.39597377e-020
C5	-2.37132819e-023
C6	2.87510939e-027
C7	-1.42065162e-031
C8	0.00000000e+000
C9	0.00000000e+000

## Asphere of lens L609

K	0.0000
C1	6.85760526e-009
C2	-4.84524868e-013
C3	-6.28751350e-018
C4	-3.72607209e-022
C5	3.25276841e-026
C6	-4.05509974e-033
C7	-3.98843079e-035
C8	0.00000000e+000
C9	0.00000000e+000

## Asphere of lens L613

K	0.0000
C1	2.24737416e-008
C2	-4.45043770e-013
C3	-4.10272049e-017
C4	4.31632628e-021
C5	-3.27538237e-025
C6	1.44053025e-029
C7	-2.76858490e-034
C8	0.00000000e+000
C9	0.00000000e+000

## Asphere of lens L616

K	0.0000
C1	-2.83553693e-008
C2	-1.12122261e-011
C3	-2.05192812e-016
C4	-1.55525080e-020
C5	-4.77093112e-024
C6	8.39331135e-028
C7	-8.97313681e-032
C8	0.00000000e+000
C9	0.00000000e+000

## Asphere of lens L622

K	0.0421
C1	7.07310826e-010
C2	-2.00157185e-014
C3	-9.33825109e-020
C4	1.27125854e-024
C5	1.94008709e-027
C6	-6.11989858e-032
C7	2.92367322e-036
C8	0.00000000e+000
C9	0.00000000e+000

## Asphere of lens L624

K	0.0000
C1	3.02835805e-010
C2	-2.40484062e-014
C3	-3.22339189e-019
C4	1.64516979e-022
C5	-8.51268614e-027
C6	2.09276792e-031
C7	-4.74605669e-036
C8	0.00000000e+000
C9	0.00000000e+000

## Asphere of lens L625

K	0.0000
C1	-3.99248993e-010
C2	5.79276562e-014
C3	3.53241478e-018
C4	-4.57872308e-023
C5	-6.29695208e-027
C6	1.57844931e-031
C7	-2.19266130e-036
C8	0.00000000e+000
C9	0.00000000e+000

## Asphere of lens L628

K	0.0000
C1	4.40737732e-008
C2	1.52385268e-012
C3	-5.44510329e-016
C4	6.32549789e-020
C5	-4.58358203e-024
C6	1.92230388e-028
C7	-3.11311258e-033
C8	0.00000000e+000
C9	0.00000000e+000

TABLE 3

L61

LENSES	RADI	THICKNESS VALUES	GLASSES	REFR. INDEX AT 157.629nm	1/2 FREE DIAMETER
0	0.000000000	34.000000000		1.00000000	82.150
	0.000000000	0.100000000		1.00000000	87.654
L801	276.724757380	40.000000000	CaF2	1.55970990	90.112
	1413.944109416AS	95.000000000		1.00000000	89.442
SP1	0.000000000	11.000000000		1.00000000	90.034
	0.000000000	433.237005445		1.00000000	90.104
L802	-195.924336384	17.295305525	CaF2	1.55970990	92.746
	-467.658808527	40.841112468		1.00000000	98.732
L803	-241.385736441	15.977235467	CaF2	1.55970990	105.512
	-857.211727400AS	21.649331094		1.00000000	118.786
SP2	0.000000000	0.000010000		1.00000000	139.325
	253.074839896	21.649331094		1.00000000	119.350
L803'	857.211727400AS	15.977235467	CaF2	1.55970990	118.986
	241.385736441	40.841112468		1.00000000	108.546
L802'	467.658808527	17.295305525	CaF2	1.55970990	102.615
	195.924336384	419.981357165		1.00000000	95.689
SP3	0.000000000	6.255658280		1.00000000	76.370
	0.000000000	42.609155219		1.00000000	76.064
Z1	0.000000000	67.449547115		1.00000000	73.981
L804	432.544479547	37.784311058	CaF2	1.55970990	90.274
	-522.188532471	113.756133662		1.00000000	92.507
L805	-263.167605725	33.768525968	CaF2	1.55970990	100.053
	-291.940616829AS	14.536591424		1.00000000	106.516
L806	589.642961222AS	20.449887046	CaF2	1.55970990	110.482
	-5539.698828792	443.944079795		1.00000000	110.523
L807	221.780582003	9.000000000	CaF2	1.55970990	108.311
	153.071443064	22.790060084		1.00000000	104.062
L808	309.446967518	38.542735318	CaF2	1.55970990	104.062
	-2660.227900099	0.100022286		1.00000000	104.098
L809	23655.354584194	12.899131182	CaF2	1.55970990	104.054
	-1473.189213176	9.318886362		1.00000000	103.931
L810	-652.136459374	16.359499814	CaF2	1.55970990	103.644
	-446.489459129	0.100000000		1.00000000	103.877
L811	174.593507050	25.900313780	CaF2	1.55970990	99.267
	392.239615259AS	14.064505431		1.00000000	96.610
	0.000000000	2.045119392		1.00000000	96.552
L812	7497.306838492	16.759051656	CaF2	1.55970990	96.383
	318.210831711	8.891640764		1.00000000	94.998
L813	428.724465129	41.295806263	CaF2	1.55970990	95.548
	3290.097860119AS	7.377912006		1.00000000	95.040
L814	721.012739719	33.927118706	CaF2	1.55970990	95.443
	-272.650872353	6.871397517		1.00000000	95.207
L815	131.257556743	38.826450065	CaF2	1.55970990	81.345
	632.112566477AS	4.409527396		1.00000000	74.847
L816	342.127616157AS	37.346293509	CaF2	1.55970990	70.394
	449.261078744	4.859754445		1.00000000	54.895
L817	144.034814702	34.792179308	CaF2	1.55970990	48.040
	-751.263321098AS	11.999872684		1.00000000	33.475
0'	0.000000000	0.000127776		1.00000000	16.430

## ASPHERIC CONSTANTS

## Asphere of lens L801

K	0.0000
C1	4.90231706e-009
C2	3.08634889e-014
C3	-9.53005325e-019
C4	-6.06316417e-024
C5	6.11462814e-028
C6	-8.64346302e-032
C7	0.00000000e+000
C8	0.00000000e+000
C9	0.00000000e+000

## Asphere of lens L803

K	0.0000
C1	-5.33460884e-009
C2	9.73867225e-014
C3	-3.28422058e-018
C4	1.50550421e-022
C5	0.00000000e+000
C6	0.00000000e+000
C7	0.00000000e+000
C8	0.00000000e+000
C9	0.00000000e+000

## Asphere of lens L803'

K	0.0000
C1	5.33460884e-009
C2	-9.73867225e-014
C3	3.28422058e-018
C4	-1.50550421e-022
C5	0.00000000e+000
C6	0.00000000e+000
C7	0.00000000e+000
C8	0.00000000e+000
C9	0.00000000e+000

## Asphere of lens L805

K	0.0000
C1	2.42569449e-009
C2	3.96137865e-014
C3	-2.47855149e-018
C4	7.95092779e-023
C5	0.00000000e+000
C6	0.00000000e+000
C7	0.00000000e+000
C8	0.00000000e+000
C9	0.00000000e+000

## Asphere of lens L806

K	0.0000
C1	-6.74111232e-009
C2	-2.57289693e-014
C3	-2.81309020e-018
C4	6.70057831e-023
C5	5.06272344e-028
C6	-4.81282974e-032
C7	0.00000000e+000
C8	0.00000000e+000
C9	0.00000000e+000

## Asphere of lens L811

K	0.0000
C1	2.28889624e-008
C2	-1.88390559e-014
C3	2.86010656e-017
C4	-3.18575336e-021
C5	1.45886017e-025
C6	-1.08492931e-029
C7	0.00000000e+000
C8	0.00000000e+000
C9	0.00000000e+000

## Asphere of lens L813

K	0.0000
C1	3.40212872e-008
C2	-1.08008877e-012
C3	4.33814531e-017
C4	-7.40125614e-021
C5	5.66856812e-025
C6	0.00000000e+000
C7	0.00000000e+000
C8	0.00000000e+000
C9	0.00000000e+000

## Asphere of lens L815

K	0.0000
C1	-3.15395039e-008
C2	4.30010133e-012
C3	3.11663337e-016
C4	-3.64089769e-020
C5	1.06073268e-024
C6	0.00000000e+000
C7	0.00000000e+000
C8	0.00000000e+000
C9	0.00000000e+000

## Asphere of lens L816

K	0.0000
C1	-2.16574623e-008
C2	-6.67182801e-013
C3	4.46519932e-016
C4	-3.71571535e-020
C5	0.00000000e+000
C6	0.00000000e+000
C7	0.00000000e+000
C8	0.00000000e+000
C9	0.00000000e+000

## Asphere of lens L817

K	0.0000
C1	2.15121397e-008
C2	-1.65301726e-011
C3	-5.03883747e-015
C4	1.03441815e-017
C5	-6.29122773e-021
C6	1.44097714e-024
C7	0.00000000e+000
C8	0.00000000e+000
C9	0.00000000e+000

## Patent Claims:

1. Objective (611, 711), in particular a projection objective for a microlithography projection exposure apparatus (81) with a plurality of lenses (L601-L630, L801-L817), with at least one fluoride crystal lens (1), characterized in that the at least one lens (1) is a (100)-lens with a lens axis (EA) that is oriented approximately perpendicular to the crystallographic {100}-planes or equivalent crystallographic planes of the fluoride crystal.
2. Objective according to claim 1, wherein the (100)-lens is a rotationally symmetric lens with a symmetry axis and wherein the symmetry axis coincides with the lens axis of the (100)-lens.
3. Objective according to one of the claims 1 to 2, with an optical axis (OA), wherein the lens axis of the (100)-lens coincides with the optical axis of the objective.
4. Objective according to one of the claims 1 to 3, wherein light rays run inside the objective from an object plane (O) to an image plane (O') and at least one light ray (609, 713, 715) inside the (100)-lens has a ray angle larger than 25°, in particular larger than 30°, relative to the lens axis.
5. Objective according to one of the claims 1 to 4, wherein light rays run inside the objective from an object plane to an image plane and all light rays inside the (100)-lens have ray angles of maximally 45°, in particular maximally  $\arcsin\left(\frac{NA}{n_{FK}}\right)$  in relation to the lens axis, wherein NA stands

for the image-side numerical aperture and  $n_{FK}$  stands for the refractive index of the fluoride crystal.

6. Objective according to one of the claims 1 to 5, with an aperture stop plane, wherein the aperture stop plane has an aperture stop diameter, wherein the (100)-lens has a lens diameter, and wherein the lens diameter is smaller than 85%, in particular smaller than 80%, of the aperture stop diameter.
7. Objective according to one of the claims 1 to 6 with an image plane, wherein the (100)-lens (L630, L817) is the lens nearest to the image plane.
8. Objective (611, 711), in particular a projection objective for a microlithography projection exposure apparatus, with at least two lenses or lens parts consisting of fluoride crystal,  
wherein the lenses or the lens parts have lens axes that point approximately in a principal crystallographic direction,  
wherein a bundle of light rays falls on an image point in an image plane, each of said rays having an azimuth angle  $\alpha_R$ , an aperture angle  $\theta_R$ , and an optical path difference  $\Delta OPL$  for two mutually orthogonal states of linear polarization,  
characterized in that  
the lenses or the lens parts are rotated relative to each other about the lens axes in such a manner that the distribution of the optical path differences  $\Delta OPL(\alpha_R, \theta_R)$  of the ray bundle as a function of the azimuth angle  $\alpha_R$  and the aperture angle  $\theta_R$  has significantly reduced values in comparison to lenses or lens parts in which the lens axes are oriented in the same principal crystallographic

direction and which are not rotated relative to each other about the lens axes.

9. Objective according to claim 8, wherein the optical path differences  $\Delta OPL$  as a function of the azimuth angle  $\alpha_R$  for a given aperture angle  $\theta_0$  vary by less than 30%, in particular by less than 20%.
10. Objective according to one of the claims 8 or 9, wherein each of the lenses or lens parts has a birefringence distribution  $\Delta n(\alpha_L, \theta_L)$  whose birefringence values  $\Delta n$  depend on azimuth angles  $\alpha_L$  relative to a reference direction that is perpendicular to the lens axis and on aperture angles  $\theta_R$  relative to the lens axis,  
wherein the birefringence distribution  $\Delta n(\alpha_L, \theta_L)$  has a k-fold azimuthal symmetry,  
wherein respective rotation angles  $\gamma$  are defined between the reference directions of the individual lenses or lens parts,  
wherein a number of n lenses or n lens parts form a group within which the lens axes point in one and the same or in an equivalent principal crystallographic direction and within which group the birefringence distributions  $\Delta n(\alpha_L, \theta_L)$  have the same azimuthal profile relative to the reference directions,  
wherein the rotation angle  $\gamma$  between each two lenses or lens parts of a group conforms to the equation:  
$$\gamma = \frac{360^\circ}{k \cdot n} + m \cdot \frac{360^\circ}{k} \pm 10^\circ,$$
wherein m represents an integer number.
11. Objective according to claim 10, wherein an outermost aperture ray (609, 713, 715) of the bundle of rays has

inside each of the lenses or lens parts a respective aperture angle  $\theta_L$  and wherein the aperture angles  $\theta_L$  within the lenses or lens parts of the group vary by no more than 30%, in particular no more than 20%.

12. Objective according to one of the claims 10 or 11, wherein an outermost aperture ray (609, 713, 715) of the bundle of rays covers inside each of the lenses or lens parts a respective ray path  $RP_L$  and wherein the ray paths  $RP_L$  within the lenses or lens parts of the group vary by no more than 30%, in particular no more than 20%.
13. Objective according to one of the claims 10 to 12, wherein the respective optical path differences  $\Delta OPL$  for an outermost aperture ray (609, 713, 715) of the bundle of rays determined at a rotation angle  $\gamma=0^\circ$  for the lenses or lens parts of a group vary by no more than 30%, in particular no more than 20%.
14. Objective according to one of the claims 10 to 13, wherein the group comprises two to four lenses or lens parts.
15. Objective according to claim 14, wherein the lenses (L629, L630) or lens parts are arranged adjacent to each other and are in particular joined to each other by wringing.
16. Objective according to one of the claims 10 to 15, wherein the objective has at least two groups of lenses or lens parts which are rotated relative to each other.
17. Objective according to one of the claims 8 to 16, wherein the lens axes point in the crystallographic <111>-direction or in equivalent principal crystallographic directions and the birefringence distribution  $\Delta n(\alpha_L, \theta_L)$  of

the lenses or lens parts has a threefold azimuthal symmetry.

18. Objective according to one of the claims 8 to 16, wherein the lens axes point in the crystallographic <100>-direction or in equivalent principal crystallographic directions and the birefringence distribution  $\Delta n(\alpha_L, \theta_L)$  of the lenses or lens parts has a fourfold azimuthal symmetry.
19. Objective according to one of the claims 8 to 16, wherein the lens axes point in the crystallographic <110>-direction or in equivalent principal crystallographic directions and the birefringence distribution  $\Delta n(\alpha_L, \theta_L)$  of the lenses or lens parts has a twofold azimuthal symmetry.
20. Objective according to one of the claims 8 to 19, wherein the lens axes of the lenses or lens parts of a first group point in the crystallographic <100>-direction or an equivalent principal crystallographic direction and the lens axes of the lenses or lens parts of a second group point in the crystallographic <111>-direction or an equivalent principal crystallographic direction.
21. Objective according to one of the claims 8 to 19, wherein the lens axes of the lenses or lens parts of a first group point in the crystallographic <100>-direction or an equivalent principal crystallographic direction and the lens axes of the lenses or lens parts of a second group point in the crystallographic <110>-direction or an equivalent principal crystallographic direction.
22. Objective according to claim 20 or 21, wherein the distribution  $\Delta OPL(\alpha_R, \theta_R)$  of the optical path differences is

composed of a first distribution  $\Delta OPL_1(\alpha_R, \theta_R)$  of the optical path differences that are due to the lenses or lens parts of all first groups and of a second distribution  $\Delta OPL_2(\alpha_R, \theta_R)$  of the optical path differences that are due to the lenses or lens parts of all second groups, and wherein the amount of the maximum value of the first distribution  $\Delta OPL_1(\alpha_R, \theta_R)$  of the optical path differences differs by no more than 30%, in particular no more than 20%, from the amount of the maximum value of the second distribution  $\Delta OPL_2(\alpha_R, \theta_R)$  of the optical path differences.

23. Objective (611) according to one of the claims 8 to 22, wherein the lenses or lens parts belong to a multitude of optical elements with optical surfaces, and wherein at least one optical surface carries a compensation coating (613), wherein the compensation coating is designed so that the distribution of the optical path differences  $\Delta OPL(\alpha_R, \theta_R)$  of the ray bundle as a function of the azimuth angle  $\alpha_R$  and the aperture angle  $\theta_R$  has significantly reduced values in comparison to an objective without a compensation coating.
24. Objective (611) according to claim 23, wherein the optical element with the compensation coating has an element axis and wherein the compensation coating has an effective birefringence distribution whose effective birefringence values depend on azimuth angles  $\alpha_F$  relative to a reference direction that is perpendicular to the element axis and on aperture angles  $\theta_F$  relative to the element axis.
25. Objective according to claim 24, wherein the effective birefringence distribution of the compensation coating for the aperture angle  $\theta_F=0^\circ$  is approximately zero.

26. Objective according to one of the claims 24 and 25, wherein the effective birefringence distribution depends primarily on the aperture angle  $\theta_F$  alone.
27. Objective according to one of the claims 23 to 26, wherein the optical element with the compensation coating is one of the lenses of fluoride crystal, and wherein the element axis is the lens axis of the fluoride crystal lens.
28. Objective according to one of the claims 23 to 27, wherein a plurality of optical elements carry compensation coatings.
29. Objective according to one of the claims 23 to 28, wherein all of the optical elements carry compensation coatings.
30. Objective according to one of the claims 1 to 29, wherein the fluoride crystal is a calcium fluoride crystal, a strontium fluoride crystal or a barium fluoride crystal.
31. Objective (611), in particular a projection objective for a microlithography projection exposure apparatus, with a plurality of optical elements, in particular lenses of fluoride crystal, with optical surfaces, wherein rays of a ray bundle meet in an image point of an image plane and each of said rays has an optical path difference  $\Delta OPL$  for two mutually orthogonal states of linear polarization, characterized in that at least one optical surface carries a compensation coating (613), wherein the compensation coating is designed so that the optical path differences  $\Delta OPL$  of the ray bundle have significantly reduced values

in comparison to an objective without a compensation coating.

32. Objective according to claim 31, wherein the optical element with the compensation coating has an element axis and wherein the compensation coating has an effective birefringence distribution whose effective birefringence values depend on azimuth angles  $\alpha_F$  relative to a reference direction that is perpendicular to the element axis and on aperture angles  $\theta_F$  relative to the element axis.
33. Objective according to claim 32, wherein the effective birefringence distribution of the compensation coating for the aperture angle  $\theta_F=0^\circ$  is approximately zero.
34. Objective according to one of the claims 32 and 33, wherein the effective birefringence distribution depends primarily on the aperture angle  $\theta_F$ .
35. Objective according to one of the claims 32 to 36, wherein the optical element with the compensation coating is interchangeable.
36. Objective according to one of the claims 31 to 35, wherein at least two optical elements are lenses or lens parts of fluoride crystal, wherein the lenses or the lens parts have lens axes, wherein the lenses or the lens parts are arranged with a rotation relative to each other about the lens axis such that the distribution of the optical path differences  $\Delta OPL(\alpha_R, \theta_R)$  of the ray bundle as a function of the azimuth angle  $\alpha_R$  and the aperture angle  $\theta_R$  has significantly reduced values in comparison to lenses or lens parts in which the lens axes are oriented in the same principal

crystallographic direction and which are not rotated relative to each other about the lens axes.

37. Objective according to claim 36, wherein the optical path differences  $\Delta OPL$  as a function of the azimuth angle  $\alpha_R$  for a given aperture angle  $\theta_0$  vary by less than 30%, in particular by less than 20%.
38. Objective according to one of the claims 36 or 37, wherein each of the lenses or lens parts has a birefringence distribution  $\Delta n(\alpha_L, \theta_L)$  whose birefringence values  $\Delta n$  depend on azimuth angles  $\alpha_L$  relative to a reference direction that is perpendicular to the lens axis and on aperture angles  $\theta_R$  relative to the lens axis,  
wherein the birefringence distribution  $\Delta n(\alpha_L, \theta_L)$  has a k-fold azimuthal symmetry,  
wherein respective rotation angles  $\gamma$  are defined between the reference directions of the individual lenses or lens parts,  
wherein a number of n lenses or n lens parts form a group within which the lens axes point in one and the same or in an equivalent principal crystallographic direction and within which group the birefringence distributions  $\Delta n(\alpha_L, \theta_L)$  have the same azimuthal profile relative to the reference directions,  
wherein the rotation angle  $\gamma$  between each two lenses or lens parts of a group conforms to the equation:  
$$\gamma = \frac{360^\circ}{k \cdot n} + m \cdot \frac{360^\circ}{k} \pm 10^\circ,$$
wherein m represents an integer number.
39. Objective according to one of the claims 36 to 38, wherein the optical element with the compensation coating is one

- of the fluoride crystal lenses, and wherein the element axis is the lens axis of the fluoride crystal lens.
40. Objective according to one of the claims 30 to 39, wherein a plurality of optical elements are coated with compensation coatings.
41. Objective according to one of the claims 1 to 40, wherein the objective has an image-side numerical aperture NA, and wherein the image-side numerical aperture NA is larger than 0.7, in particular larger than 0.8.
42. Objective according to one of the claims 1 to 41, wherein the objective is designed for wavelengths shorter than 200 nm.
43. Objective according to one of the claims 1 to 42, wherein the objective is designed for wavelengths shorter than 160 nm.
44. Objective according to one of the claims 1 to 43, wherein the Objective (611) is a refractive objective.
45. Objective according to one of the claims 1 to 44, wherein the objective is a catadioptric objective (711) with lenses and with at least one mirror (Sp2).
46. Objective according to one of the claims 1 to 45, wherein all of the lenses are of calcium fluoride.
47. Microlithography projection exposure apparatus (81), comprising  
- an illumination system (83),

- an objective (85) according to one of the claims 1 to 46 which projects a structure-carrying mask (89) onto a light-sensitive substrate (815).
48. Method for the manufacture of semiconductor components by means of a microlithography projection exposure apparatus (81) according to claim 47.
49. Method for the manufacture of objectives, in particular projection objectives for a microlithography projection exposure apparatus,  
with at least two lenses or lens parts consisting of fluoride crystal,  
wherein the lenses or the lens parts have lens axes pointing approximately in a respective principal crystallographic direction,  
characterized in that  
for a ray bundle wherein each of the rays of the bundle has a respective azimuth angle  $\alpha_R$ , a respective aperture angle  $\theta_R$ , and a respective optical path difference  $\Delta OPL$  for two mutually orthogonal states of linear polarization in an image plane, the distribution  $\Delta OPL(\theta_R, \alpha_R)$  is determined for lenses and lens parts, and  
the lenses or lens parts are arranged with a rotation relative to each other about the lens axes such that the distribution of the optical path differences  $\Delta OPL(\alpha_R, \theta_R)$  of the ray bundle has significantly reduced values in comparison to lenses or lens parts in which the lens axes point in the same principal crystallographic direction and which are not arranged with a rotation relative to each other about the lens axes.
50. Method according to claim 49, wherein the objective comprises a first group with lenses or lens parts and a

second group with lenses or lens parts, wherein the lens axes of the lenses or lens parts of the first group point in the crystallographic <100>-direction or an equivalent principal crystallographic direction, and wherein the lens axes of the lenses or lens parts of the second group point in the crystallographic <111>-direction or an equivalent principal crystallographic direction.

51. Method according to claim 49, wherein the objective comprises a first group with lenses or lens parts and a second group with lenses or lens parts, wherein the lens axes of the lenses or lens parts of the first group point in the crystallographic <100>-direction or an equivalent principal crystallographic direction, and wherein the lens axes of the lenses or lens parts of the second group point in the crystallographic <110>-direction or an equivalent principal crystallographic direction.
52. Method according to one of the claims 49 to 51, wherein a distribution of the optical path differences  $\Delta OPL(\alpha_R, \theta_R)$  [is determined?] for a ray bundle with rays that have respective azimuth angles  $\alpha_R$ , aperture angles  $\theta_R$ , and optical path differences  $\Delta OPL$  for two mutually orthogonal states of linear polarization in an image plane,  
wherein based on the distribution of the optical path differences  $\Delta OPL(\alpha_R, \theta_R)$ , an effective birefringence distribution is determined for a compensation coating designed to reduce the optical path differences  $\Delta OPL(\alpha_R, \theta_R)$ ,  
wherein the effective birefringence values of the compensation coating depend on azimuth angles  $\alpha_F$  relative to a reference direction that is perpendicular to an element axis of the optical element and on aperture angles

$\theta_F$  relative to the element axis,  
wherein the design of a compensation coating is determined  
from the birefringence distribution, and  
wherein the compensation coating is applied to an optical  
element of the objective.

53. Method for the compensation of birefringence effects in objectives, particularly in projection objectives for a microlithography projection exposure apparatus, wherein the objective has a plurality of optical elements, in particular lenses of fluoride crystal, with optical surfaces,  
wherein at least one optical element is interchangeable, wherein the rays of a ray bundle meet in an image point of an image plane, each of said rays having a respective azimuth angle  $\alpha_R$ , a respective aperture angle  $\theta_R$  and a respective optical path difference  $\Delta OPL$  for two mutually orthogonal states of linear polarization in an image plane,  
wherein a distribution of the optical path differences  $\Delta OPL(\alpha_R, \theta_R)$  is determined,  
wherein based on the distribution of the optical path differences  $\Delta OPL(\alpha_R, \theta_R)$ , an effective birefringence distribution for a compensation coating is determined with effective birefringence values depending on azimuth angles  $\alpha_F$  relative to a reference direction that is perpendicular to an element axis of the optical element and on aperture angles  $\theta_F$  relative to the element axis,  
wherein the design of a compensation coating is determined from the birefringence distribution,  
wherein the interchangeable optical element is removed from the objective,  
wherein the compensation coating is applied to the interchangeable optical element, and

wherein the interchangeable optical element with the compensation coating is reinstalled in the objective.

54. Method for the manufacture of lenses, characterized in that a plurality of plates consisting of a crystal material, preferably fluoride crystal and in particular calcium fluoride, which are rotated relative to each other in regard to the respective crystallographic orientations of the crystal material, are joined together in an optically seamless manner, in particular by wringing, and are subsequently shaped and polished as a unitary blank.
55. Method for the manufacture of lenses according to claim 54, wherein each of the plates has a birefringence distribution  $\Delta n(\alpha_L, \theta_L)$  with birefringence values  $\Delta n$  dependent on azimuth angles  $\alpha_L$  relative to a reference direction that is perpendicular to the lens axis and further dependent on aperture angles  $\theta_L$  relative to the lens axis, and wherein said birefringence distribution has a k-fold azimuthal symmetry,  
wherein for a number of N plates the surface normal vectors point in one and the same or an equivalent principal crystallographic direction and the birefringence distributions  $\Delta n(\alpha_L, \theta_L)$  have the same azimuthal profile relative to the reference directions,  
wherein angles of rotation  $\gamma$  are defined between the reference directions of the individual plates, and wherein the rotation angle  $\gamma$  between each two plates conforms to the equation:  
$$\gamma = \frac{360^\circ}{k \cdot n} + m \cdot \frac{360^\circ}{k} \pm 10^\circ, \text{ wherein } m \text{ is an integer number.}$$
56. Method for the manufacture of lenses according to claim 55, wherein two plates are seamlessly joined.

57. Method for the manufacture of lenses according to one of the claims 55 and 56, wherein the plates are of approximately equal thickness.
58. Method for the manufacture of lenses according to one of the claims 54 to 57, wherein in first plates the normal vectors of the plate surfaces point in the crystallographic <111>-direction or an equivalent principal crystallographic direction, and wherein in second plates the normal vectors of the plate surfaces point in the crystallographic <100>-direction or an equivalent principal crystallographic direction.
59. Method for the manufacture of lenses according to claim 58, wherein the first plates have an approximately equal first thickness and the second plates have an approximately equal second thickness, and wherein the ratio between the sum of the first thicknesses and the sum of the second thicknesses is  $1.5 \pm 0.2$ .
60. Method for the manufacture of lenses according to one of the claims 54 to 57, wherein in first plates the normal vectors of the plate surfaces point in the crystallographic <110>-direction or an equivalent principal crystallographic direction, and wherein in second plates the normal vectors of the plate surfaces point in the crystallographic <100>-direction or an equivalent principal crystallographic direction.
61. Method for the manufacture of lenses according to claim 60, wherein the first plates have an approximately equal first thickness and the second plates have an approximately equal second thickness, and wherein the

- ratio between the sum of the first thicknesses and the sum of the second thicknesses is  $4.0 \pm 0.4$ .
62. Method for the manufacture of lenses according to one of the claims 60 and 61, wherein two first plates are seamlessly joined with a second plate.
63. Method for the manufacture of lenses according to one of the claims 60 and 61, wherein four first plates are seamlessly joined with two second plates.
64. Lens, characterized by the manufacture according to one of the claims 54 to 63.
65. Objective, in particular a projection objective (611, 711) for a microlithography projection exposure apparatus (81), characterized in that the objective comprises a lens according to claim 64.
66. Objective according to at least one of the claims 1 to 46, characterized in that it comprises a lens according to claim 64.

---

Attached hereto: 27 page(s) of drawings

---

**Summary:****Objective with Crystal Lenses**

(Fig. 1)

Objective, in particular a projection objective for a microlithography projection exposure apparatus with at least one fluoride crystal lens. A reduction of the undesirable influence of birefringence is achieved if this lens is a (100)-lens with a lens axis that is oriented approximately perpendicular to the crystallographic {100}-planes or equivalent crystallographic planes of the fluoride crystal. In objectives with at least two fluoride crystal lenses, it is advantageous if the fluoride crystal lenses are arranged with a rotation relative to each other. In addition to the crystallographic <100>-direction, the lens axes of the fluoride crystal lenses can also be oriented in the crystallographic <111>- or <110>-direction. A further reduction in the undesirable influence of birefringence is achieved by using groups of mutually rotated (100)-lenses in simultaneous combination with groups of mutually rotated (111)-lenses or (110)-lenses. A further reduction in the undesirable influence of birefringence is achieved by applying a compensation coating to an optical element.